Alluvial river response to active tectonics in the Dehradun region, Northwest India: A case study of the Ganga and Yamuna rivers.

PICKERING, JACK

Abstract

In environments characterised by active tectonics, it is widely accepted that river morphology will be affected by active fault displacement. For example, there is documented evidence of change in channel slope, channel width, channel braiding patterns, grain size distribution trends, and stream power in response to active faults. Therefore, river morphology can carry a measurable signature of tectonic activity. Furthermore, it can be hypothesised that fluvial systems are in fact more sensitive to local faulting than raw topographic expression. This would mean that young active faults will affect river morphology before they are expressed in the local topography. Therefore, detailed morphological measurements of rivers in tectonic settings could allow for an early detection of faulting which is not yet expressed in the landscape.

The Dehradun region of the Northwest Himalayan foothills is an ideal test case for this hypothesis. In this area, the Ganges and Yamuna rivers flow across an active thrust fault system, which is not yet clearly visible in the landscape. Therefore, longitudinal river profiles of the Ganges and Yamuna rivers from the Lesser Himalaya mountain front to ~35 km into the Gangetic Plain were extracted from a 90 m Digital Elevation Model and hydraulic features, including width of channel belt, channel slope, and geomorphic characteristics, were collected from IRS 23.5 m satellite images. Stream power was calculated by using channel slope and monthly discharge data. These data were complemented by field measurements of bed material grain sizes at ~5 km intervals. All data were analysed for the ~80 km Ganges and Yamuna reaches flowing from the Main Boundary Thrust, through the alluvial Dehra Dun valley and across the suspected active Himalayan Frontal Thrust, and ~35 km out into the Indo-Gangetic foreland.

The longitudinal profile, width of channel belt, channel slope, braiding relationship, pattern of stream power, and grain size distribution all indicate river response to active slip on the Himalayan Frontal Thrust. Most importantly, channel slope (0.063) increases in response to an uplifted bed, and elevation drop over the fault axis. The Yamuna channel slope shallows upstream of, and proximal to the HFT (~0.0025) and steepens across the fault axis to (~0.0035) in response to an uplifted bed and elevation drop. Width of channel belts narrow across the HFT in response to constriction by uplifted topography from ~1500 m upstream to ~500 m across the HFT. This is reflected in the braiding index as both rivers flow as one channel across the HFT and as many channels in the Dun and foreland. The grain size trend along the Ganges reflects downstream fining by selective entrainment throughout the entire study reach with no variation interpreted as having a high enough stream power to move all sediment. The Yamuna indicates downstream fining through the Dun valley, yet grain size increases immediately, upstream of the HFT. This is interpreted as being due to low stream power within the Mohand Anticline caused by a low discharge and shallowing channel slope.

This study concludes that the Ganges and Yamuna rivers are responding to active tectonic uplift of the HFT in the Dehradun basin, Northwest India.

Alluvial river response to active tectonics in the Dehradun region, Northwest India: A case study of the Ganga and Yamuna rivers.

Jack Pickering

MSc by Research

Department of Geography

University of Durham

2010

Contents *Page No.*

Figures

Tables

Statement of Copyright

Acknowledgements

I would like give a huge thanks to my supervisors Dr Alexander Densmore and Dr Patrice Carbonneau for the opportunity to be involved in a fantastic research collaboration. I would also like to thank them for all of their time and commitment invested in me, their help and guidance over the last two years has been instrumental to the success of my thesis.

I would also like to thank Dr Jason Barnes for all of his help, both technically, and in the field. His experience has been invaluable. I thank Dr Vikrant Jain for his advice with sections of the analysis, and I would like to acknowledge Dr Jeff Warburton and Dr Rajiv Sinha for their comments that have helped improve this manuscript.

Finally, I would like to say a huge thank you to my parents for their financial support throughout the entire project. Without it the last two years would not have been possible.

1. Introduction

It is well documented that rivers respond rapidly and consistently to active tectonic deformation of the Earth's surface (Seeber and Gornitz, 1983; Ouchi, 1985; Holbrook and Schumm, 1999; Jain and Sinha, 2005; Turowski *et al*. 2006; Amos and Burbank, 2007). They do this by altering their width of channel belt, channel slope, and geomorphology to drive the system toward a 'steady state' whereby uplift and erosion are balanced (Willett and Brandon, 2002).

Active tectonics in a river system can be seen by alterations in the longitudinal profile, even where spatial gradients between two points of a river, for example an upstream and lower stream point, rock uplift rates of 2-3 mm/yr can induce morphological changes (Schumm *et al*. 2002). Width of channel belt should decrease as a river flows over an active fault, and this may also be reflected in the braiding pattern. Figure 1.1 illustrates the expected river response to tectonic uplift (Holbrook and Schumm, 1999). Braiding decreases as a river flows over an active fault as width decreases, and increase downstream of the fault as width increases (Holbrook and Schumm, 1999). Channel slope should decrease upstream of an active fault and increase immediately downstream of the fault (Holbrook and Schumm, 1999). In turn, this should cause predictable patterns of grain size variation, with clast size increasing as slope begins to decrease, as by reducing slope, the energy available to transport sediment is reduced (Paola *et al*., 1992). Grain size distribution can therefore be used to identify rock uplift on a fault. Stream power can also be used as a proxy for tectonic uplift as a result of changing slope. Stream power is known to be a main control on sediment transport capacity, and therefore as slope decreases stream power decreases, influencing the transport capacity of the river (Whipple, 2004). A tenet of tectonic geomorphology is that we can look for those expected relationships in areas of known or suspected tectonic deformation, to see if the rivers have been affected by faulting and fold growth. As previous studies have observed some of the relationships between river morphology and tectonics (Seeber and Gornitz, 1983; Ouchi, 1985; Holbrook and Schumm, 1999), the likely relationships can be implemented and contrasted as hypotheses for larger river response in poorly understood regions, where individual faults are thought to be active.

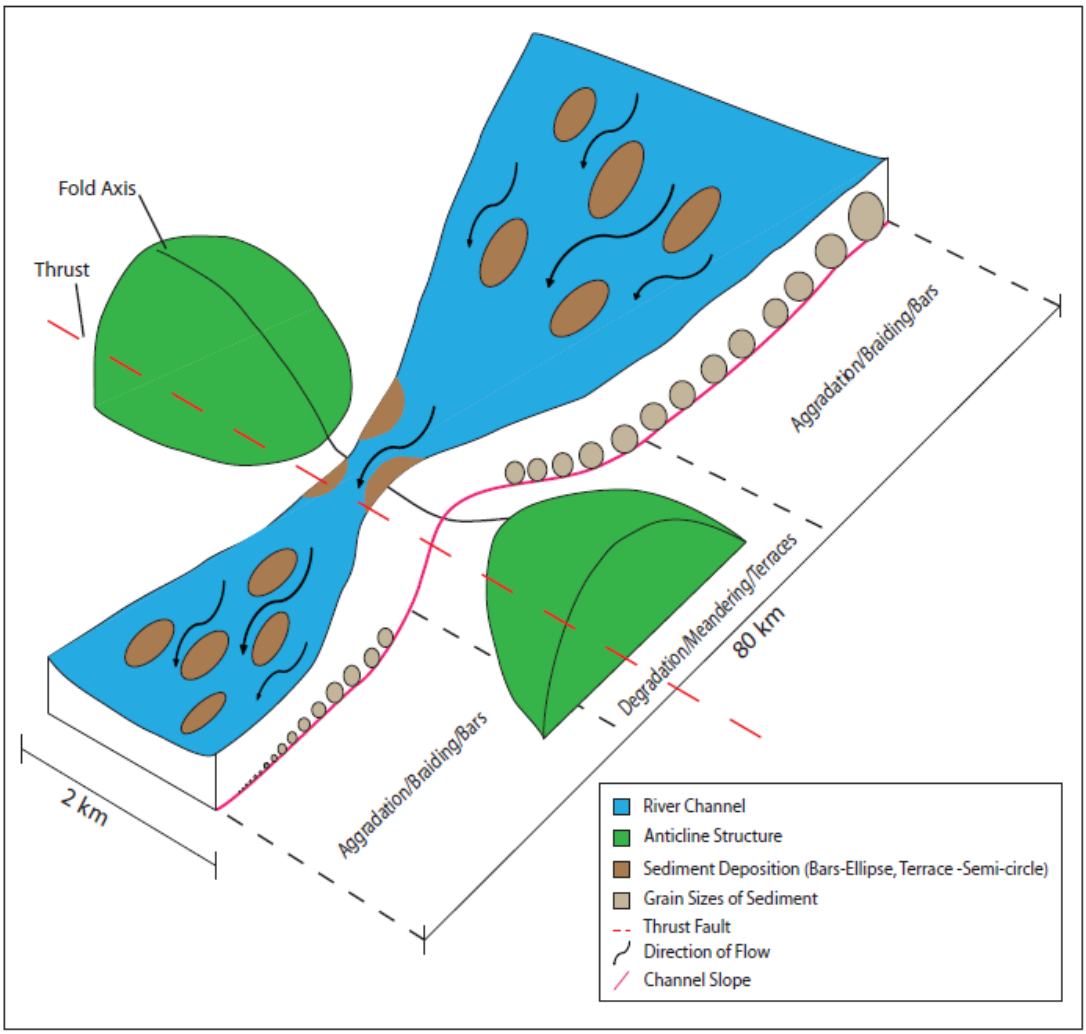

Fig 1.1. A simple river system diagram illustrating the changes in channel morphology in a river flowing over an uplifting fault axis (dashed red line). The figure shows the river response according to previous studies (Holbrook and Schumm, 1999, Ouchi, 1985). The river is represented by the blue, the channel slope indicated by the pink line, the anticline structure in green, the depositional features in brown, grain size change in grey circles, and the sedimentation/river sinuosity/deposition feature type labelled in the dashed line cells. The direction of flow has been identified by an arrow.

The Dehra Dun area in Northwest India is an ideal place to apply this model because the Ganges and Yamuna rivers both drain through an alluvial valley bound by two thrust faults. It is thought that the faults are active, but the effect of faulting on the Himalayan Frontal Thrust on the Ganges and Yamuna has never before been examined. This important reach of the two rivers is in a very large and relatively remote area of Northwest India (Fig 1.2). Therefore, it is inevitable that there are regions where local data is not available. Due to this limitation, remotely sensed data will be essential to the project in order to construct a useful and detailed dataset. Both the Ganges and Yamuna rivers are subject to anthropogenic impacts in the form of large damming and canalling networks, as well as intense local mining operations. It will be important to address any obscurity that these anthropogenic sources of influence might have. It will be of particular importance when investigating grain size data due to the selective removal of grains, as well as the more macro scale influence of river deflection and damming, and thus anthropogenic forcing of slope derived variables such as unit stream power.

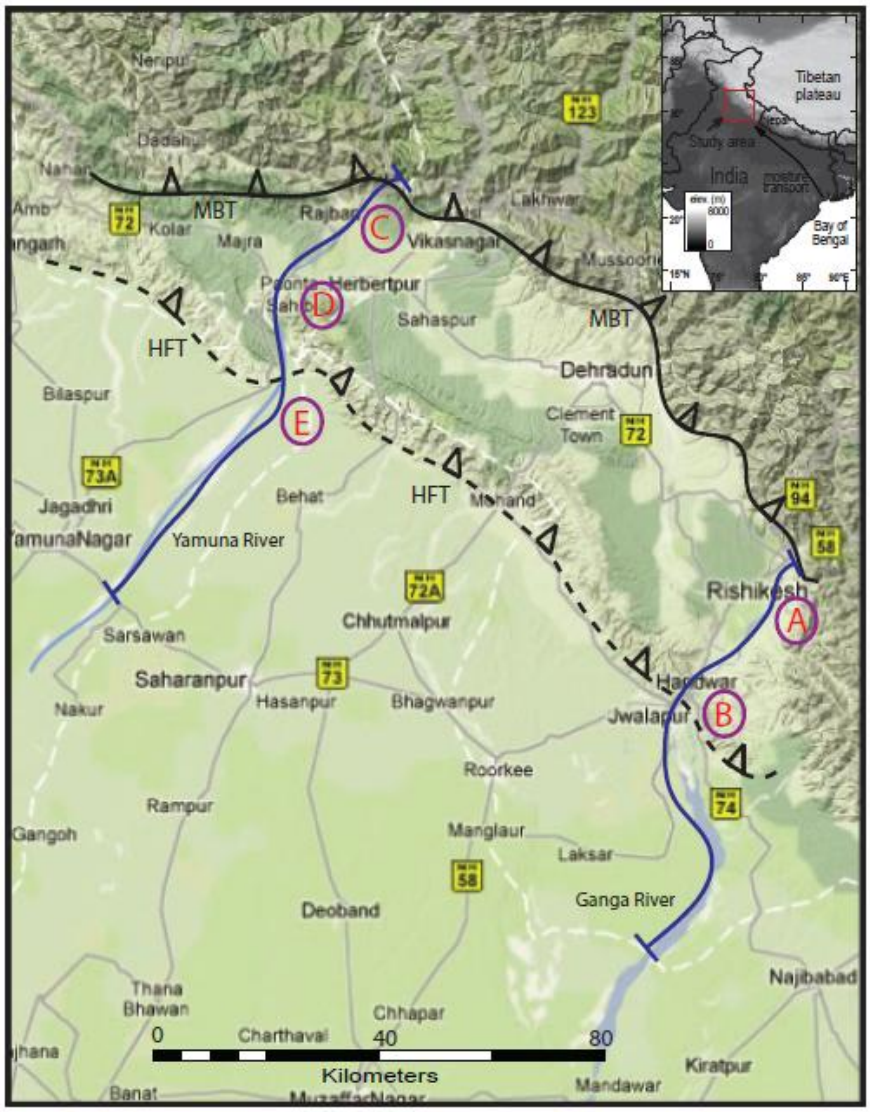

Fig 1.2. A map indicating the study region in Dehradun, Northwest India. The map shows the key geological features (black lines) important to the study, the Main Boundary Thrust (MBT) as the solid black line, and the Himalayan Frontal Thrust (HFT) as the dashed black line. The river reaches that are used in the study are mapped in dark blue, and the positions of major dams are labelled A-E. The major towns and cities are also marked. The map has been modified from Google maps.

The majority of dams in place along both rivers have been installed for the main purpose of irrigation, and to control the high flow and low flow discharges (Fig 1.2). During monsoon the reservoirs are filled in order to store water for the remaining months of the year, as more than 75% of rainfall falls within the period of June-September (Singh, 2006). Large canal networks feed off from the main reservoirs and run off into surrounding areas in the foreland, delivering water mainly for irrigation, but also providing drinking and bathing areas for the local population. The largest and most well known engineering project is the Upper Ganges Canal System (UGC).

Fig 1.3a. The two satellite images above illustrate the two main river diversions on the Ganges within the study reach. The red letters correspond to the letters on Fig 1.2 above. A is located at Rishikesh, and B, the more significant river deflection, shows the Upper Ganges Canal (UGC) at Haridwar.

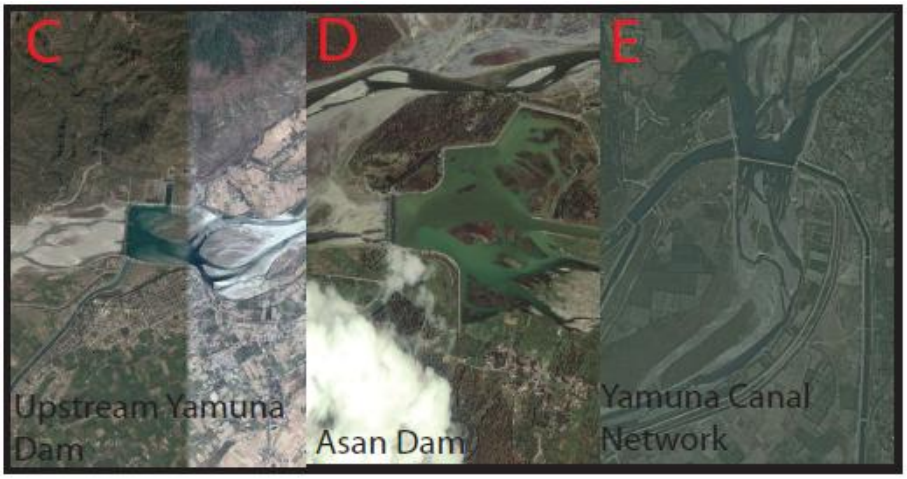

Fig 1.3b. The three satellite images above illustrate the three main river diversions on the Yamuna within the study reach. The red letters correspond to the red letters on Fig 1.2. C is located upstream (west) of Vikasnagar, D is located immediately upstream of Paonta Sahib, and E shows the Eastern and Western Yamuna Canal Network. The satellite image is from Google maps.

The UGC was originally constructed to combat drought in the western region of the current Uttar Pradesh state. The UGC draws its supply from a diversion of the Ganges at Haridwar, and runs for a length of 290 km and extends over an area of 24'000 km^2. The main Yamuna canal systems exist in the form of the Eastern Yamuna Canal and the Western Yamuna Canal (Jain *et al*., 2007). Main cities that are supported by the Yamuna and Ganges rivers in the foreland include Delhi (Yamuna), Kanpur (Ganges), Lucknow (Ganges), Allahabad (confluence of Yamuna and Ganges), and Varanasi (Ganges).

Both river networks are heavily regulated due to the importance of water storage for the dry season and are heavily gravel mined. It is not clear yet, however, whether these diversion schemes and selective removal of gravel have had a subsequent effect on the drainage systems and river morphology. These could be very significant as by regulating the flow through these confined areas of the region, channel morphology and river hydrology (discharge/stream

power) could potentially be heavily controlled/anthropogenically manipulated, impacting the accuracy and natural variance of the rivers. Another limitation to the project will be the unknown contribution of the tributaries to the main river channels. The important issue of the influence of dams will be addressed in the project by observing grain size data, discharge and stream power/unit stream power variability in the human-influenced regions, obtained from both the remotely sensed data and the field collected data.

The following key research questions are therefore raised:

1. What fluvial geomorphologic changes happen to the Ganges and Yamuna rivers as they flow through the alluvial Dun Valley, from the Lesser Himalayan mountain front, across the Himalayan Frontal Thrust, and into the Indo-Gangetic Plain?
2. To what extent is the fluvial response to active tectonics obscured by anthropogenic influences in this environment?

The objectives that will be used to help answer these questions are:

1. Using remotely sensed data, measure the geomorphic variables width of channel belt, channel slope and braiding index, to answer question 1 and 2.
2. Obtain grain size data in the field at predetermined intervals along both the Ganges and Yamuna rivers. Obtain discharge data and combine with previously collected channel slope data to calculate unit stream power, to answer questions 1, 2.

The thesis consists of six chapters: the Introduction, Study Region, Methodology, Results, Discussion, and Conclusions. The study region chapter will introduce the Dehra Dun valley, its geological framework, geographical setting relative to the Himalaya, and river processes in the region. The methodology chapter will describe the remote sensing methods, fieldwork methods, and analysis methods used to collate the data needed to examine any changes in behaviour of the rivers as they flow over the suspected active fault. The results chapter will display and describe the characteristics that we see and indicate any potential signals that should be further discussed in the fifth chapter, the discussion. The discussion will interpret the signals highlighted in the results and attribute them to a cause. The sixth and final chapter is the conclusions, in which the key research questions will be revisited and further work proposed.

2. Study Region

Geological and Geographical setting:

The topography, geologic structures, and earthquakes of the Himalaya and surrounding regions are a consequence of the northward progression and collision of India into Eurasia, a process that has accommodated an estimated 2000-3000 km of convergence since the Late Cretaceous (Molnar and Tapponnier, 1977) and is thought to continue today at a rate of ~55 to 60 mm/yr (DeMets *et al*., 1994; Bilham *et al*., 1997, 1998). The Himalayan orogen is characterized by the activation and successive abandonment of large thrust faults whose lateral continuity and large inferred displacement identify them as primary zones of intracontinental thrusting during the Himalayan orogeny (Meigs *et al*., 1995; Gansser, 1981; Molnar, 1988; Seeber *et al*., 1981).

Intracontinental mountain building in convergent settings usually occurs as a result of the nucleation and growth of thrust faults. As thrust faults emerge as topographic entities, they define intermontane basins in which the detritus eroded from the bounding ranges accumulates, forming alluvial deposits (Burbank *et al*., 1999). There are at least three patterns of deformation that accommodate shortening as convergence continues. These are thought to be (1) the early formed thrusts continue to move and accumulate more and more displacement; (2) the zone of deformation widens as new thrusts emerge along the flanks of the mountain belt; or (3) new thrusts can develop within and between the existing mountains during densification of the thrust system (Burbank *et al*., 1999). The intracontinental basin in the study region fits under the first pattern of deformation and the Main Boundary Thrust (MBT) and the distal Himalayan Frontal Thrust (HFT) define the northern and southern boundaries (Fig 2.1)

The Himalaya represents one of the few places on Earth where continental crust (Indian plate) is attempting to underthrust continental crust (Eurasian Plate) (Zhao *et al.*, 1993). The Indus-Tsangpo suture zone separating India from Tibet marks the Paleogene collision of India with Eurasia (Gansser, 1964: Powers *et al*., 1998; Thakur, 1992). To the south of the suture zone, Precambrian basement (High Himalaya) and a relatively complete cover of Phanerozoic rock (Tethys Himalaya) are believed to have been thrust southwards over a discontinuous sedimentary sequence along the Main Central Thrust (Fig 2.2). The Precambrian and younger rocks of the Himalaya were originally part of India's northern passive margin (Powers *et al.*, 1998). South of the Main Central Thrust, Proterozoic and younger rocks of the Lesser Himalaya are thrust southwards over the Miocene-Pleistocene Siwalik Group along the Main Boundary Thrust (MBT). The MBT is defined throughout the literature as the southernmost thrust that places metasedimentary rocks of the Lesser Himalaya over unmetamorphosed granitic rocks of the Himalayan foredeep. Because the MBT folds the Main Central Thrust and cuts Quaternary sedimentary rocks preserved in the Himalayan foreland, the MBT is deduced to have formed some time since ~25-20 Ma (Hodges *et al*., 1988; Macfarlane, 1993). However, as Meigs *et al.* (1995) explained, there are no overlapping or crosscutting relations that closely define the MBT deformation history and therefore there can be no direct dating of fault activity. Subsidence histories across the western Himalayan foreland, sediment provenance data, and cooling ages

from the leading edge of the MBT have been used to define its formation at >10 Ma along at least 1000 km of the Himalayan frontal zone (Meigs *et al*., 1995), and deformation continues today (Valdiya, 1992).

As a result of the Himalayan orogeny, many rivers, in this context, the Ganges, and Yamuna, have formed as a response of uplift, contributing to the transport of water away from the uplifted collision zone. The rivers carried detritus generated by the denudation of the fast-emerging Himalayas and deposited it in the foreland basin, beginning at ~23 Ma (Validya, 2002). Another fluvial foreland basin, the Siwaliks, began to form at ~18 Ma in front of the rapidly rising orogen and was filled with river born sediments at the rate of ~30 cm/1000 yr in the early stage, and at ~50-55 cm/1000 yr in the late Miocene (~9-7.5 Ma) (Gautam and Fujiwara, 1999). After about 0.8 Ma, deformation stepped-out into the foreland to form the Himalayan Frontal Thrust (HFT) which caused the partitioning of the foreland basin into the rising Siwalik Hills and the subsiding Indo-Gangetic Plain, and also may have initiated glaciation in the uplifted domain of the great Himalaya (Valdiya, 2002).

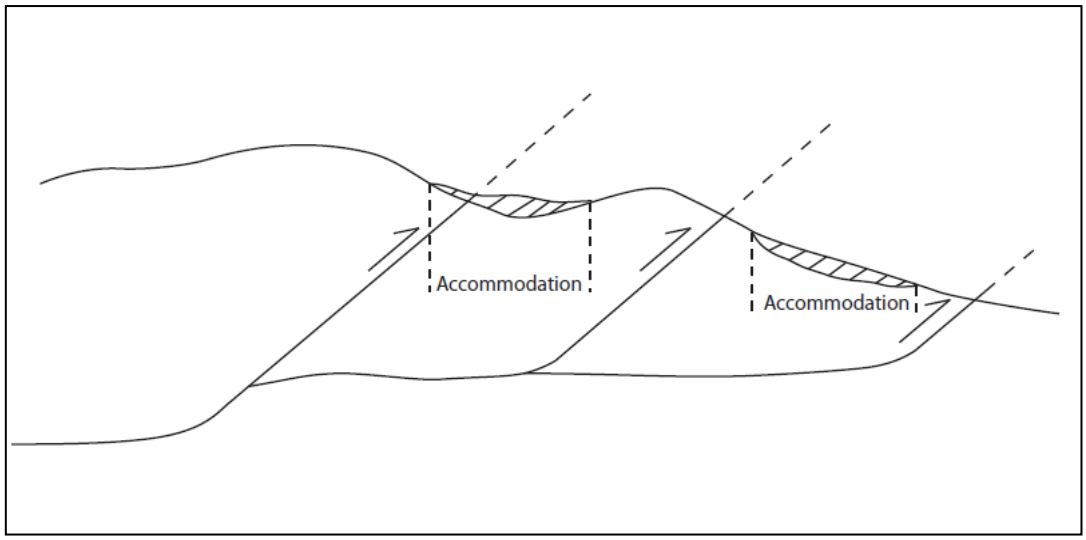

Fig 2.1. A simple thrust fault diagram. As the thrust propagate, they create accommodation space behind in which sediment fills in (dashed area). When there are a number of faults together with fill behind, they create a piggy-back basin as shown above. The deformation in the study region belongs to this type of thrust fault formation.

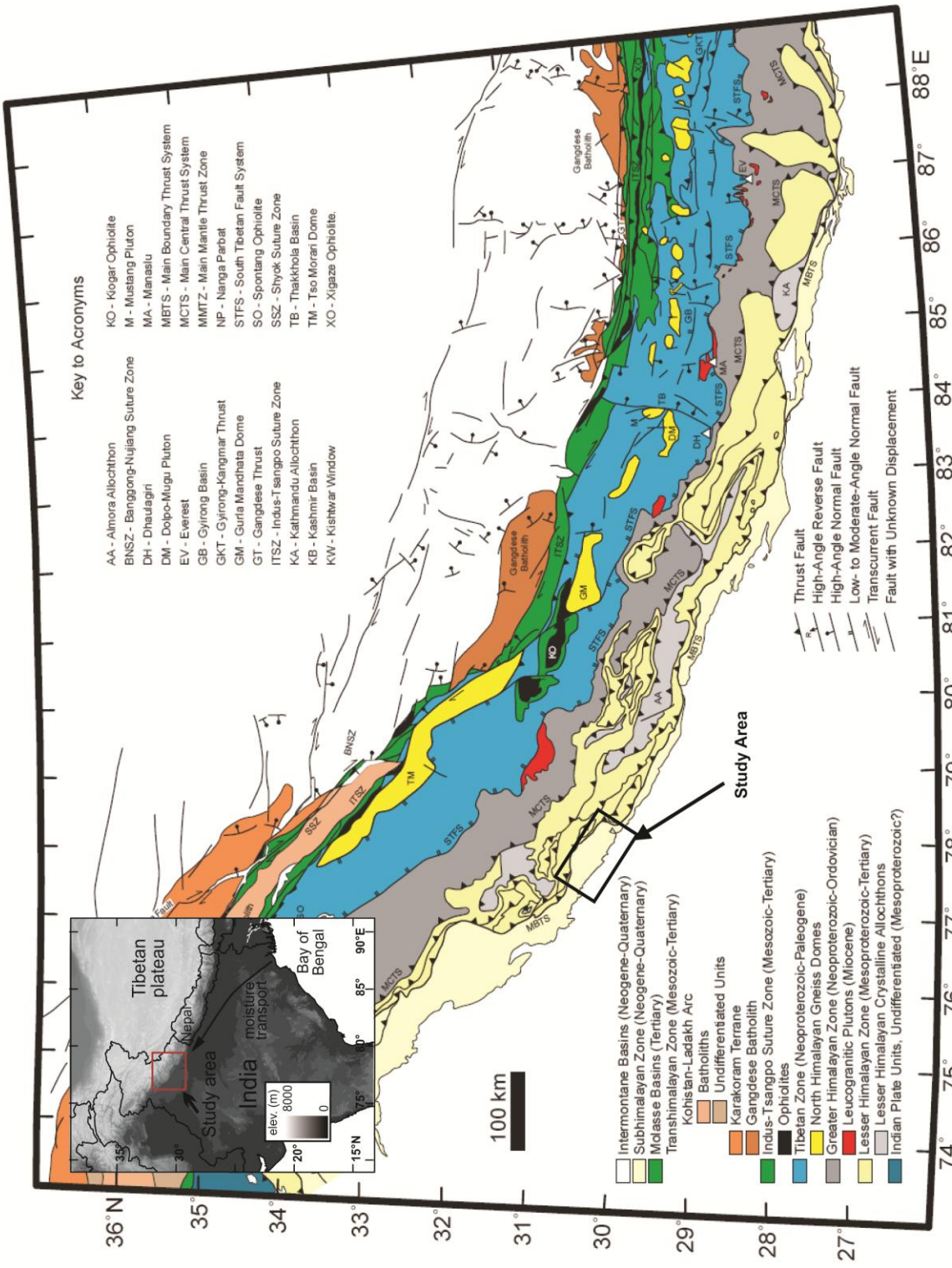

Fig 2.2. Regional geology and major structures of the Himalayan orogenic belt, modified from Hodges (2000). The small box identifies the study region with a larger index map in the top left corner of the map, modified from Powers *et al*. (1998).

The region that we are interested in is the Dehra Dun Basin (Dun valley). This is because the Dun valley falls in a complex and tectonically active zone. The Dun valley is located in the north-western region of Uttarakhand State, India. The specific study region is constrained between the Ganges River in the east and the Yamuna River in the west. The basin stretches approximately 80 km in a NW-SE direction having a maximum width of approximately 25 km. The research area covers various locations in this region protruding up to 40 km into the Indo Gangetic foreland on both rivers. The region is situated between latitudes 30°31'N to 30°6'N and 77°46'E to 78°25'E (northern parameters), 30°13'N to 29°42'N and 77°31'E and 78°10'E (southern parameters) (Fig 2.3).

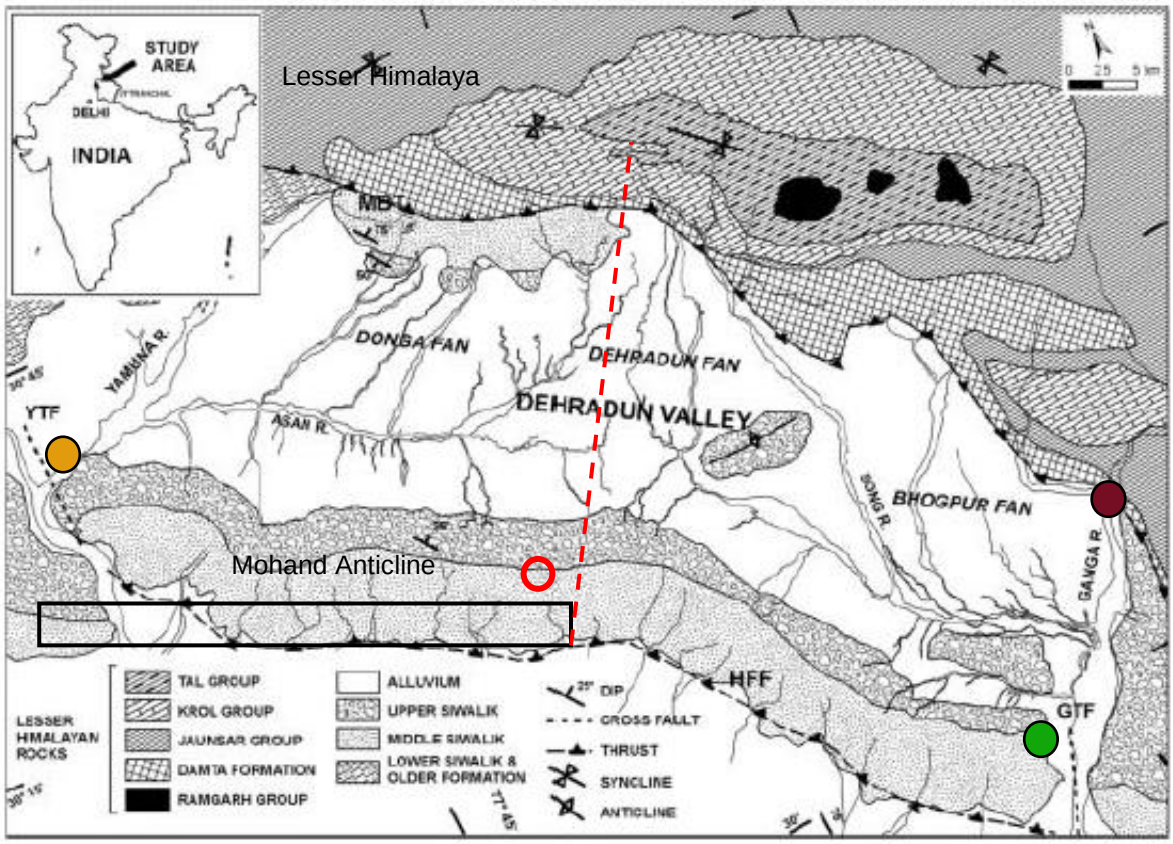

Fig 2.3. Location and regional geology of Dehra Dun area (modified from Singh *et al*. (2007) and Rupke (1974). HFF, Himalayan Frontal Fault; GTF, Ganges Tear Fault; MBT, Main Boundary Thrust; and YTF, Yamuna Tear Fault. The HFF is also referred to as the HFT, Himalayan Frontal Thrust. The red circle identifies the drill hole site used by Wesnousky *et al*. (1999) for radio carbon dating and the black box indicates the location of their calculated uplift rate of ~6.9 ± 1.8 mm/yr. The red dashed line indicates the position of the cross section (Fig 2.3) taken by Thakur and Pandey, (2004). The maroon circle identifies the location of the town Rishikesh, the green circle identifies the town of Haridwar, and the orange circle identifies the town of Paonta Sahib.

The elevation of the study area ranges from ~260 m above sea level at Roorkee to ~350 m north of Rishikesh near the MBT. The Dun valley is an alluvial valley that is bounded by the Lesser Himalaya range in the north, and the Siwalik Hills to the south. The Siwalik Hills are uplifted areas in the Dehra Dun basin, which in this area refers to the Mohand Anticline formed by uplift on the HFT. The Mohand Anticline is a long prominent ridge that trends NW-SE with ranging altitudes from 750 m to ~977 m. The main ridge is composed of a gentle northern slope with a much steeper southern slope. The drainage divide is offset from the fold axis by approximately 10 km, resulting in two peaks in elevation. This is due to a kink in the HFT geometry at depth (Fig 2.4). As the thrust kinks, it creates differences in dip along the fault and as the fault begins to bend and to exhume it creates the first peak in uplift, the drainage divide. The second peak in elevation is due to the fold axis. This is the steepest dip of the HFT driving up the topography above. Due to this uplifted zone, numerous parallel to sub-parallel streams drain the ridge to the north or to the south in consequent entrenched channels.

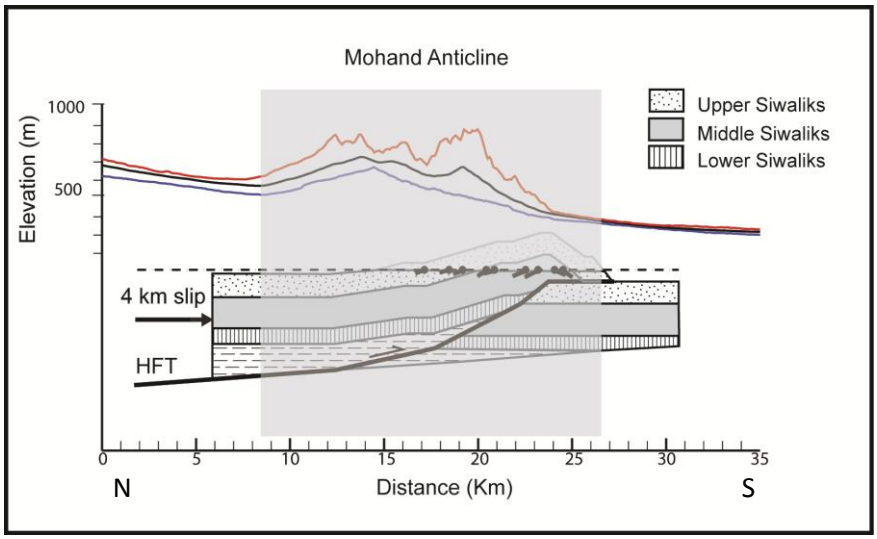

Fig 2.4. Schematic diagram of HFT geometry and bedrock lithology (Mishra and Mukhopadhyay, 2002). The grey box indicates the lateral extent of the Mohand Anticline, with N indicating North and S indicating south.

The HFT provides the southern boundary of the Dun basin. The Ganges and Yamuna rivers cut across the HFT at either end of the Mohand Anticline. It is this geometry that makes this an ideal area to observe and record the response of alluvial rivers to active uplift (Philip and Sah, 1999).

Accommodation in the Dun valley is created by a combination of subsidence in the footwall of the MBT and trapping of sediments behind the rising Mohand Anticline. The alluvial basin is thought to have started forming sometime after 700 ka (Sangode *et al*., 1996), with sediment deposited by debouching streams from the Lesser Himalaya forming three large fans (from east to west – the Bhogpur Fan, Dehra Dun Fan and the Donga Fan (Fig.2.3)) . The sediments that underlie the Dehra Dun basin are the Siwalik Group (Fig 2.5). These were deposited in 3 stages: first the Lower Siwaliks, consisting of a high percentage of mudstone, then the Middle Siwaliks, consisting primarily of gray sandstone, and then the Upper Siwaliks, dominated by cobble conglomerate. These are thought to have been deposited between ~20 and 0.2 Ma (Mid-

Miocene – Pleistocene) (Ranga Rao *et al*., 1988; Singh *et al*., 2001; Kumar *et al*., 2003b). The sediments that then overlie these, in essence the youngest fill deposits, are known as the Dun gravels or the post-Siwalik gravels (Medlicott, 1864). OSL dating by Singh *et al*. (2001) suggested that the Dun gravels are Late Pleistocene to recent in age, however, they only dated the exposed sections, therefore making this an uncertain assessment. The Brunhes-Matuyama geomagnetic transition at ~780 ka, however, is preserved near the top of the Upper Siwaliks in the Mohand, giving us a more accurate age of the initiation of folding of the Siwalik Group (Sangode *et al*., 1996) (Fig 2.5). The Mohand Anticline partitions the Siwalik Group basin sediments from the Gangetic alluvial plains (Singh *et al*., 2007).

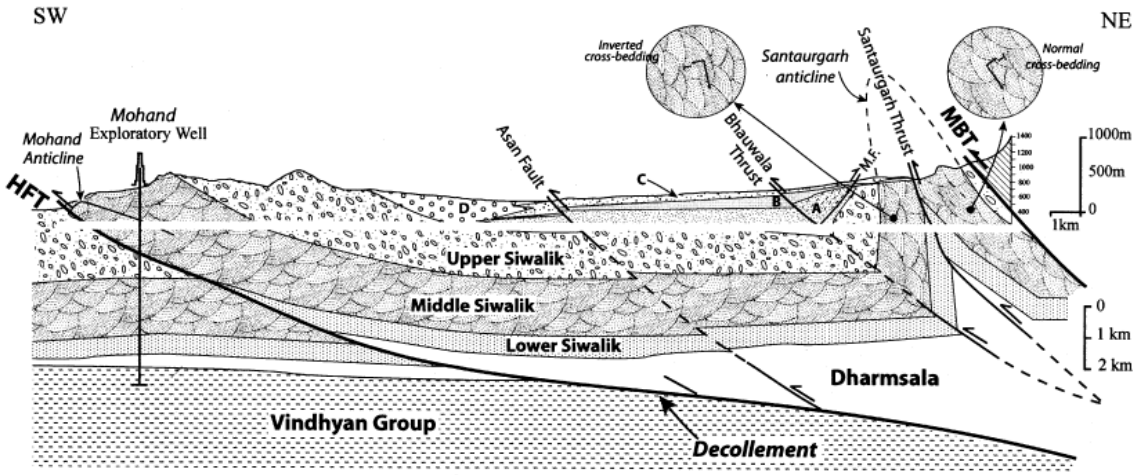

Fig 2.5. Geological cross-section across the Dehra Dun Basin (Dun valley). Upper position of the cross-section (above white strip) is vertically exaggerated for better depiction of structural deposition of post-Siwalik Dun gravels. Subsurface structure (below white strip) based on seismic reflection profile of Dun valley by ONGC, India is adopted after Powers *et al*., 1998. MBT, Main Boundary Thrust; MF, Majhauan back-thrust; HFT, Himalayan Frontal Thrust (taken from Thakur and Pandey, 2004).

Structural Setting of the Dun Valley:

The Dun basin is confined to the north by a large active thrust fault (MBT) and confined by another active thrust fault to the south (HFT) (Wesnousky *et al*., 1999) (Fig 2.3). Near Rajpur and Rispana Rao in the Dehra Dun Basin, the MBT dips north and thrusts the Chandpur phyllite of the Krol Group over the Late Quaternary – Holocene Dun gravels, indicating Holocene to recent tectonic activity along the MBT (Thakur and Pandey, 2004). The Siwalik Group strata are folded into the asymmetric Mohand Anticline in the frontal Siwalik range, the broad Dun syncline occupying the Dehra Dun basin behind, and the overturned Santaurgarh anticline in the north west of the Dehra Dun Basin (Karunakaran and Rao, 1979) (Fig 2.6). The HFT axial trace runs NW-SE between Ganges and Yamuna rivers. The forelimb of the fold dips steeply both north and south, and the back limb dips NE at 15-30°. The HFT is extremely important to this study as both rivers flow across the fault axis. The HFT therefore provides a good study area to look for a response to uplift from the two rivers.

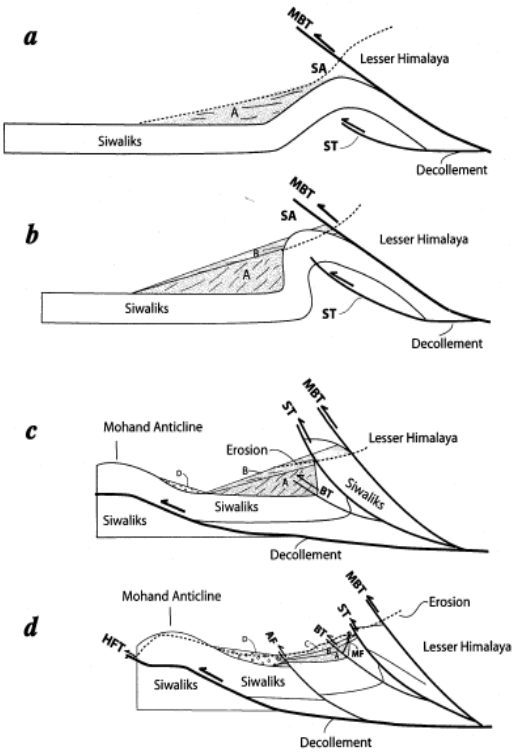

Fig 2.6. Schematic diagram showing Late Quaternary evolution of structure of the Dun valley. A, Initiation of the growth of Santaurgarh anticline (SA) as fault propagation fold over the blind Santaurgarh Thrust (ST) and synchronous deposition of Unit A of Dun gravel. B, Further growth of SA and accompanied steepening of limbs led to the tilting of Unit A gravel. Strath erosion of the crest of growing SA and deposition of horizontally disposed Unit B. c, Steepening of MBT and ST causes locking of thrust that resulted in southward propagation of decollement fault from MBT to HFT. This led to the growth of the Mohand anticline and corresponding Dun syncline as fault-bend fold on the decollement. d, Formation of Bhauwala Thrust (BT), coeval Majhaun Fault/back thrust (MF) and Asan Fault (AF) as out-of-sequence thrusts resulting due to further shortening of strata in the Dun. Taken from Thakur & Pandey (2004).

The HFT thrusts Upper and Middle Siwaliks over Upper Siwaliks, although Upper Siwaliks are not observed on the northern flank of the Mohand due to erosion of the conglomerate strata (Powers *et al.,* 1998; Mishra & Mukhopadhyay, 2002). Wesnousky *et al*. (1999) have calculated an uplift rate on the HFT of ~6.9 ± 1.8 mm/yr on the Mohand Anticline from a radio carbon date of strath terraces near the southern flank of the anticline. They assumed a dip of ~30º on the HFT from drill hole data at the town of Mohand indicated on Fig 2.2. Assuming this dip and uplift rate, Wesnousky *et al*. (1999) calculated the slip on the HFT to be ~13.8 ± 3.6 mm/yr which, when combined with a total displacement of ~4 km (Mishra & Mukhopadhyay, 2002), means the HFT is likely to have activated ~0.3 Ma-0.7 Ma ago. In summary, the Ganges and Yamuna

rivers flow across the HFT in the Mohand Anticline exits to the Gangetic Plain. These areas of the rivers and the reaches in the basin behind the Mohand are key for the study.

Regional Surface Processes and River Morphology:

The following subsection will cover the regional and local surface processes before focussing on the Ganges and Yamuna rivers in more detail.

As the Himalayas continued to rise, orographic forcing of rainfall weather patterns strengthened, which, combined with the creation of a high plateau, became favourable for formation of a monsoon system, with low pressure on the high plateau in the summer months, and the transport of latent heat from the Indian Ocean. This shaped the weather system that has been present since the Mid-Miocene (France-Lanord, 1997; An, 2000). The annual high precipitation values are therefore distributed seasonally with the main contributor being the Indian Monsoon in June – September (Sinha, 2005). Fig 2.7 identifies the precipitation pattern across the Dehra Dun region, with blue indicating the areas of very high rainfall, up to 5.5 meters per year. It can be seen from the image that there are two main zones of high precipitation, one across the Lesser Himalaya mountain front and the second across the Higher Himalaya mountain front. There is also a secondary smaller zone of high precipitation across the northern flank of the Mohand. Bookhagen and Burbank (2006) explained that heavy rainfall is induced by the first considerable topography that the moist air mass meets. Using a decade of TRMM (Tropical Rainfall Measurement Mission) data, they showed that the maximum rainfall occurs consistently along the frontal Himalaya zone rather than further north in the Higher Himalaya. They found that these zones of high rainfall occur most commonly at an average elevation of ~0.95 km or average relief of ~1.2 km.

The drainage system of the Gangetic rivers also takes them through a distinct rainfall gradient that runs from east to west. Generally the west receives less rainfall (~60 – 140 cm/yr), and the east more (~90 - >160 cm/yr) (Sinha, 2005). This high precipitation along the Lesser Himalaya zone (Fig.2.7) provides the Ganges and Yamuna rivers with a high discharge through the monsoon months, providing a potentially high amount of energy to transport sediment downstream.

The monsoon provides the main source of discharge for the Ganges and Yamuna rivers. The Yamuna receives a comparable discharge to the Ganges from a drainage area 66% smaller by the time the rivers are flowing through the Mohand Anticline. According to a value from Jha *et al*. 1988, the peak seasonal discharge at Tajewala (Fig 2.8a) records 777 m^3s^{-1}. This value is provided by a catchment of 9572 km^2. In comparison, discharge data provided by a Gauge at Rishikesh on the Ganges (Fig 2.8b) records an average monthly discharge of 1232 m^3s^{-1} from a catchment area of 21467 km^2. The hydrology of the rivers are therefore somewhat comparable, however, the discharge data for the Yamuna reflects a less than half the size of the Ganges. The Yamuna data is also not valid, as it is a single value from dated literature, and the average peak monthly discharge is inferred from seasonal run off data. Unfortunately, any current gauge data for the Yamuna is not available.

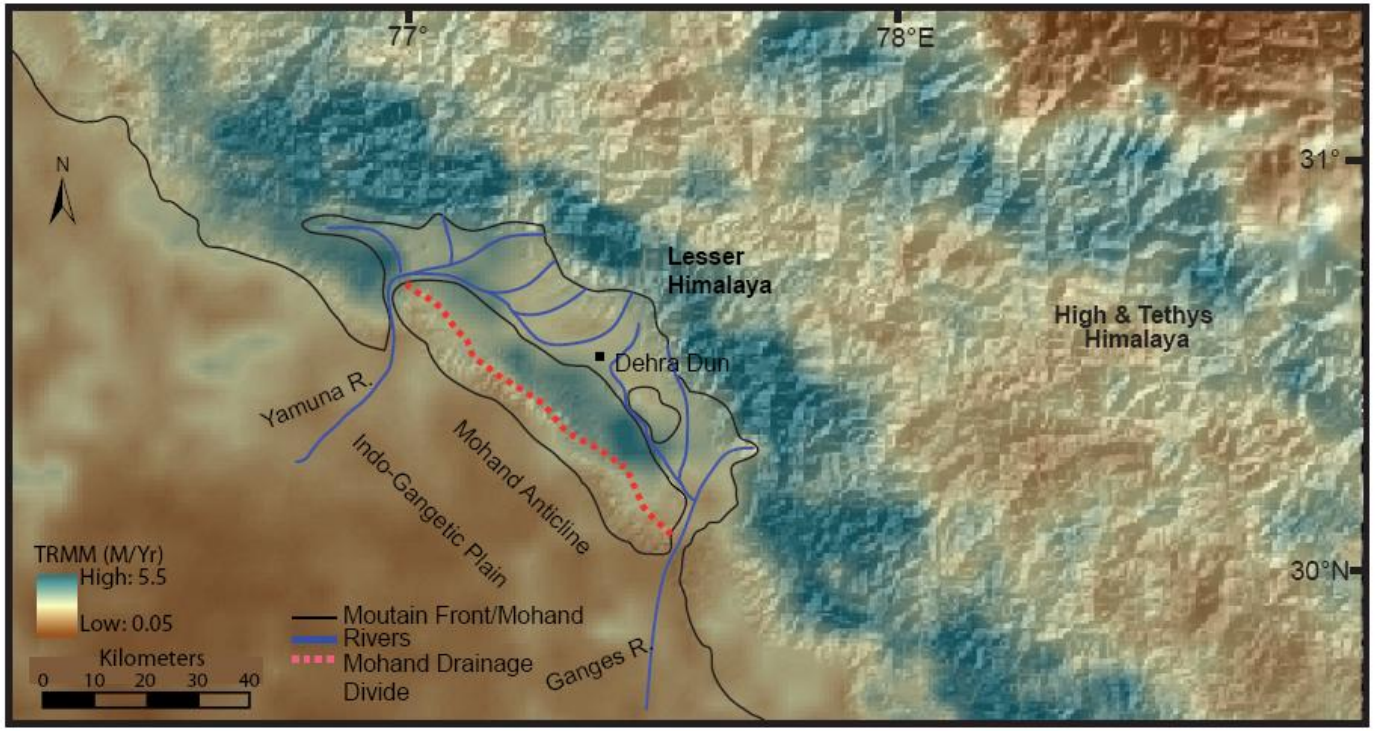

Fig 2.7. TRMM (Tropical Rainfall Measuring Mission) data overlain on a hillshaded DEM for the Dehra Dun region. Blue colours indicate the highest precipitation, brown indicates the lowest precipitation. The Ganges River is located to the east, the Yamuna to the west. TRMM data provided by Bodo Bookhagen.

River Morphology:

The Ganges is formed at Devaprayag by the confluence of the Bhagirathi and the Alaknanda rivers, while the Yamuna originates from the Yamunotri glacier in the Higher Himalaya. Both the Ganges and Yamuna rivers flow through the Gangetic Plain before their confluence at Allahabad.

The Ganges flows out into the Dehra Dun Basin at Rishikesh and flows along the eastern boundary of the valley for approximately 24 km to Haridwar. Along the course of this 24 km reach, the number of channels that constitute the Ganges River varies between just a couple of active channels during the dry season to 7+ during monsoon. Downstream of Haridwar the river again occupies one channel as it is confined by the steep topography of the uplifted Siwalik range (known as the Mohand Anticline). The river then flows for another ~7 km before leaving the mountain front and beginning to bifurcate again. This is observed for the remaining reach of river down to Bālāwāli where the study region terminates (Fig 2.8a).

The Yamuna River flows out into the Dun Valley ~2 km north of Haripur and flows along the western boundary of the valley for approximately 35 km to Paonta Sahib. As with the Ganges, along this stretch of river the number of channels varies between just a couple of active channels during the dry season to 7+ during the wet season to accommodate the extremely high monsoonal discharge. These channels then congregate into a single channel as the river passes through the uplifted Mohand region before splitting again into multiple active channels south of the mountain front. A braiding signature is observed for the remaining reach of river down to Shāhjahānpur where the study region ends (Fig 2.8b).

The rivers are controlled by the strong split in seasonal discharges defined by the wet season (monsoon) and the dry season. Annual river discharges at Allahabad have been recorded as ~59,000 $Mm^3\ s^{-1}$ and ~96,100 $Mm^3\ s^{-1}$ for the Ganges and Yamuna respectively (Jain *et al*., 2007). Fig 2.9a and Fig 2.9b show the measured seasonality of annual discharge in the two rivers. The discharge of the Ganges has been recorded in 4 gauges upstream of the MBT. They all consistently show a significant increase in discharge for the monsoon months June through to September. The discharge for the Yamuna has been recorded at 5 gauges downstream of the MBT but still show the significant increase in discharge in the monsoon season.

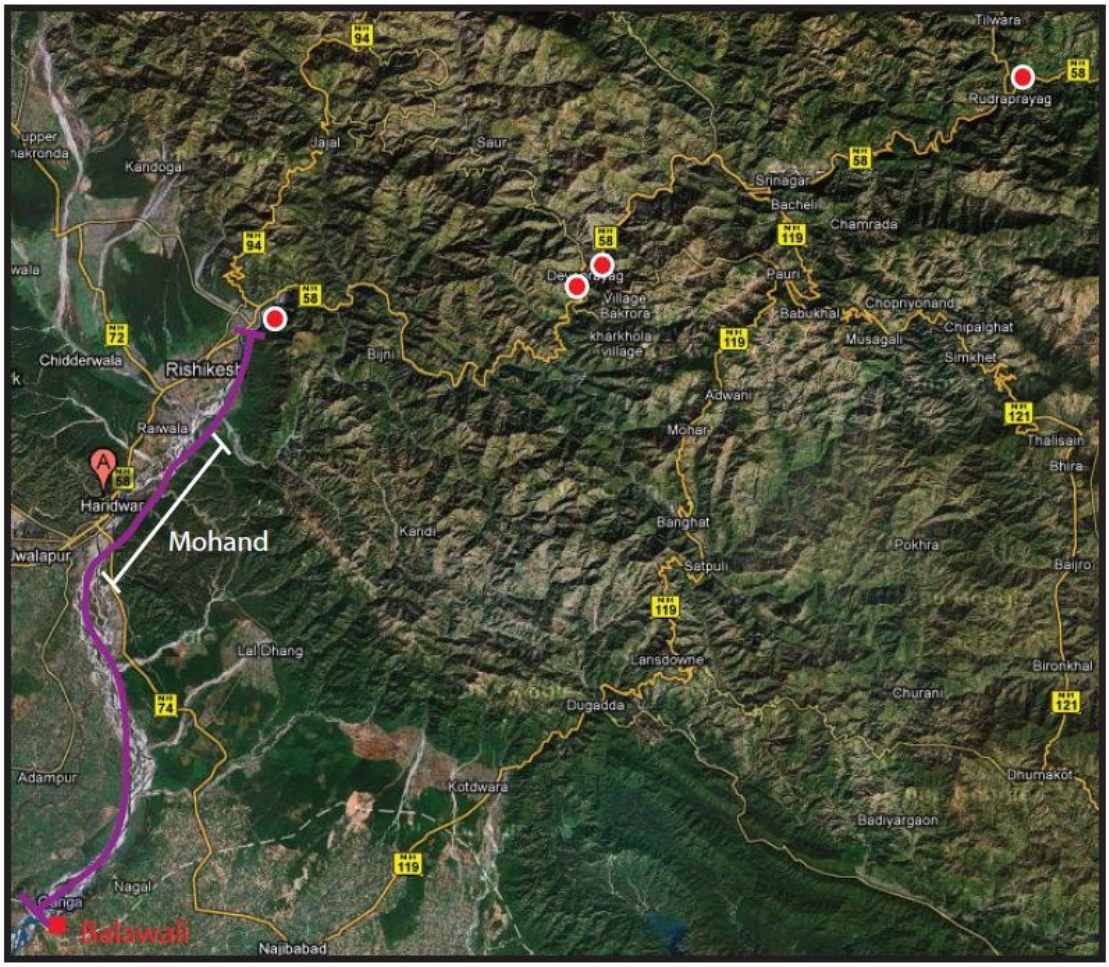

Fig 2.8a. A map showing the route of the Ganges as it flows out of the Lesser Himalayan mountain front at Rishikesh, down to the furthest downstream point of the study reach at Balawali (purple line). The white outlined red dots indicate the location of gauging stations, from right to left: Rudraprayag, Devaprayag – Alaknanda, Ganges, and finally Rishikesh. The gauge at Rishikesh is the upstream point of the study reach. Haridwar (A) is located in the Mohand, with the Mohand reach (15 km long) indicated by the white scale bar.

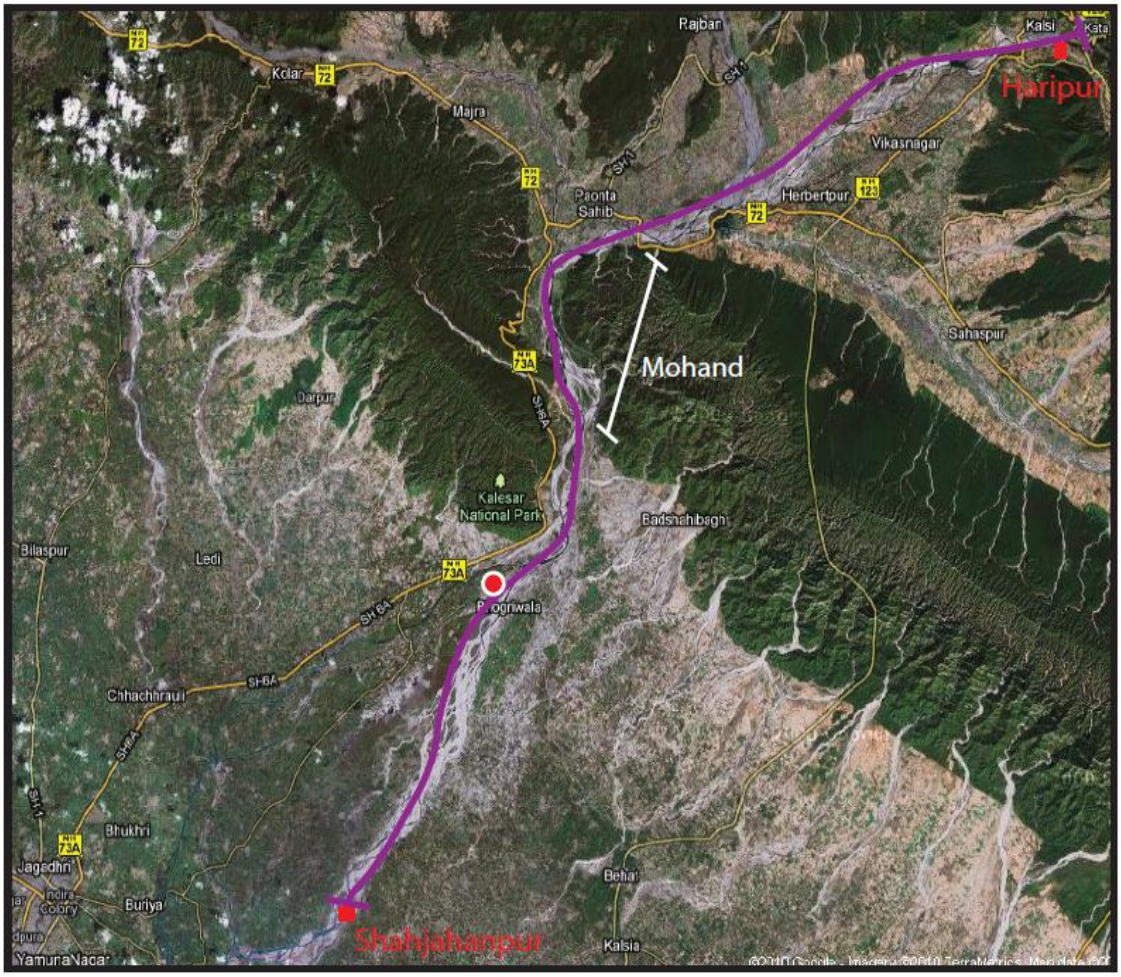

Fig 2.8b. A map showing the route of the Yamuna as it flows out of the Lesser Himalayan mountain front at Haripur, down to the furthest downstream point of the study reach at Shahjahanpur (purple line). The white outlined red dot indicates the location the gauging station at Tajiwala. The Mohand reach (12 km long) is indicated by the white scale bar.

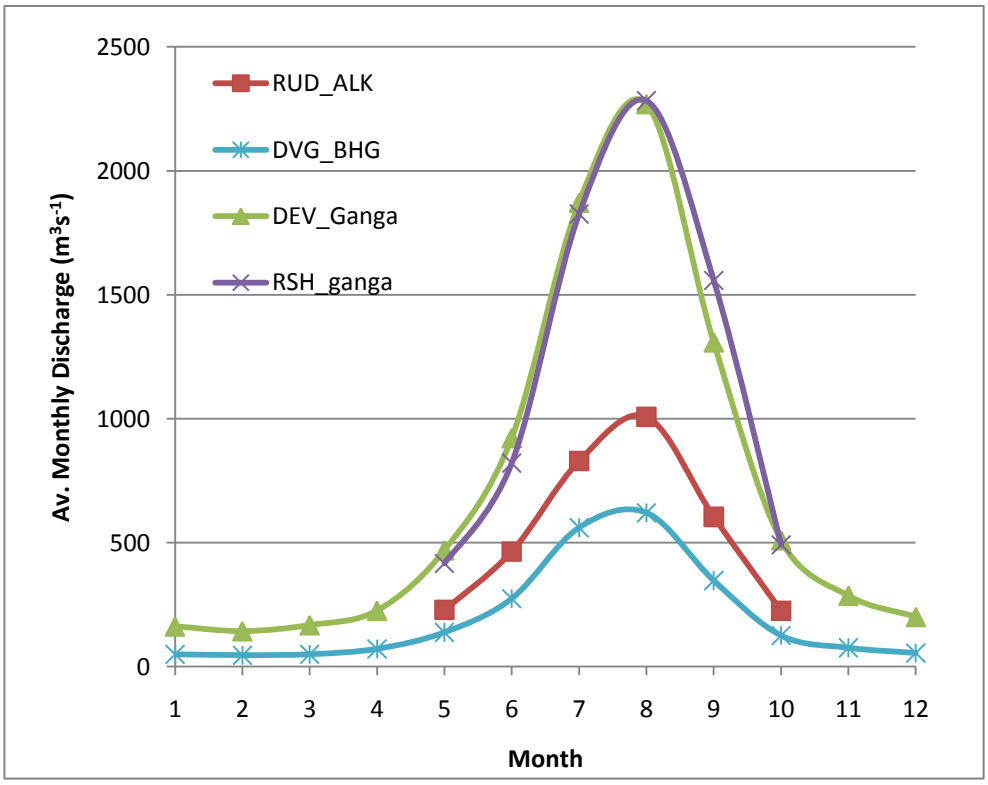

Fig 2.9a. A graph illustrating the average monthly discharge measured along the Ganges at 4 different gauging stations; Rudraprayag (Alaknanda), Devaprayag (Bhagirathi), Devaprayag (Ganges), and Rishikesh (Ganges).

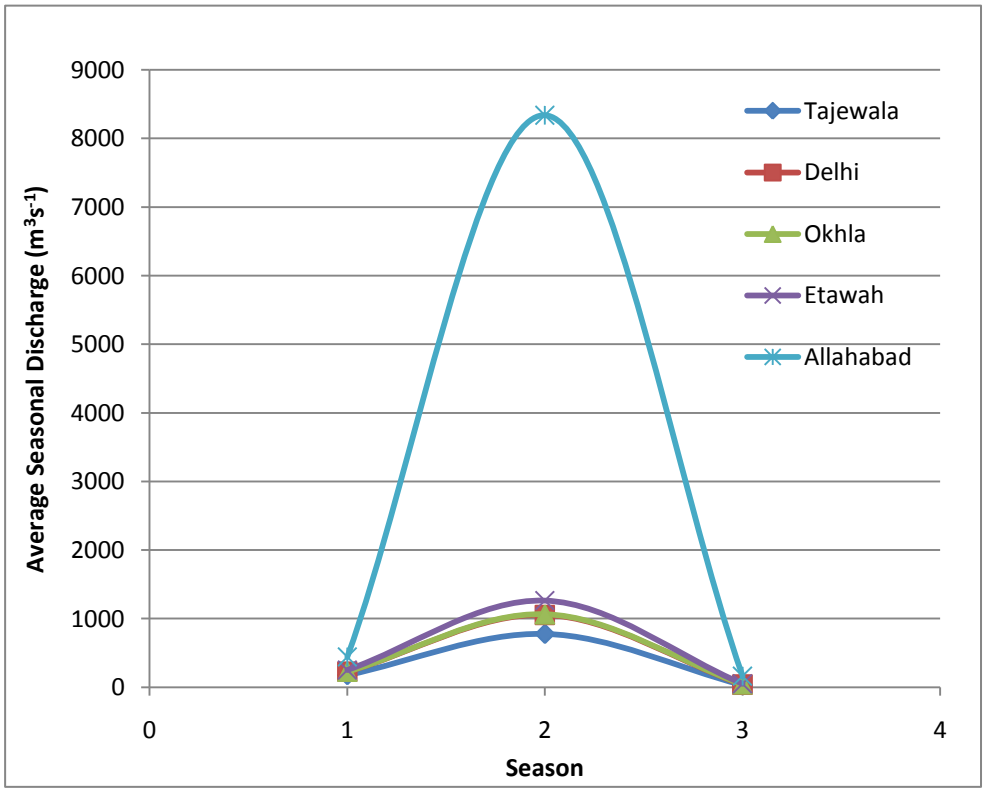

Fig.2.9b. A graph illustrating the average seasonal discharge measured along the Yamuna at 5 different gauging stations. Season axis (1 represents summer discharge March-May, 2 monsoon discharge Jun-Sept, and 3 winter discharge Oct-Feb). The legend identifies the name of the town where the gauging stations are located. Data from Jha *et al*. (1988).

Hydrological and sediment transport characteristics are two main fluvial parameters affecting the aggradation and degradation behaviour of the Ganges and Yamuna river systems. Sinha (2005) found that stream power in the dominantly degradational rivers in the Western Gangetic Plain (WGP) was significantly higher than that in the dominantly aggradational rivers in the Eastern Gangetic Plain (EGP), at ~ 40-43 W/m^2 and ~ 6-20 W/m^2, respectively. Thus, large-scale patterns of incision or aggradation appear to be linked to spatial variations in stream power. The Gangetic rivers erode a large volume of sediment from the upstream Himalayan region, depositing a part of this in the alluvial Indo-Gangetic plain, but routing ~90% of the annual sediment flux into the Bay of Bengal (Jain and Sinha, 2003). The Ganges and Yamuna are both degradational rivers incising into the foreland basin sediments of the Indo-Gangetic Plain. Recent work by Wasson (2003) showed that the Ganges erodes ~794 million tonnes of sediment per year (measured at Farakka close to the India-Bangladesh border), with ~65 million tonnes being deposited on the alluvial plains. It has been noted that the Ganges average sediment load (Mt/yr) measured at Haridwar in the Mohand anticline is 14 Mt/yr, and a sediment yield of $0.15x10^3$ $t/yr/km^2$ (Jain and Sinha, 2003). The sediment load for the Yamuna is however, uncertain, as it is not clear where the measurement is made. The literature states that the average sediment load is 125 Mt/yr, with a sediment yield of $0.34x10^3$ $t/yr/km^2$ (Jain and Sinha, 2003). The study of Sr and Nd isotopes by Singh *et al*. (2008) suggested that >65% of the sediments in the Ganges are derived from Higher Himalaya Crystalline rocks. Wasson (2003) delegates 20 ± 10 % of the 794 million tonnes to a Lesser Himalayan source, and < 10% to Siwalik source. The erosion of the Siwaliks across the HFT results in the fault being weakly expressed in the landscape, requiring the use of river morphology to detect recent uplift.

The Ganges and Yamuna rivers thus have similar geomorphology between the Lesser Himalaya and the Indo-Gangetic Plain. They both undergo a transition from a tightly constrained bedrock channel, bounded by steep topography changes in the Lesser Himalaya, to wide, braided, low gradient alluvial channels in the Dehra Dun Basin and Indo-Gangetic Plain.

Braided channels tend to form where stream energy is high, the channel gradient is steep, sediment supply from hill slopes, tributaries, or glaciers is high and a large amount of coarse material is transported as bed load, and bank material is erodible, allowing the channel to shift laterally fairly effortlessly (Huggett 2003). Both river systems are extremely braided. The braided channels are essentially depositional forms that occur where the flow divides into a series of braids separated by islands or bars of accumulated sediment. The islands support vegetation and can remain stable in the system for a long period of time whilst bars are more impermanent. In this case, the islands and bars are formed during the monsoon flow as a large discharge is required to move the high sediment supply from the Lesser Himalaya. Once bars form in the braided rivers they are rapidly colonised by vegetation and therefore stabilizing the bar sediments and forming islands. However, counteracting the stabilization process is a highly variable stream discharge, which encourages alternate phases of degradation and aggradation in the channel and militates against vegetation establishment Fig (2.9a)

Summarising Points

The important points to draw on from this chapter are: the geological setting of the Dehradun Basin, the Siwaliks and the Mohand anticline setting, the fact that both rivers have similar geomorphology and hydrological characteristics as they flow through the Dehradun basin and Mohand anticline. And finally, the presence of anthropogenic structures along both rivers explained in the introduction is extremely important when relating the possible effects on the natural discharge and sediment transport system. The combination of these highlighted points is critical to the investigation of tectonic imprint on the rivers, and using the rivers to highlight tectonic uplift. The next chapter will build upon these points and describe the methodology adopted for the research.

3. Methodology

This chapter will describe the remote sensing techniques used to collect the width of channel belt, channel slope, and geomorphology data. It will also describe the field work methods used to collect the grain size data and the method of calculating stream power. There were limitations with some of the methods adopted, and there is a section at the end of this chapter that notes them.

Geomorphology and remote sensing methods

As the study region is located in a large, remote area, it can be extremely difficult to collect a detailed data set from local sources, therefore, by using remotely sensed data, a dataset for a large area can be relatively easily collected. There are three main sources of remotely sensed data (Table 3.1), which are; Shuttle Radar Topography Mission (SRTM) data in the form of a Digital Elevation Model (DEM), Satellite image data in the form of Indian Remote Sensing images (IRS), and Topographical Survey Maps. There are two main pieces of software used to manipulate these forms of data which are ArcGIS and RiverTools.

Type of Data	Resolution of Data	Type of Data	Year Data Published
SRTM	90 m	Type 2	2000
IRS	23.5 m	LISS III	2004
Topographical Maps	1:50'000 m	First Edition	1965-87

Table 3.1. The table identifies the 3 types of data used, their resolution, source, and age.

The Data:

Shuttle Radar Topography Mission (SRTM):

SRTM data were used in the form of Digital Elevation Model (DEM) data as described by Javis *et al*. (2006) (Fig 3.1 – which shows a clipped DEM section from a larger DEM that covered the whole NW Himalaya region). The data were used to represent the topography of the study region with 90 m resolution. Standard hydrological analysis techniques in ArcGIS were used to generate a data set for the two river basins. Flow accumulation tools were used to find the centre line of both the Ganges and the Yamuna, along with the catchment areas of both networks. These products were then used to identify the reaches and channels to be measured (width of channel belt and braiding).

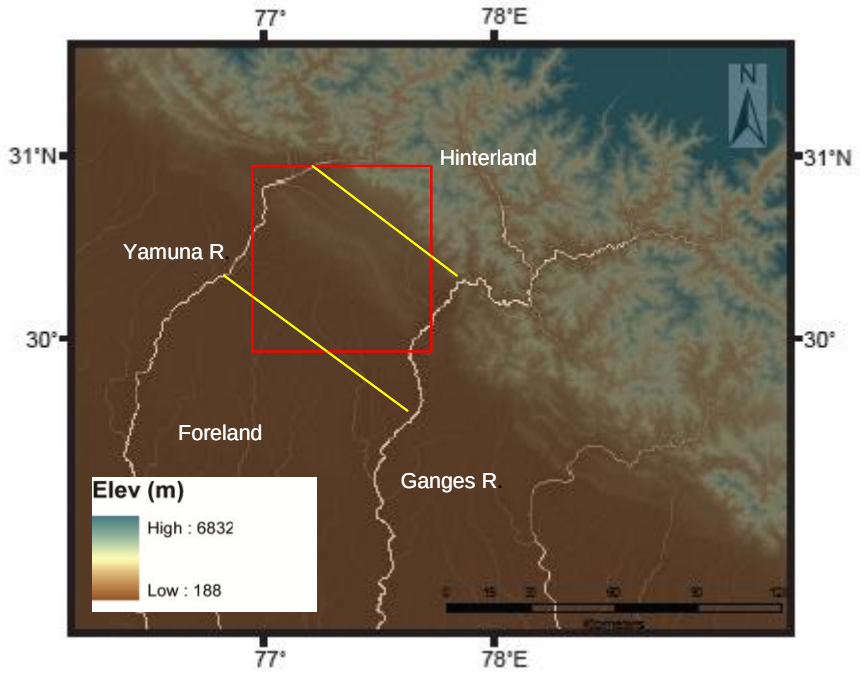

Fig 3.1. Clipped DEM coverage of Dehra Dun Basin and Mohand (red box), Ganges and Yamuna rivers, Hinterland, and Foreland (brown indicating lower lying elevation, rising to white then blue representing the highest elevation. The white lines represent drainage networks in the study region, the yellow lines represent the upstream and downstream ends of the studied river reaches.

RiverTools:

The DEM was imported from ArcGIS into the software RiverTools and manipulated to extract a more clearly illustrated data set for the Ganges and Yamuna river basins, illustrated in Fig 3.2. By using these river basins, specific reaches could be selected and an upstream data output point defined. The MBT was selected as the upstream point for data extraction, as this study was primarily concerned with the river morphology downstream from this point. By defining the upstream and downstream x and y co-ordinates of the desired reaches, RiverTools was used to extract the elevation and cumulative drainage area for every pixel in the defined river reaches. This data was used to analyse the longitudinal river profiles and calculate slope, as well as calculate stream power. Fig 3.2 also helps illustrate the difference in catchment area between the two rivers.

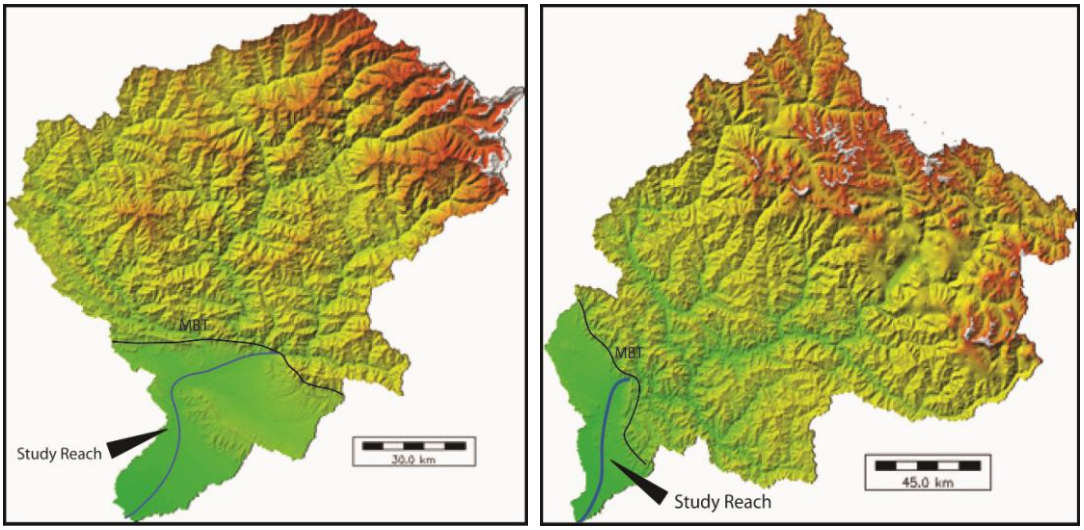

Fig 3.2: Ganges (right) and Yamuna (left) river basins. The basins above have been extracted using RiverTools and were used to extract river profiles and basin drainage areas from the MBT outlet points. The blue line indicates the rivers and the Study reaches have been identified. The black line shows the approximate position of the MBT for reference.

Topographical Maps:

Scanned topographical maps were provided by Vikrant Jain (Delhi University) and Rajiv Sinha (IIT Kanpur). These maps were 1:50,000 scale and covered the quadrants 53F, 53G, 53J, and 53F. They were surveyed and produced in 1987. The topographical maps were georeferenced in order to match contours to the DEM. The contours were used to infer channel slope information, and were used along with the DEM to aid in the analysis of channel slope and elevation.

Satellite Imagery:

Satellite imagery covering the study area consisted of two images from the Indian Remote Sensing (IRS) satellite IRS-P6 (Resourcesat-1) (Fig 3.3). The image is a digitally processed IRS P6 WiFS image with 4 bands: red (520-590 nm), green (620-680 nm), near infrared (770-860 nm) and shortwave infrared (1550-1700 nm). The pixel size of the imagery is 23.5 m.

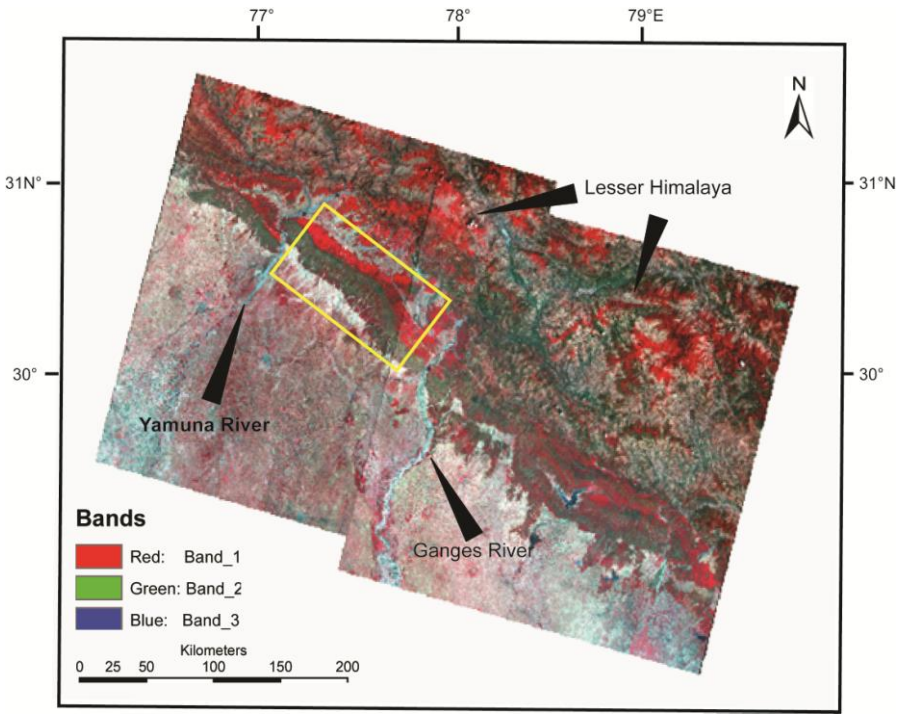

Fig 3.3. IRS images of Dehra Dun and Mohand Region (yellow box), North West India. The legend indicates the 3 bands of colour within the image.

The images (Fig 3.3) were overlaid on the DEM so that the width of channel belt and braiding could be measured by using the colour change between land and water (red/green) to define the river banks. All data were projected to the UTM coordinate system, zones 43 and 44, using the WGS84 datum.

Channel Morphology:

The topographical maps and DEM were used to collate a data set for channel slope, width of channel belt, and channel geomorphology. The methods are identified below.

Longitudinal River Profile and Channel Slope:

The channel slope for the Ganges and Yamuna reaches were calculated using both the SRTM data and the topographical maps. Working in ArcGIS, the contour tool in (under Data Management – Raster) was selected and the contours were generated every 5 m. These contours were compared with those on the scanned topographic maps, which had a spacing of 20 m. As another comparison, which proved to be a more accurate and efficient way of extracting data from the DEM, RiverTools was used to extract the river long profiles on each river, providing elevation data for each pixel in the reach. The topographical maps were difficult to follow as the scale was too small to count small lines of the contours, therefore the DEM became the primary source of channel elevation data. A new point shapefile was created to mark the intersection of the river with the DEM-derived contours. For both the SRTM and the topographical maps, the contours were measured at the point they crossed the river channel and the distance between each contour downstream was recorded. This was then plotted as

two graphs, one showing the long river profile, the second showing the local channel slope, calculated by the equation:

$$S = \frac{\Delta H}{\Delta L} \quad (1)$$

Where ΔH and ΔL are height differences and channel length between the two successive contour crossings, respectively. ArcGIS methods produced unsatisfactory preliminary results for the longitudinal river profiles and channel slope data, because measurement of the elevation and channel slope was done by hand. Elevation measurements were also made difficult by the presence of sinks and pits in the DEM. This limitation was overcome by removing the sinks and pits by smoothing the DEM in RiverTools. This method provided elevation data for every pixel in the ~80 km defined study reach for each river (Fig 3.2), which was used to plot a more accurate longitudinal river profile and a more accurate calculation of channel slope over 2 km downstream intervals. The interval of 2 km was selected as the interval to give an acceptable spatial distribution of data for slope calculation. By using 2 km, there are enough points to calculate and indentify any substantial changes in the downstream channel slope relationship, and reduce uncertainty from the DEM accuracy that a smaller interval might have included e.g. a compromise was made so that minute changes or no change in elevation over 90-100 m wasn't picked up. 2 km accommodated elevation change for a good channel slope calculation. The interval spacing was kept at 2 km in order to generate estimates of stream power, at a consistent spacing. Due to the smoothing of the data and the fact that there is some variation in the accuracy of elevation between pixels, as 1 pixel represents 86 m^2, some inaccuracies in slope are derived, which can be accepted as noise.

Width of Channel Belt:

Using ArcGIS v9.2, a point shapefile was created and points were added at intervals of 500 m downstream along both river reaches. This process was started at the MBT and continued downstream to the lower end of the study reaches. The river trace in map view was defined by the flow accumulation tool on the DEM (Fig 3.1), which did not consequently match to the IRS map of the river channel There was some displacement between the two sources, however, the DEM was taken to be the middle of the channel belt as the DEM would be used for the other parameter measurements. At each of the points the width of channel belt was measured from the IRS satellite imagery. The width of channel belt was defined as the entire channel including inactive channels due to low river levels. The boundary for the entire channel was marked by the change from water (blue) to vegetation (green and red, Fig 3.3). The width was measured using the measure tool on the ArcGIS tool bar. Width of channel belt (m) measurements were then plotted against distance (m) downstream.

Channel Braid Index:

The braiding index used by Chew and Ashmore (2001) was adopted to record the degree of channel braiding in the Ganges and Yamuna rivers. This method works by counting the number

of wet channels in a given cross section. Here, we used the same shapefiles used to calculate width of channel belt to demark the location of a cross section measurement on the IRS-P6 WiFS image. The braiding index was calculated at 500 m intervals downstream and the river boundaries were defined by transition from river (blue) to vegetation (green/red) on the downstream right to left banks. 500 m was chosen as the interval for measurement for both the width of channel belt and braid index to collect a satisfactory amount of data to indentify a more consistent and accurate portrayal of the river morphology. 500 m was again a compromise between time and amount of data collected, while giving a good representation of the channel morphology changes. For example, the index yields a value of 1 for a single channel, 2 for two channels and 3 for three channels. This process then clearly identified the braiding/anastomosing trend and how the systems were increasing or decreasing in intensity as the rivers progressed downstream from the MBT (Fig 3.4). The figure below, for the purpose of explanation, has the river channels traced in red, so for every yellow line, the number of red channels intersecting it were counted.

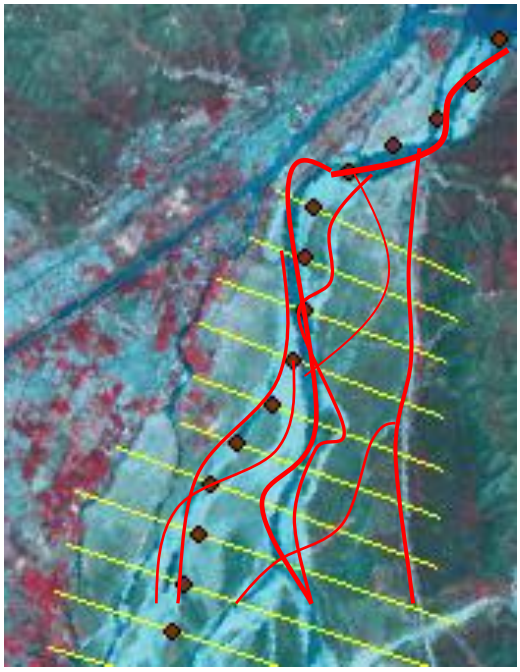

Fig 3.4: Visual description of the braiding index method. The image above has been cropped from the IRS image. The yellow lines show the width of the channel over which braids were counted. This was a crude method of counting how many channels of water (blue) crossed any one yellow line. The brown dots identify the points where width of channel belt was measured and therefore it to be consistent with channel counting, the same points of measurement were used.

Fieldwork:

Fieldwork was needed to compile a data set for grain size in the study area. The grain size distribution reflects stream power and stream power is a function of channel slope, which is affected by uplift. Therefore, the grain size distribution can be used to identify river response to tectonic activity. This subsection will explain the method used for data collection and will explain how the data were processed.

Grain size data collection:

Grain size data was needed to understand the depositional processes of the rivers and relate those patterns seen to the other hydrological variables in the study. Grain size data is extremely important to help identify river response of channel slope to tectonic uplift (Fig 1.1). The study region of both the Ganges and the Yamuna rivers covered a reach of approximately 80 km on the eastern and western boundaries of the Dun valley. Over these 80 km, potential sites for sampling were identified by using both topographical maps and Google Earth. Potential sites were provisionally selected approximately every 5 km from the river outlets at the MBT to the downstream study reach limits approximately 40 km into the foreland. However, it was quickly realised that intervals on this scale weren't going to be possible, and therefore the focus shifted to places with suitable access to the river channel. Google Earth was used to identify potential transect sites, as the topographical maps that were available were of poor resolution and much older (1985) than the higher resolution Google satellite images, and therefore didn't show recent infrastructure. The main problem with access was that the bars ideal for sampling were often on the opposing river bank to the access, and the active channels were frequently too large to cross. Grain sizes (*b*-axis) were measured and sampled by using a photography technique at 15 sampling sites along each river (Table 3.2 and 3.3).

Transect	UTM_x_WGS84_43N	UTM_y_WGS84 43N
1	0775511	3379324
2	0772474	3378998
3	0766760	3377295
4	0763498	3374996
5	0760395	3372462
6	0756496	3371206
7	0747623	3367468
8	0747566	3365888
9	0749359	3360562
10	0749036	3357913
11	0749038	3357913
12	0747359	3354766
13	0737970	3340274
14	07322835	3336816
15	0726586	3328696

Table 3.2. The data above indicates the position of each of the 15 transects taken along the Yamuna River. The data is in the coordinate system WGS84 Zone 43N. Table corresponds to Fig 3.5b.

Transect	UTM_x_WGS84 44N	UTM_y_WGS84 44N
1	0226616	3315699
2	0226229	3310804
3	0226703	3306245
4	0227231	3304397
5	0226803	3303591
6	0241427	3335507
7	0240678	3334267
8	0237872	3328720
9	0238031	3328636
10	0232922	3323930
11	0230630	3321216
12	0227623	3298869
13	0228381	0228381
14	0227887	0227887
15	0219840	0219840

Table 3.3. The data above indicates the position of each of the 15 transects taken along the Ganges River. The data is in the coordinate system WGS84 Zone 44N. Table corresponds to Fig 3.5b.

Grain size data were collected with a photosieving method modified from Carbonneau *et al*. (2004). Photosieving dramatically reduces the time in the field by replacing labour intensive field measurements with rapid image acquisition. Therefore the higher volumes of data that can be gathered offset the errors associated with photosieving. A Canon IXUS50 5.0 megapixel digital camera was used to capture the images. The camera was mounted onto a monopod at a height of 1.5 m to keep the scale of each photo constant (Fig 3.5a). In order to quantify this scale, a 400 mm ruler was photographed in the first image of each series. In certain cases, it was found that the bed material was so coarse that the fixed camera height was too low to capture a significant number of clasts. In such cases, the monopod height was increased to 1.7 m and another photograph of the scale ruler was acquired. When a sample site had been located, the primary method used to collect data was by photographing along transects across the river channel orientated perpendicular to the flow direction. This was repeated at a series of distances along the length of either reach. Because the transect sites were located near to access points along the river, their spatial distribution of them was not uniform. The transects were composed of ~31 photos at 10 m intervals in a zigzag type walk so that the true grain size distribution could be recorded (Fig 3.5a). As one person walked along taking the photos, another recorded the position of the images with a Garmin GPSmap 60CSx hand held GPS. The GPS was also used to record the start and end points of each transect, with an absolute positional accuracy ranging from +/- 3 – 5 m. The GPS was pre-programmed to record waypoints every 10 metres so that at a later date, the transect path could be added as a layer in

ArcGIS. Images from Google Earth were georeferenced and the tracks from the GPS downloaded and displayed on the images to visualise the spatial coverage of the transects (Fig 3.5b and 3.5c.)

Additional transects were taken in key areas, for example, 1-2 km upstream and downstream of any significant blockade or dam, to help resolve any external influence on downstream fining.

When particles were larger than 400 mm, or in the case of submerged gravels, imagery was ineffective as a grain size measurement method. Therefore a secondary method of recording grain size data was adopted by measuring grain *b*-axes at 2 m intervals over a transect distance of 200 m. This method involved laying out a 15 m tape measure, and at every 2 metres, the grain that was directly below the tape was measured. The measurement was taken of the axis perpendicular to the longest axis, this is the *b*-axis (Fig 3.6). This method was only used for one transect out of the 30 taken across the two rivers, located at Rishikesh (see Fig 3.5b).

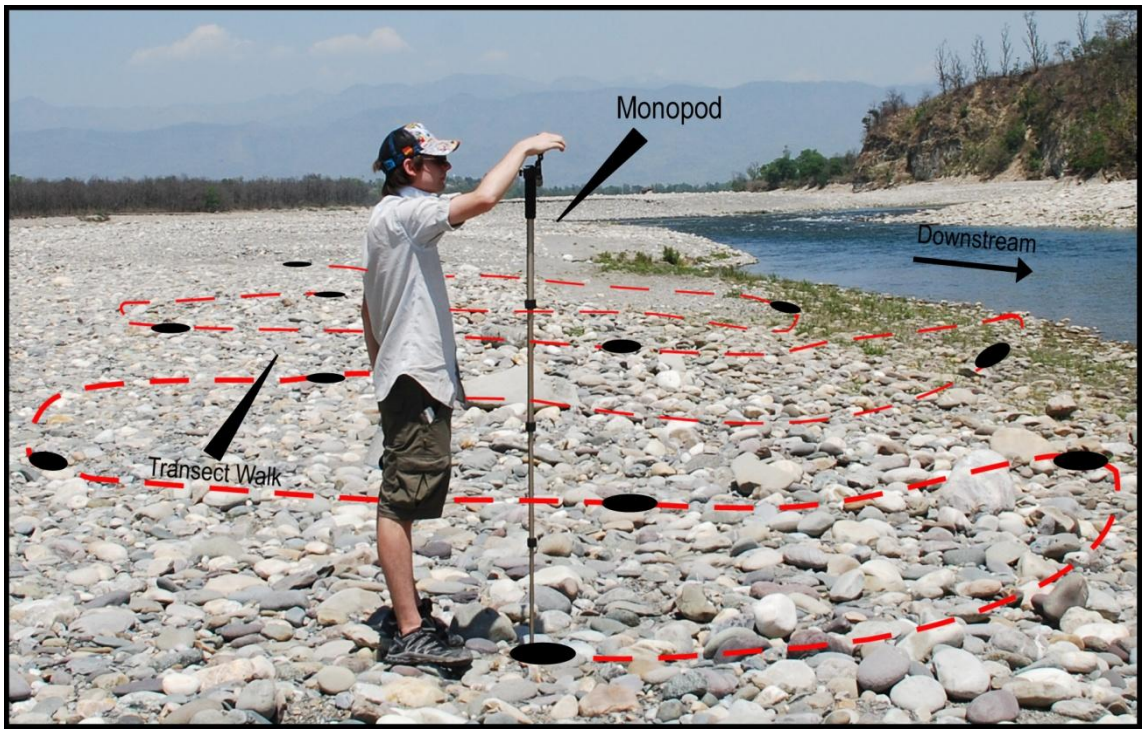

Fig 3.5a. Grain size data collection adopted from (Carbonneau *et al*. 2004). The monopod has the camera mounted on to it, the camera lens at 90 degrees to the ground. The red dashed line indicates the path taken, with the picture looking upstream. The black ellipses illustrate an example of points where photographs were taken. The Monopod can be used for scale with its length of 1700 mm.

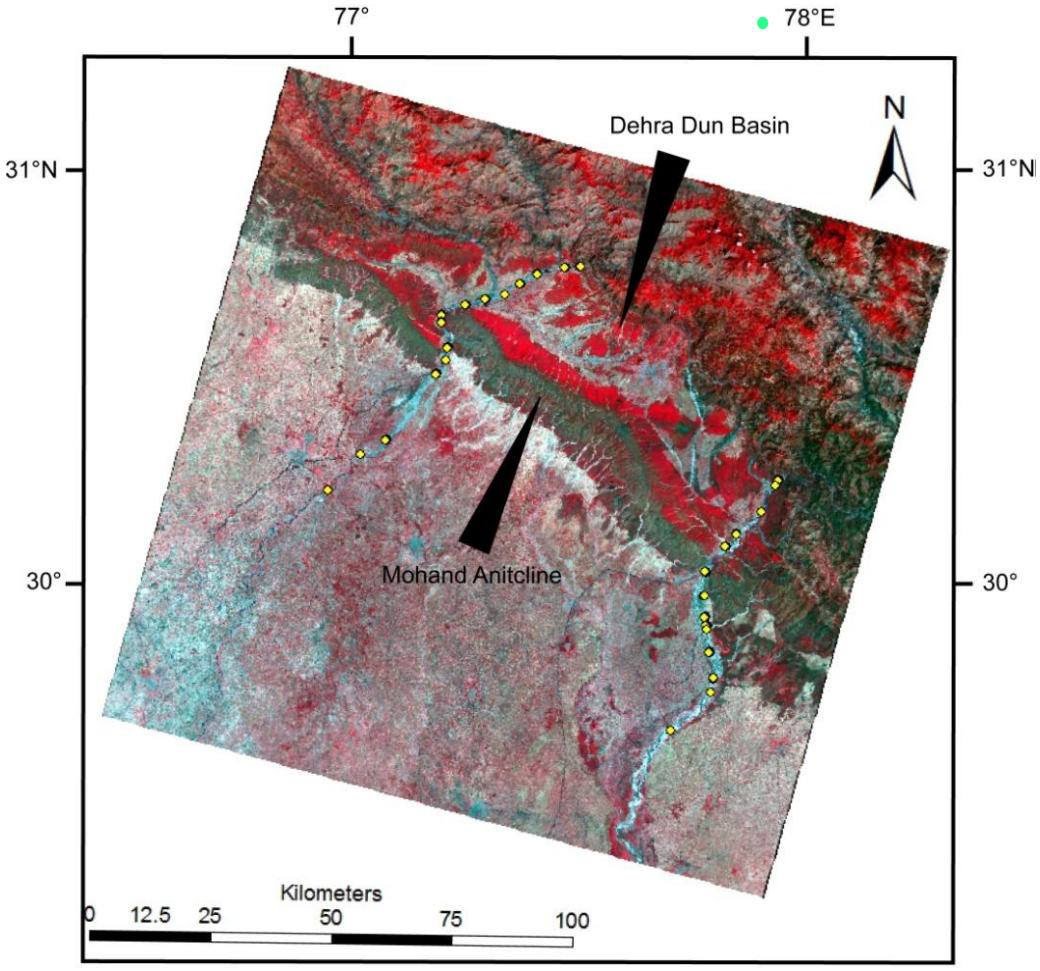

Fig 3.5b. Locations of grain size transects. The transects taken in the study area are marked using yellow dots. The Ganges river and transects in the east and the Yamuna river and transects in the west. The Dehra Dun Basin and Mohand Anticline are identified and the town of Rishikesh is marked by a green dot.

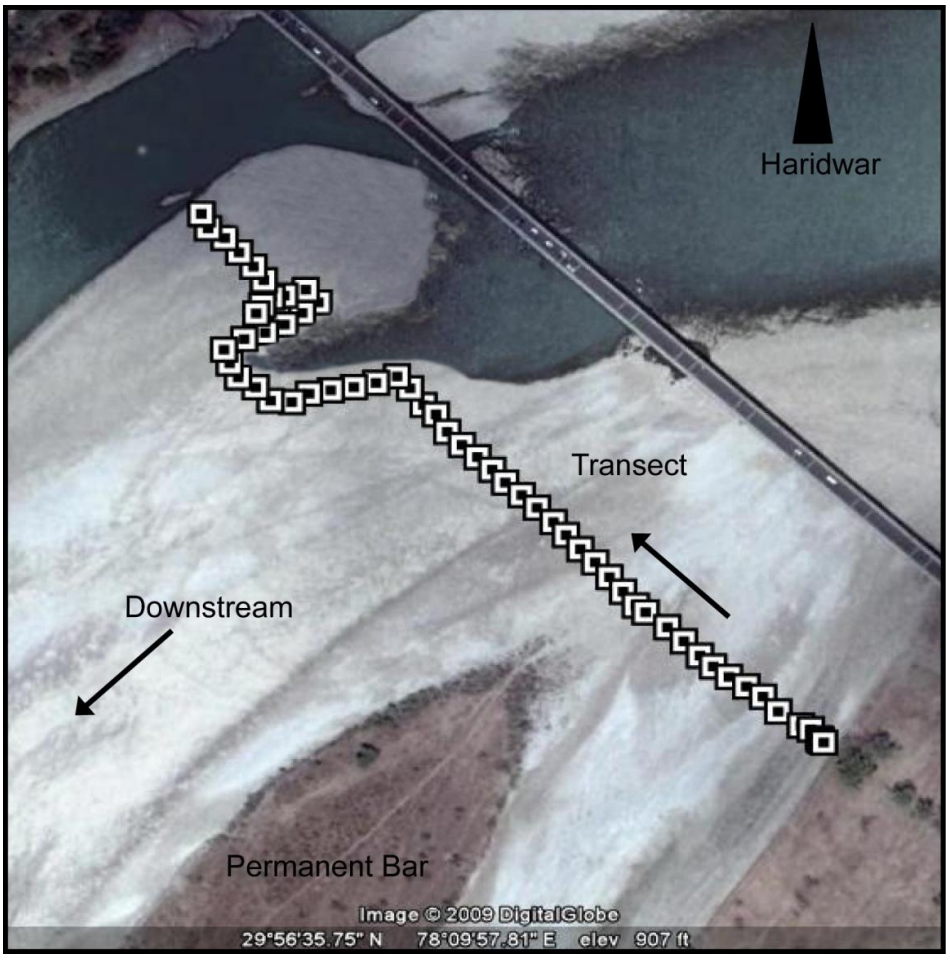

Fig 3.5c. An example of a transect path; the image illustrates the path of a transect taken ~1.5 km south of the Haridwar Dam. The arrow below the label transect indicates the direction the photographs were taken. The white outlined squares indicate the position of each photo taken with a GPS point recorded. Water flow is to the bottom left as indicated, with a stable vegetated bar shown. The river bank is seen in the bottom right and top left of the image. The image was taken from Google Earth. Transect in image is approximately 200 m long

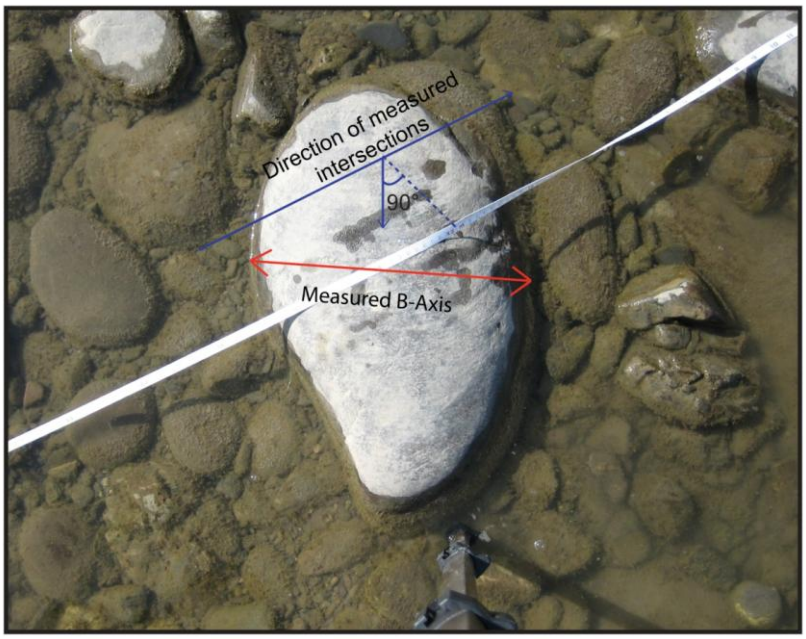

Fig. 3.6. Secondary method of grain size collection. The tape measure extends from left to right, representing the path taken between subsequent measured grains. The tape measure is held tight, so that the grain that is located perpendicular to the tape can be identified. The grain is then measured across its *b*-axis, the axis perpendicular to the longest axis. A minimum of 100 grains were recorded with this method.

Analysis Methods:

Matlab code for photosieving was used to process the grain size photos obtained in the field, adapted from the method used by Carbonneau *et al*. (2004). Grain sizes for the close range images were determined with a graphic user interface (GUI) programmed in the Matlab environment. A 7 X 8 grid was superimposed over the images, and the user manually identified the *b* axis of grains lying on the 56 grid intersections. The program then calculated D16, D50, and D84 for the image as well as returning the full distribution of measurements. A value of 0 mm was assigned to sand surfaces (Fig 3.7).

Paths are then set to the directory containing the photos, which are processed sequentially. The first photo of each transect had the image scale included in the form of a rule. This was 400 mm long of which this value was set before the analysis began. Once done, each grain that was manually indentified was measured. The *b*-axis was measured by clicking on either end of the axis and then a red circle appeared to mark the grain as measured, then the next grain would proceed to be measured. Approximately 31 photos in each transect, and 15 transects for each of the Ganges and Yamuna Rivers. The processing method relies on the assumption that the *a*-and-*b* axes are in the horizontal plane, so that what is actually being measured is close to the true *b*-axis. Graham *et al*. (2005b) termed the error arising from this assumption 'fabric error', This type of error assumed by Graham *et al*. (2005b) is consistent with my findings, that a photograph in two-dimensions cannot take into account the three-dimensional nature of a sediment surface. These associated fabric errors are widely recognised in the literature but do not appear to be large (~1ψ) (Adams, 1979; Butler *et al*., 2001; Sime and Ferguson, 2003).

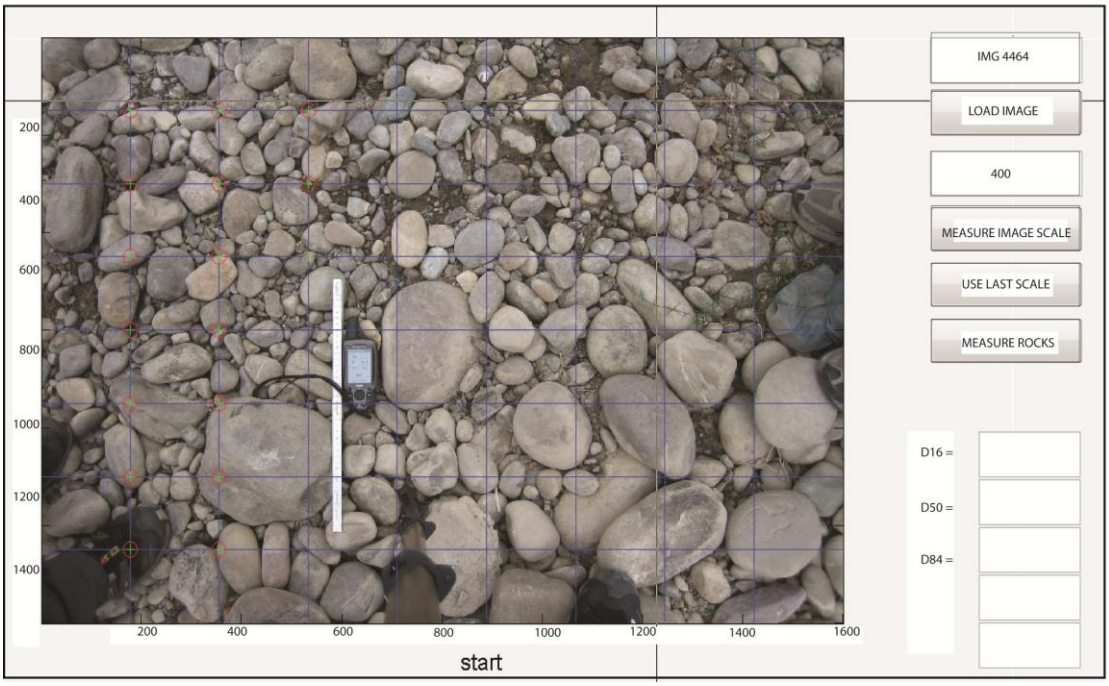

Fig 3.7. Screenshot from the Matlab photosieving program used to calculate grain size. The blue grids providing the cross hairs of which grains lying perpendicular to were measured, much in the same way as illustrated in Fig 3.6. The scale is recorded in this image as it is the first photo of a transect. At each intersection point on the grid, the apparent b-axis of the subjacent grain was measured.

Once each transect had been processed, the percentiles D16, D50, and D84 were extracted to be correlated with the other river characteristics.

Once all of the photos had been analysed, the data for each river were reshaped into a single matrix with 15 columns to hold the data for all 15 transects. The largest transect on the Ganges had 46 photos, and therefore the largest column had 2622 rows (46X57). This was set as the default number of rows for this file, filling in the empty cells on other transects with 'NaN' so that graphs could easily be created. This process was repeated for the Yamuna so that just two files held the entire grain size data set. These two files, named 'all_data_g 'and 'all_data_y' for the Ganges and Yamuna respectively, were then exported to Microsoft Excel to be further manipulated.

The grain size data were then correlated with the previous morphology data collected earlier in the project: elevation, slope, width, braiding, stream power and unit stream power.

Stream Power:

Stream power is an essential hydraulic variable to understand in this study as it is a function of the variable channel slope. When channel slope is altered by tectonic uplift, a change in stream power is induced. Therefore, by calculating stream power, it can be directly compared with channel slope changes and width of channel belt to identify reaches of rivers responding to active slip on the HFT. Stream power is extremely important to the study because it provides information regarding the potential of a river to move sediment. Because stream power is a

function of channel slope, any induced change in slope from tectonic uplift can have a direct affect on stream power, and therefore an influence on the rivers ability to transport sediment. The relationship between stream power and channel slope is therefore important when identifying and explaining and patterns in grain size distribution that may be seen. With higher stream power there is more energy in the system available to move larger grains, a lower stream power would mean less energy to move larger grains. Stream power (W m^{-1}) is commonly defined as:

$$\Omega = \gamma . Q . s \quad (2)$$

Where γ = specific weight of water (= 9800 N/m^3), Q = water discharge (m^3 s^{-1}), and s = slope (m/m).

Stream power is thus dependant on two variables, discharge and slope. Because discharge data are only available for a few sites in the study area (Chapter 2, p. 18), a continuous distribution of discharge (Q) must be established on the basis of discharge-area relationships for the given study area. Discharge for the Yamuna was assumed to be uniform, using a value from Jha *et al*. (1988) as gauge data on the Yamuna were not available. This is clearly an oversimplification, but represents the best possible option with extant published data. The value however, is not valid, and therefore the variability of discharge and stream power throughout the Yamuna is extremely poor. By only having access to one, dated, gauge reading, a power law could not be fitted and any figures calculated for the Yamuna would be taken lightly. For the Ganges, water discharge can be represented as a power law function of drainage area:

$$Q = a . A^b \quad (3)$$

Where A is the contributing catchment area in kilometres squared and a and b are empirical coefficients.

The coefficients in equation (3) can be evaluated by using the discharge data from Chapter 2 (p. 14). Discharge data were available from 4 gauging stations upstream of Rishikesh on the Ganges. Drainage area was derived from the DEM data using RiverTools. Fig 3.8 is the product of the data presented in Table 3.3. Notice all four gauges are upstream of the study region, and therefore no accurate stream power variability can be calculated throughout the study reaches (Fig 2.8a And Fig 2.8b).

Location	A_d (km^2)	Q ($m^3 s^{-1}$)
Rudraprayag (Alaknanda)	1647.991	287
Devaprayag (Alaknanda)	10141.81	1008
Devaprayag (Ganges)	10919.77	2269
Rishikesh (Ganges)	21467.67	2283

Table 3.4. Hydrological data used to calculate a continuous relationship between water discharge and drainage area using equation (3). Q = highest value of monthly discharge observed in an average year (m^3s^{-1}), A_d = drainage area (km^2). The data are from the period 1985 to 1997 and were provided by Prof Rajiv Sinha, IIT Kanpur.

A value for the highest monthly discharge observed in an average year was used in the calculation of stream power because it is widely known in river dynamics that the highest and largest sediment load is transported during the period of highest flow. Therefore by using peak monthly discharge, a value of peak stream power can be calculated and used to explain grain size trends observed throughout the reaches during the monsoon season.

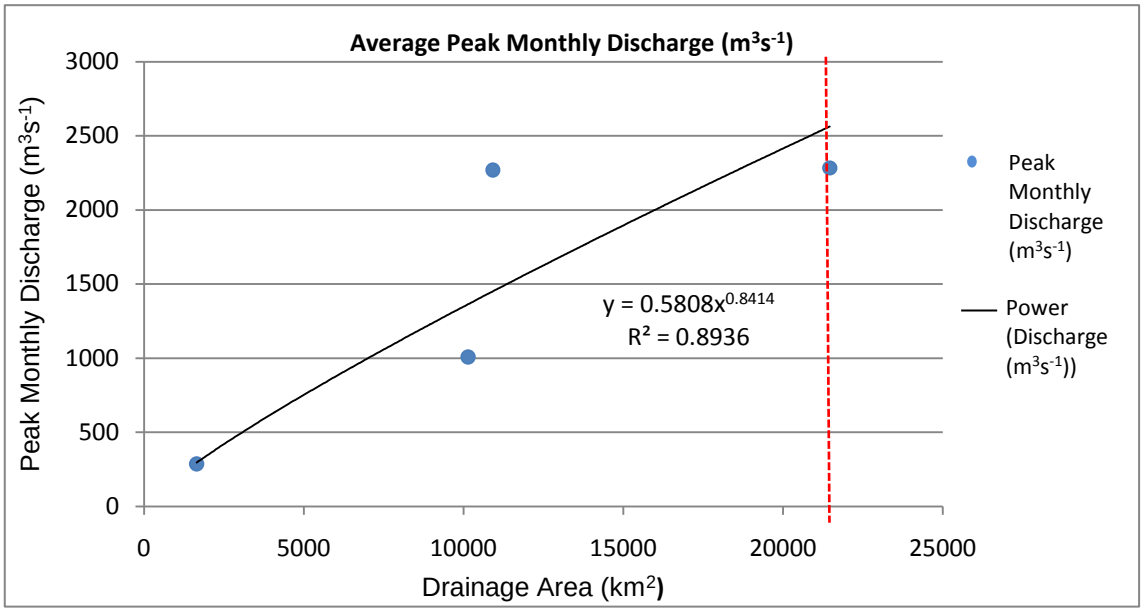

Fig 3.8. Ganges power law relationship between peak monthly discharge (m^3s^{-1}) and drainage area (km^2). The data were obtained from four gauging stations along the Ganges River (table 3.3). Each gauge is identified by a blue circle. From left to right with increasing discharge and drainage area, the gauges are from Rudraprayag (Alaknanda), Devaprayag (Alaknanda), Devaprayag (Ganges), and Rishikesh (Ganges) (see Fig 2.8a and 2.8b) – The upstream limit of the study reach is identified by the red dashed line, with the study reach being to the right of the line.

Once stream power was calculated using equations (2) and (3), stream power per unit area could be estimated along the study reach. Stream power per unit area was defined as:

$$w = (\gamma.(a.A^b).s)/W \quad (4)$$

Where W is the width of channel belt, γ = specific weight of water (= 9800 N/m^3), A is the contributing catchment area in kilometres squared, a and b are empirical coefficients and s = slope (m/m). This allows the competing effects of width and slope variations to be examined, because unit stream power accounts for variations in both factors.

Both stream power and stream power per unit area were then plotted against distance downstream and channel slope.

Assessment of Errors:

Errors in ArcGIS:

Burrough (1986) defined three main categories of error in GIS: (1) obvious sources of error; (2) errors resulting from natural variations or from original measurements; (3) errors arising through processing.

The obvious sources of error reside in such forms as the age of the data, the scale of the maps, density of observations, formatting of the data, accessibility, and cost.

Type of Error	Possible Ramifications of Error	Overcoming the Error
Outdated SRTM (DEM), Satellite Image (IRS) and Topographical Survey Maps.	From all three sources of data, river properties such as channel position, river aggradational and degradational features may be inaccurate.	Obtaining newer data.
Topographical map resolution too low.	Using 1:250'000 and 1:50'000 m maps creates inaccuracy when reading river position and contour data. When zoomed in to trace contours, the lines become distorted and impossible to read accurately. This is more of a problem when calculating elevation and slope changes from inaccurately extracted data.	Using higher resolution maps preferably 1:5'000, 1:1'000 m maps would be the best solution, however, they might not exist for such a remote region.
SRTM and Satellite data resolution too low.	Using 90 m DEM and 23.5 m satellite image create inaccuracies when reading river position and channel features such as thalweg position and channel positions.	Using a better resolution ASTER data at 30 m, and better IRS image – 5 m.

Spatial coverage of Grain size data not 100 % perfect due to inaccessible areas.	By not having a complete coverage of grain size data, important relationships like the gravel/sand transition zone were missed. Large areas of the reach on the Yamuna were not accessible due to quarrying (see fig 5.3 and limitations section of Discussion chapter).	Fuller coverage of grain size data could be obtained by using an Aerial survey approach, specifically using a U.A.V.
Handheld GPS accuracy in the field inconsistent between two handsets.	By not securing a consistent GPS position throughout the field work. The data may have been mapped incorrectly in some places. This was a small error.	Using more accurate and more handsets could achieve a more consistent reading between n handsets.

Table 3.5. A summary table outlining the main limitations and errors in the methodology.

Errors in Matlab:

The processes involved in photosieving introduced some error. The main problem revolved around the measurement of the individual grains in any given image. The pixel size of the computer screen was the main issue, as the GUI used did not allow for zoom capability. Grain measurement was therefore only possible at the screen resolution and depended critically on the ability of the observer to discriminate grain boundaries. This limitation could cause inaccuracy in D16, D50 and D84 (Carbonneau *et al.* 2004; Verdú *et al.* 2005).

This will have varied to some degree over the course of the entire measuring procedure. Some grains were lying at an angle so that the entire *b*-axis was slightly skewed by an overlying grain, or were submerged slightly in water/silt so that it was made difficult to interpret the true *b*-axis. The most likely error with this particle type is an over-estimation of size because of the hiding of portions of the larger grains within the three-dimensional fabric of the sediment bed (Buscombe and Masselink, 2009). Error increases as the grain size decreases due to the likelihood of grains not being truly horizontal (Buscombe and Masselink, 2009). However, as stated earlier in the chapter, fabric error is widely acknowledged in the literature and is accepted to not be a large error, ~1ψ (Sime and Ferguson, 2002).

4. Results

The geomorphological variables quantified in this study are presented in this section in the following order: long river profile, channel slope, width of channel belt, braiding index, stream power and grain size.

Longitudinal River Profile:

The elevation of the Ganges decreases relatively systematically along the study reach. In general, the elevation decreases at an even rate through the Dun and decreases at a faster rate through the Mohand Anticline before decreasing at a much slower rate in the foreland (Fig 4.1). In detail, the long river profile of the Ganges shows three main breaks in slope, one ~10 km downstream of the Lesser Himalaya mountain front with elevation dropping from ~315 m to 300 m, and the other within the Mohand Anticline ~28 km downstream of mountain front, reflecting a 15 m drop in elevation. The first drop in elevation is not likely to be a manifestation of the MBT as it is over 10 km downstream of the fault. It is in fact, more likely to be a hole in the DEM that has been filled using the Fill function in ArcGIS. The second is likely to be the HFT, as it is ~25 km downstream of the MBT which is consistent with the placement by Wesnousky *et al* (1999) - the hanging wall thrusts upward, creating a larger drop in elevation localised to the fault axis. The profile shows a very roughly stepped pattern throughout the reach flowing through the Dehra Dun basin. It is clear that the longitudinal river profile is split into a steeper section in the reach from the MBT to the HFT (in the Dun Valley), then a more shallow profile between the HFT and the downstream end of the study reach (in the Gangetic plain), indicating a slowing rate of decrease in elevation. The river profile drops a total of ~110 m over the 80 km of measured reach. It must be noted that the two steps in the profile may be errors in the DEM, thus accentuating the elevation change.

The elevation of the Yamuna decreases relatively systematically along the study reach. In general, the elevation decreases at an even rate through the Dun and decreases at a faster rate through the Mohand Anticline before decreasing elevation at a much slower rate in the foreland (Fig 4.2). In detail, the Yamuna river profile is much more linear than the Ganges. The measurements begin at the Lesser Himalaya mountain front, with the elevation at 472 m. This elevation decreases at a rate of 10 m over the first 2 km in the Dun. The gradient continues to decrease at approximately the same rate for another 2 km before showing one obvious step down by 7 m between 4.76 km and 5.97 km. This could also be accentuated by irregularities in the DEM but is likely to be showing a manifestation of the MBT. The elevation then drops at a much slower rate, decreasing from 433 m elevation to 423 m over a distance of 5 km which is approximately the rate observed through the remainder of the study reach. The Yamuna elevation decrease slows slightly as it flows into the Mohand, with a brief increase in rate of decrease immediately downstream of the potential location of the HFT. The rate of decrease in elevation then begins to slow as the river flows out into the Indo-Gangetic plain. The overall change in elevation through the reach is ~200 m.

The most interesting points that the longitudinal river profiles identify are the considerable steps in elevation on the Ganges River, the second being more important as it occurs in the Mohand Anticline. There are also two steps, smaller in scale, on the Yamuna river profile, one at the upstream end of the measurements, and the other in the Mohand Anticline, which will be discussed in the next chapter. By comparing the two graphs, the Yamuna drops in elevation by nearly twice that of the Ganges. By comparing both graphs, the Yamuna clearly has a steeper profile and drops by a considerably larger amount of 90 m over a similar distance.

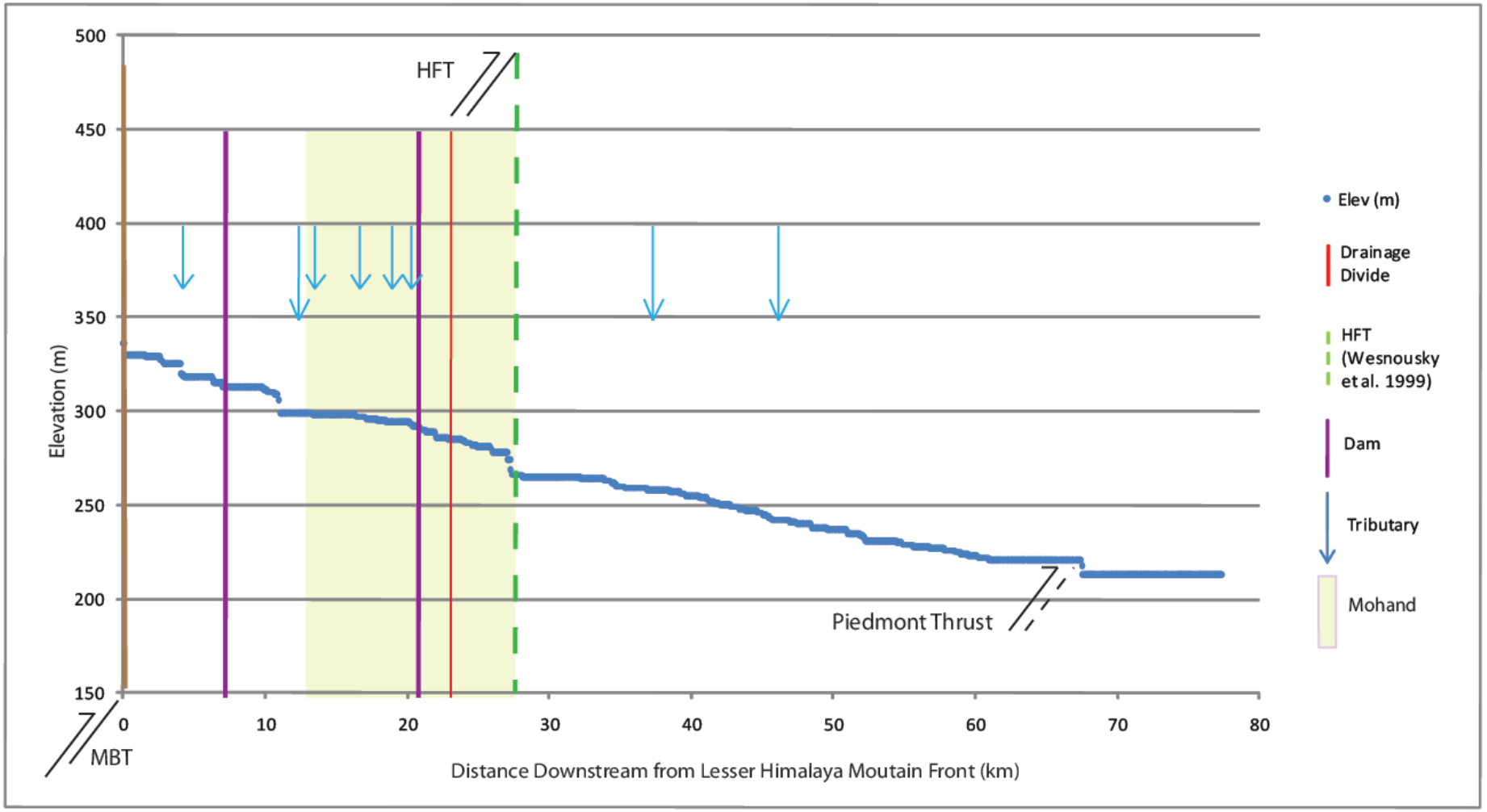

Fig 4.1. Longitudinal profile variations for the Ganges River as a function of distance downstream from the MBT. The orange box indicates the Mohand Anticline region, the red solid line indicates the drainage divide, and the dashed green line indicates the location of the HFT (from Wesnousky *et al.* 1999). Additional tributary locations have been indicated by blue arrows and dams by purple lines. The MBT has been identified by a brown line along with the possible Piedmont Thrust location.

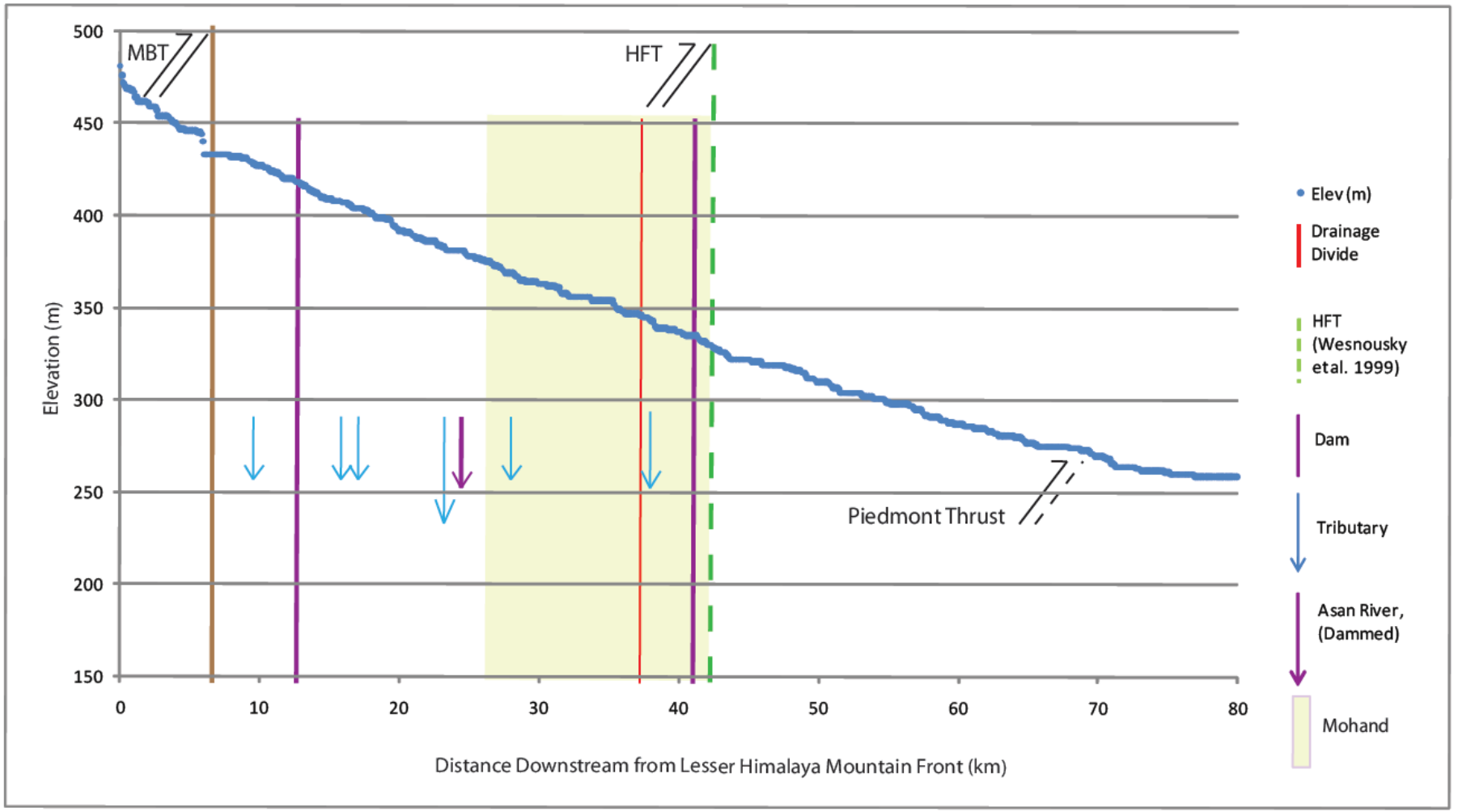

Fig 4.2. Longitudinal profile variations for the Yamuna River as a function of distance downstream from the MBT. The orange box indicates the Mohand Anticline region, the red solid line indicates the drainage divide, and the dashed green line indicates the location of the HFT (from Wesnousky *et al.* 1999). Additional tributary locations have been indicated by blue arrows and dams by purple lines. The MBT has been identified by a brown line along with the possible Piedmont Thrust location.

Channel Slope:

Channel slope is derived from the longitudinal river profiles. The Ganges channel slope shows a general decrease through the study reach except at the upstream end of the measurements and within the channel reach in the Mohand Anticline (Fig 4.3), where channel slope steepens caused by a sink in the data ~10 km from the MBT position, and upstream proximal to the HFT location.. In detail, the channel slope has been calculated for approximately every 2 km using equation (4) from the methodology. The first channel slope point is 2.11 km from the Lesser Himalaya mountain front with a value of ~0.003. Channel slope then increases before increasing rapidly, corresponding to the sink in the DEM, before decreasing gradually through the Dun as the river flows towards, and into the Mohand Anticline. The Ganges slope then briefly increases and decreases by ~0.00015 before increasing significantly as before, as the river flows across the HFT and through the southern flank of the Mohand, a key point for later discussion. Once the slope reaches a peak of 0.0063, it begins a significant decrease as the river flows out of the Mohand. Channel slope then sequentially decreases as the river flows into the Indo-Gangetic plain with a net increase ~15 km from the HFT for ~10 km. Channel slope reaches a value of ~0.0008 towards the final downstream measurement, ~ 80 km from the MBT. The overall decrease in channel slope observed over the reach is ~0.002. Due to this channel slope data being of relatively low resolution, any detailed interpretation is difficult as can be seen by the very undulating trend. The two main areas of interest however, (MBT and HFT) do show more exaggeration of the slope in these areas.

The Yamuna channel slope, similar to the Ganges shows an increase within the first 7 km of the upstream measurement, reflecting the presence of the MBT (Fig 4.4). The channel slope then shows a general decrease downstream of this point, with an increased rate of shallowing upstream of the HFT. In detail, the Yamuna channel slope starts off high at 0.0086 2.1 km downstream of the Lesser Himalaya mountain front, potentially indentifying the presence of the MBT. This rate sharply decreases as the Yamuna flows downstream before increasing to a slope of ~0.003 ~13 km into the Dehra Dun basin. This marks the start of fluctuating slope between ~0.003 – <0.002 for ~12 – 65 km downstream from the MBT. During this phase of fluctuating slope the river flows through the Mohand Anticline. The slope in this section of the reach decreases in a more controlled manner, shallowing as the channel approaches the HFT. The river channel steepens proximal to the HFT and continues to as the river flows over the fold axis. This section of reach ~29-42 km downstream of the MBT is extremely important for determining tectonic influence on channel morphology and will be revisited. As the river flows out into the Indo-Gangetic plain the river channel slope is ~0.002 – 0.003 for ~30 km before decreasing to <0.001 at the downstream end of the study reach. The overall decrease in channel slope observed over the reach is ~0.008.

It is interesting that the Ganges channel slope increases as the river flows progressively further into the Mohand Anticline as it isn't what we would expect (Holbrook and Schumm, 1999) (Fig 1.1). The Yamuna slope shows important changes in morphology in the Mohand as it shallows upstream of the fold axis. It is also interesting that the Ganges slope increases in the

foreland, ~15 km from the HFT, correlating with the decrease in width of channel belt and braiding frequency. This will be discussed in detail in the next chapter.

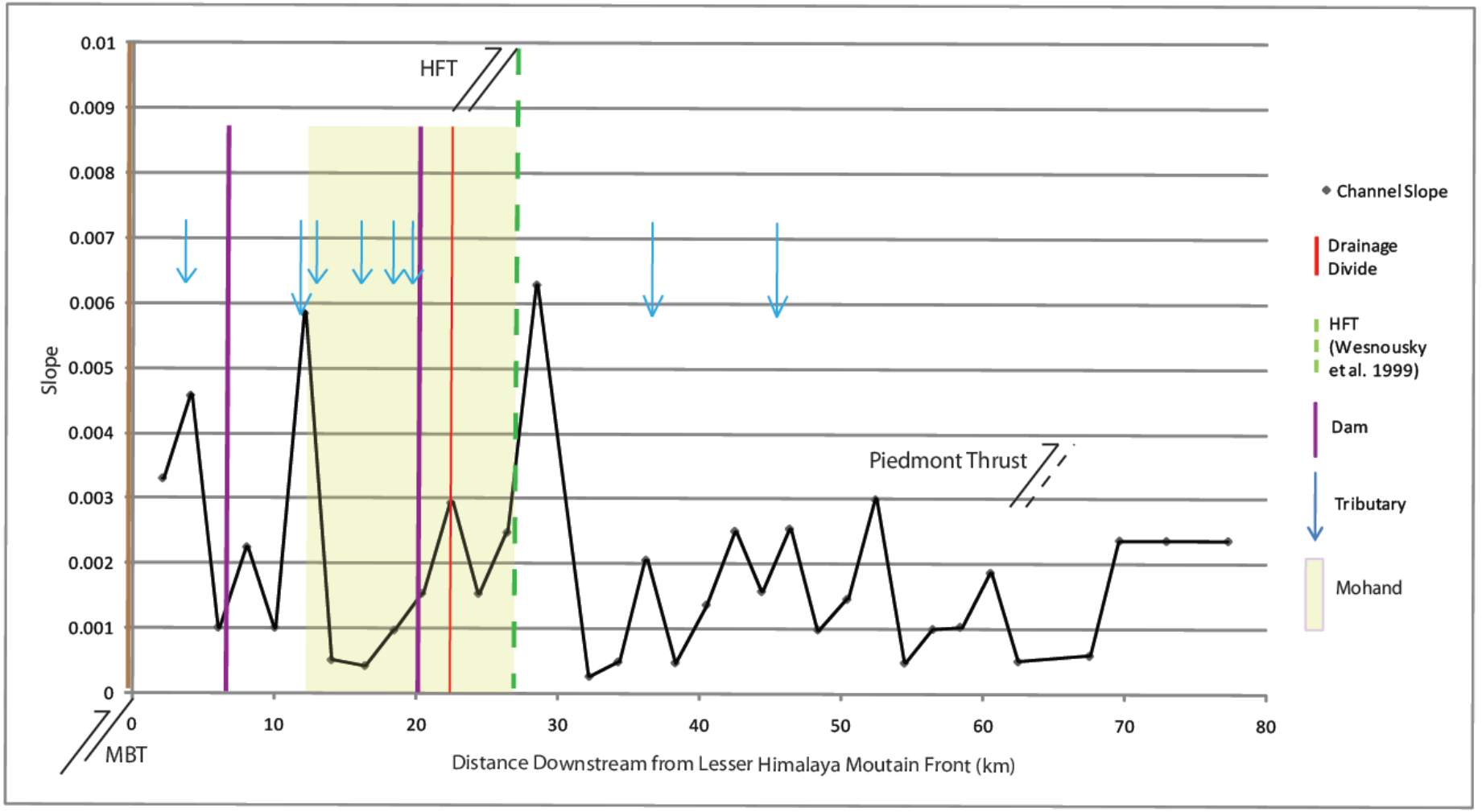

Fig 4.3. Channel slope variations for the Ganges River as a function of distance downstream from the MBT. The orange box indicates the Mohand Anticline region, the red solid line indicates the drainage divide, and the dashed green line indicates the location of the HFT (from Wesnousky *et al.* 1999). Additional tributary locations have been indicated by blue arrows and dams by purple lines. The MBT has been identified by a brown line along with the possible Piedmont Thrust location.

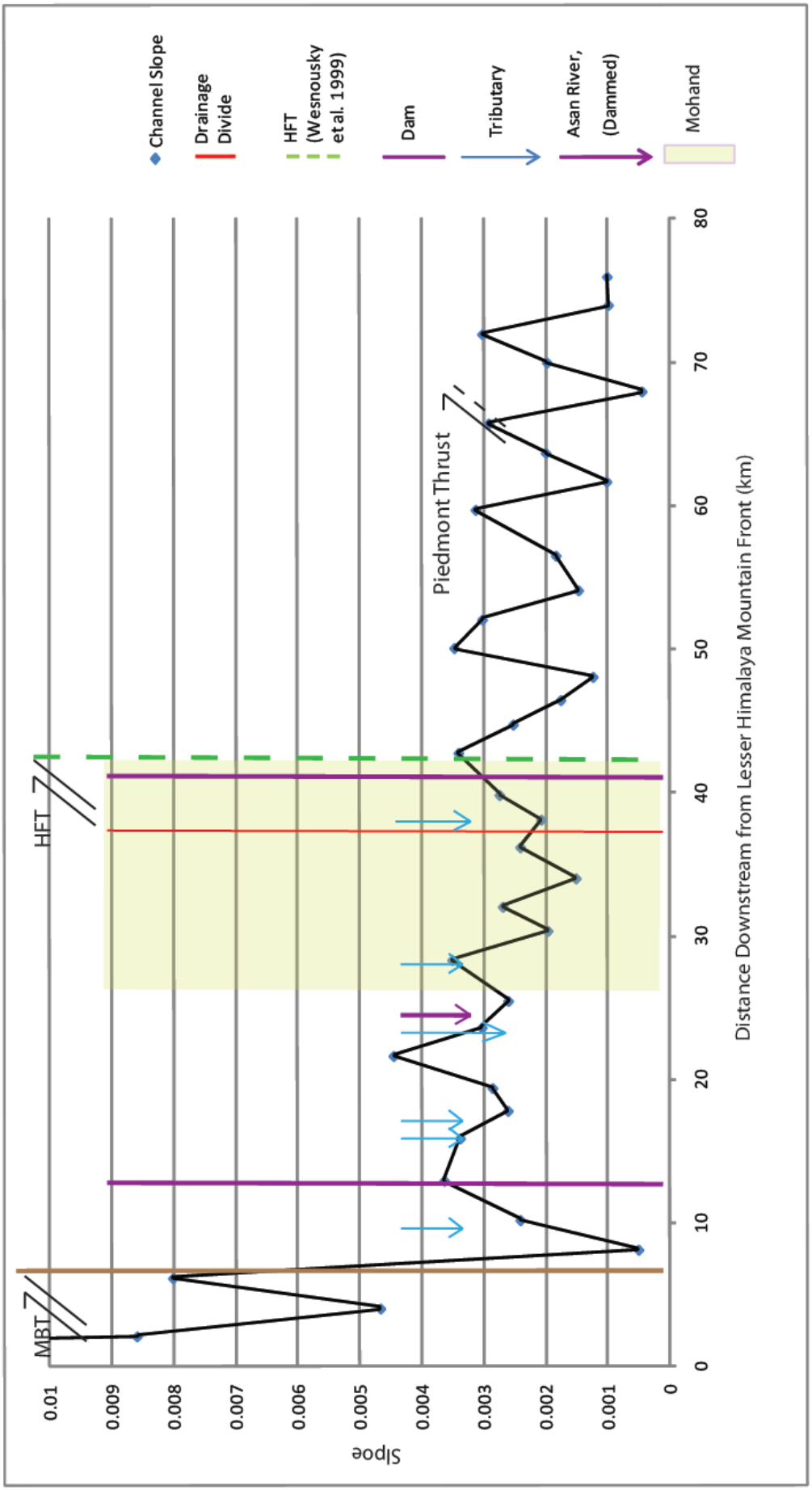

Fig 4.4. Channel slope variations for the Yamuna River as a function of distance downstream from the MBT. The orange box indicates the Mohand Anticline region, the red solid line indicates the drainage divide, and the dashed green line indicates the location of the HFT (from Wesnousky *et al.* 1999). Additional tributary locations have been indicated by blue arrows and dams by purple lines. The MBT has been identified by a brown line along with the possible Piedmont Thrust location.

Width of channel belt:

Ganges Width of channel belt varies systematically with distance downstream from the MBT (Fig 4.5). In general, width of channel belt increases through the Dun and decreases in the Mohand Anticline, constricted by topography. The channel continues to decrease as it flows over the HFT to ~400 m. Width of channel belt then begins to widen as the river flows into the foreland reaching a maximum of 3.5 km ~ 15 km downstream of the HFT. Width of channel belt then decreases through the remainder of the study reach. In detail, the channel at the MBT is ~240 m in width. The channel then progressively increases in width but remains below 500 m over the first 10km downstream of the MBT. Width then increases over the following 10 km of river flowing towards the drainage divide of the Mohand Anticline, peaking at ~2200 m. The channel narrows upstream proximal to the HFT, and continues to narrow as the river flows over the HFT fold axis. The channel then begins to substantially widen as it flows further out into the Indo-Gangetic plan for ~10 km before reaching the widest part of the Ganges in the study reach at 3500 m. The channel then begins a relatively steady decrease in width over the remaining 35 km of the study reach.

Width of channel belt of the Yamuna varies systematically with distance downstream from the MBT (Fig 4.6). In general, the trend shows a fluctuating width through the Dun basin before becoming more constrained in the Mohand Anticline occupied reach. This is the only obvious controlled section of the channel. As the river flows over the HFT is continuing to narrow for ~3-4 km before that control is released. The channel, now in the Gangetic Plain, begins to increase as the river becomes more distal from the HFT. During the final kms of the study reach, the channel begins to narrow once again, in detail, the lowest value of width of channel belt is ~500 m at the MBT. Width of channel belt then fluctuates with a general increasing trend as it flows through the Dehra Dun basin for 15 km to reach a peak width of 1599 m. As the river flows into the Mohand Anticline the river channel narrows, before flowing through the Mohand drainage divide 35 km downstream from the MBT with a width of 256 m. The river channel then widens briefly upstream of the HFT before narrowing as the river flows over the HFT. The channel then widens as the river flows out into the Indo-Gangetic plain reaching a peak of 2382 m ~15 km from the HFT. Width of channel belt then proceeds to decrease over the remainder of the study reach.

By using an interval of 0.5 km, an acceptable number of measurements have been made without compromising too much time invested in the one variable. 0.5 km supports identification of a natural trend in the graphs. The most interesting point to raise from the width of channel belt results is the decrease in width on both rivers due to the Mohand anticline and the HFT. The width measurements, when compared to channel slope could be interpreted to show a steepening channel where width of channel belt decreases, although the channel slope graphs are of low resolution, and therefore not a 100% reliable source for interpretation. By using the labelled tributaries, width of channel belt increases also seem to co-inside with larger confluences (see fig 4.5 ~12 km, 18, 19 km). It is also interesting that both rivers should begin to

narrow ~15 km into the foreland. By comparing the two graphs of width of channel belt, the Yamuna is overall narrower throughout the reach than the Ganges, reflecting a lower discharge

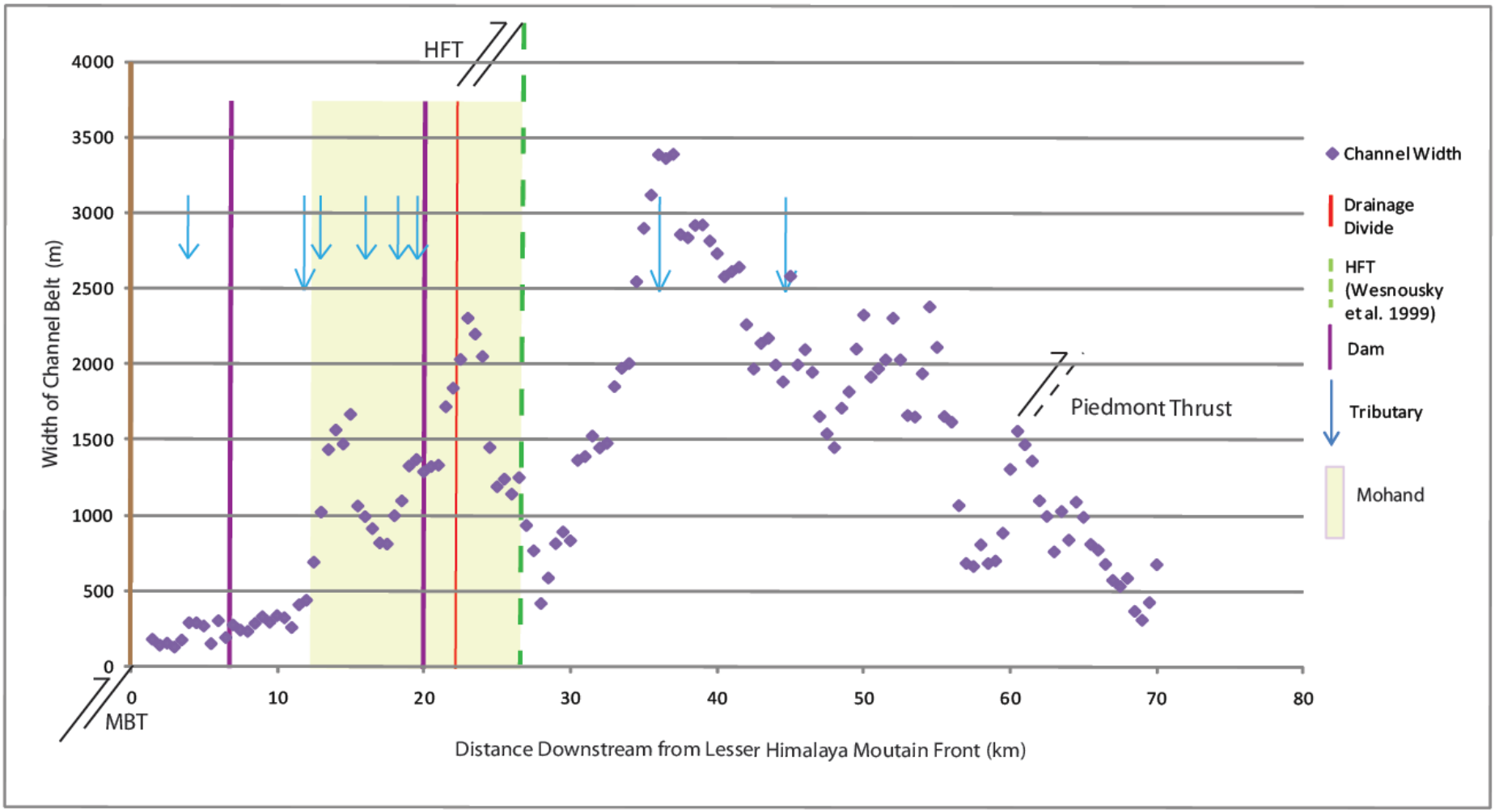

Fig 4.5. Width of channel belt variations for the Ganges River as a function of distance downstream from the MBT. The orange box indicates the Mohand Anticline region, the red solid line indicates the drainage divide, and the dashed green line indicates the location of the HFT (from Wesnousky *et al*. 1999). Additional tributary locations have been indicated by blue arrows and dams by purple lines. The MBT has been identified by a brown line along with the possible Piedmont Thrust location.

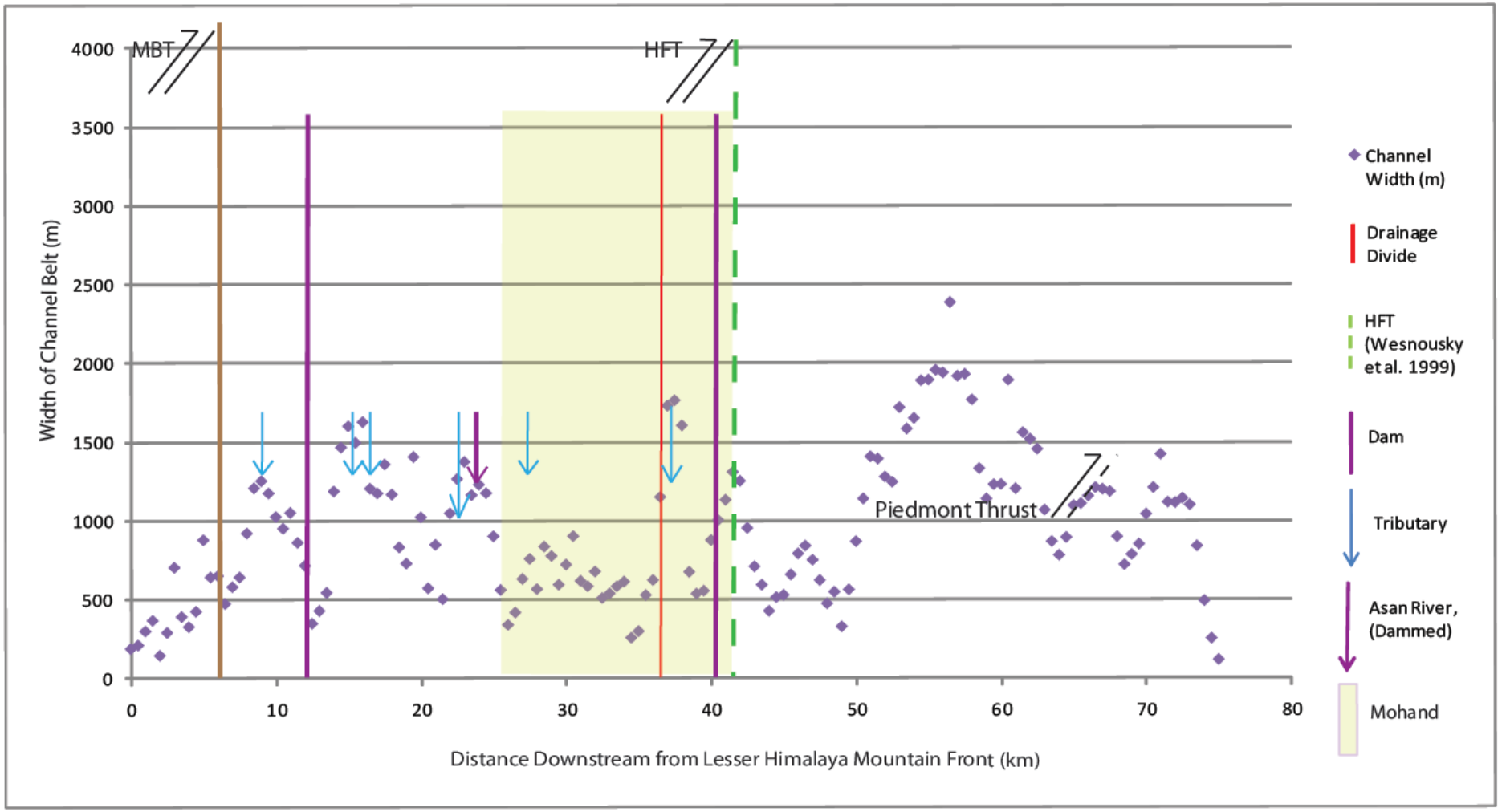

Fig 4.6. Width of channel belt variations for the Yamuna River as a function of distance downstream from the MBT. The orange box indicates the Mohand Anticline region, the red solid line indicates the drainage divide, and the dashed green line indicates the location of the HFT (from Wesnousky *et al.* 1999). Additional tributary locations have been indicated by blue arrows and dams by purple lines. The MBT has been identified by a brown line along with the possible Piedmont Thrust location.

Braiding Index:

The pattern of braiding on the Ganges, as quantified by a channel count varies substantially downstream from the MBT (Fig 4.7) to the downstream end of the study reach. In general, there is an overall increase into the Dehra Dun basin, a decrease into the Mohand Anticline, and an increase into the foreland, reaching a peak ~15 km from the MBT where braiding begins to decrease through the remainder of the study reach. In detail, the Ganges flows into the Dehra Dun basin as one channel before bifurcating into four channels ~10 km from the MBT. The river then flows in a braiding pattern through the Dun basin before flowing back into a single channel, 15.5 km from the MBT. The number of channels then increases again as the river flows into the Mohand Anticline, reaching a peak of eight channels at the drainage divide. The river then flows into a single channel as it flows across the HFT, 36 km from the MBT. As the river flows out into the Indo-Gangetic plain it bifurcates and flows in a braiding pattern, increasing in channels to a peak of 11 ~15 km downstream of the HFT. The river then continues to flow in a braiding pattern, decreasing in channels through the remainder of the study reach.

The nature of braiding in the Yamuna as quantified by a channel count varies substantially downstream from the MBT (Fig 4.8) to the downstream end of the study reach. In general, there is an overall increase into the Dehra Dun basin, a decrease into the Mohand Anticline, and an increase into the foreland, reaching a peak ~15 km from the HFT where braiding begins to decrease through the remainder of the study reach. In detail, the Yamuna flows into the Dehra Dun basin as one channel before bifurcating ~2 km from the MBT. The Yamuna River then fluctuates between one and five channels as it flows into the Mohand Anticline. The river then flows across the HFT as one channel flowing out into the Indo-Gangetic plain before systematically increasing in the number of channels the further the river flows from the MBT. The river flows for ~15 km after exiting the Mohand before the number of channels begins to decrease so that the river is flowing in one channel at the downstream end of the study reach.

The most interesting point raised from the braiding index results is the decrease in braiding due to the Mohand Anticline and HFT. It is also interesting that the braiding decreases in conjunction with width of channel belt ~15 km from the HFT. This distance of ~15 km could be important as all channel morphology appears to be altering in this area of the reach. The Yamuna and Ganges rivers are comparable in the amount of braiding throughout their reaches.

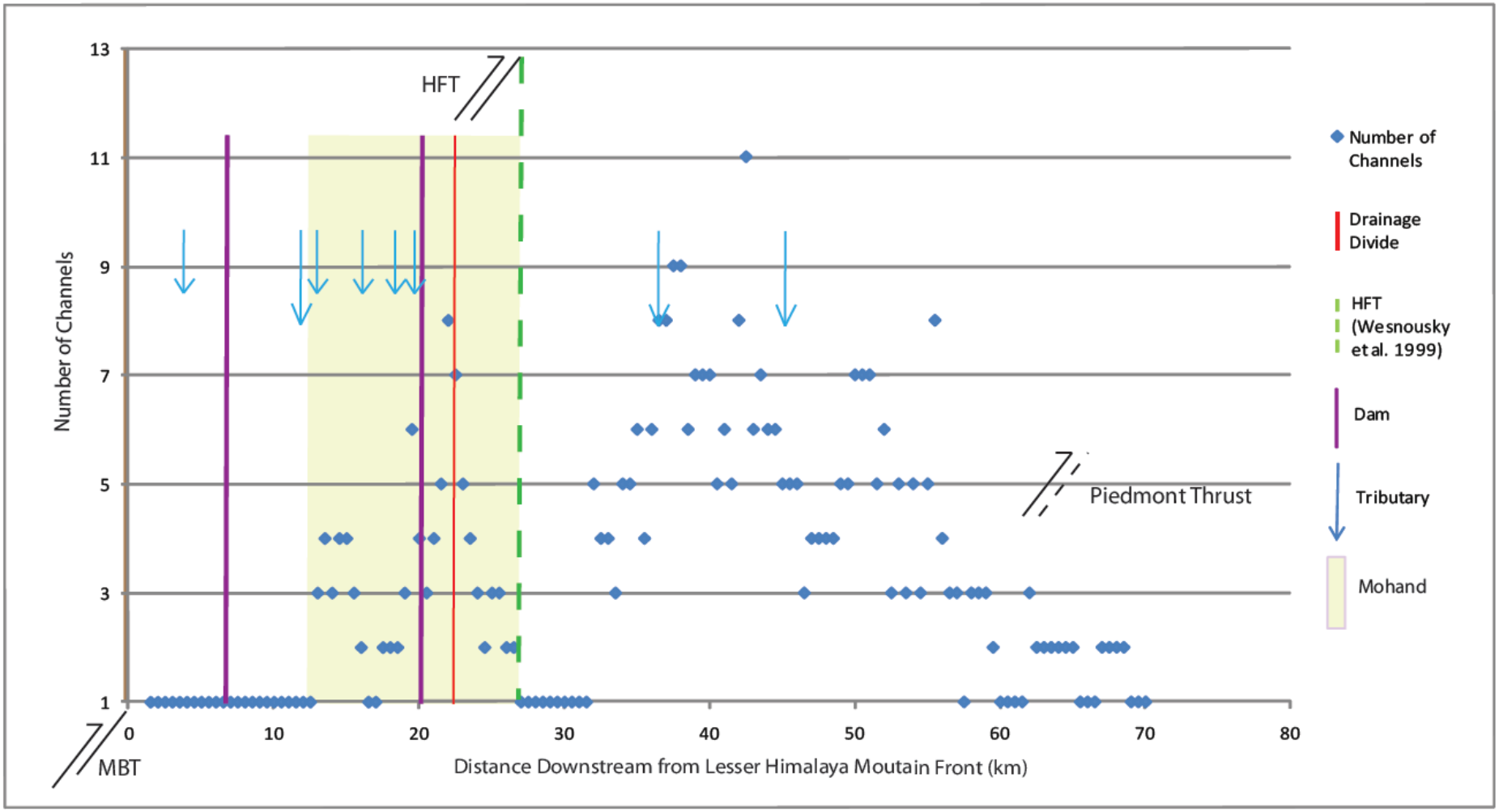

Fig 4.7. Channel braiding variations for the Ganges River as a function of distance downstream from the MBT. The orange box indicates the Mohand Anticline region, the red solid line indicates the drainage divide, and the dashed green line indicates the location of the HFT (from Wesnousky *et al.* 1999). Additional tributary locations have been indicated by blue arrows and dams by purple lines. The MBT has been identified by a brown line along with the possible Piedmont Thrust location.

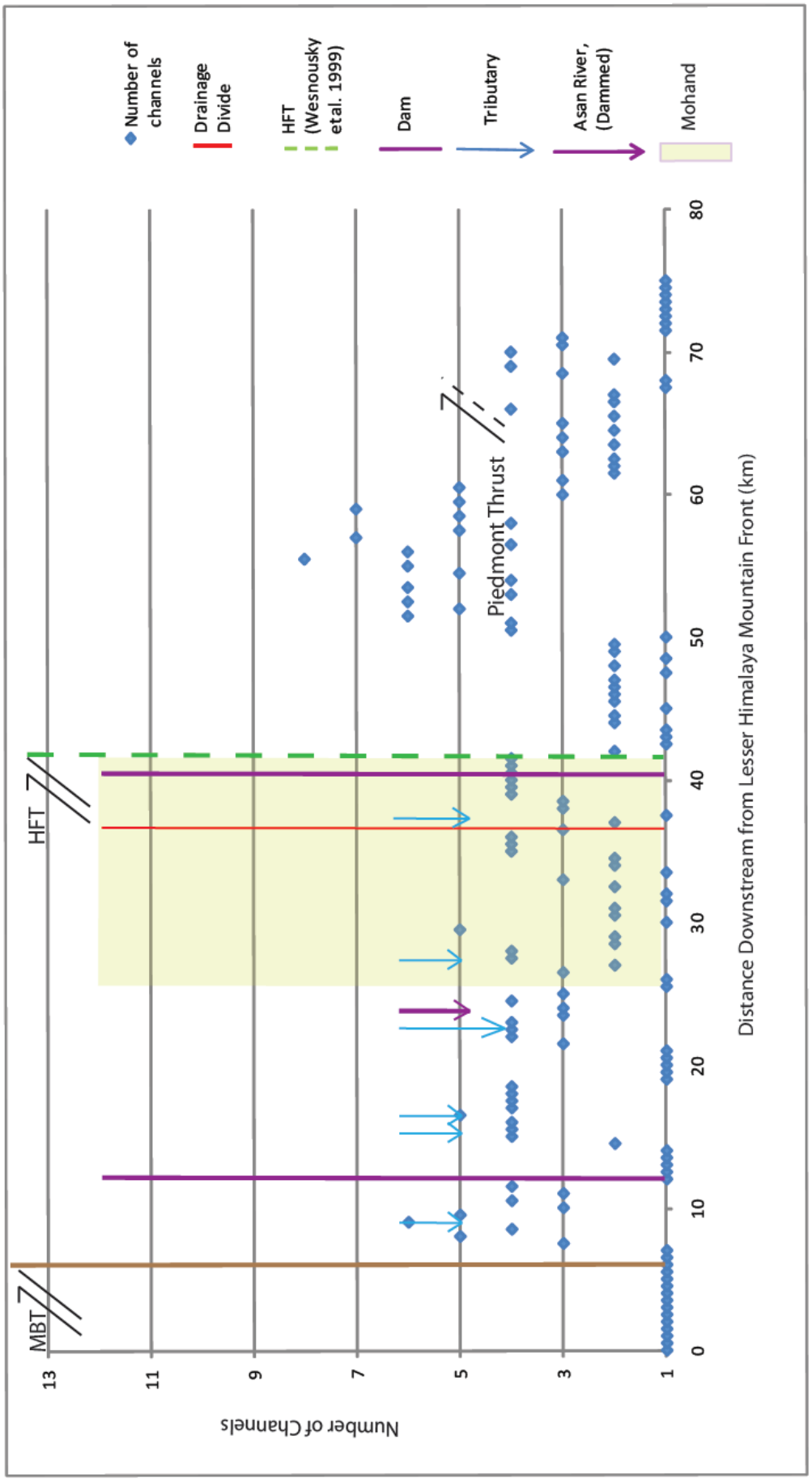

Fig 4.8. Channel braiding variations for the Yamuna River as a function of distance downstream from the MBT. The orange box indicates the Mohand Anticline region, the red solid line indicates the drainage divide, and the dashed green line indicates the location of the HFT (from Wesnousky *et al.* 1999). Additional tributary locations have been indicated by blue arrows and dams by purple lines. The MBT has been identified by a brown line along with the possible Piedmont Thrust location.

Stream Power and Unit Stream Power

Stream power has been calculated and incorporated into stream power per unit area. By plotting unit stream power, the more important relationship between stream power (a function of slope) and width of channel belt can be visualised.

The general pattern shows stream power per unit area systematically decaying through the Dun with a peak just upstream of the HFT. There is then a rapid decrease as the river base level drops considerably over the HFT. Stream power per unit area then gently rises as the river flows into the Indo-Gangetic plain. In detail, stream power per unit area just downstream of the MBT is ~650 Wm^{-2} (Fig 4.9). This is the highest stream power per unit area measured in the reach. Stream power per unit area then decreases at almost the same rate as stream power down to a value of ~140 Wm^{-2}, 6 km from the MBT. Stream power per unit area then fluctuates through the remaining 5 km of the Dun valley, most likely responding to the sink in the DEM. Stream power per unit area gradually increases through the Mohand from ~10 Wm^{-2} to ~100 Wm^{-2}, corresponding to the increased slope as the river flows over the HFT. Over the next 3 km as the river flows out of the Mohand, stream power per unit area decreases back to values of ~10 Wm^{-2}, responding to the shallowed channel slope downstream proximal to the HFT. Stream power per unit area then fluctuates through values of ~10 Wm^{-2} - 60 Wm^{-2} as the river flows through the Gangetic plain. Stream power per unit area seems to increase in the far distal region of the study reach, however, as stream power per unit area is a function of slope, any inaccuracies in slope may cause some inaccuracy to be carried though. The overall change in stream power per unit area is ~350 Wm^{-2} for the entire study reach.

In general, stream power per unit area on the Yamuna decreases through the Dun, remains relatively constant through the Mohand Anticline and decreases into the foreland (Fig 4.10). In detail, stream power per unit area decreases across the MBT from 450 Wm^{-2} to ~100 Wm^{-2}, which corresponds to the shallowing of channel slope downstream, proximal to the MBT. Power per unit area decays through the Dehra Dun basin with no systematic variation across most of the river profile. Stream power per unit area does not change through the HFT which is another key point that will be addressed in the discussion chapter. Power decreases downstream of the HFT slightly from ~37 Wm^{-2} to ~20 Wm^{-2} before an approximately uniform stream power per unit area is observed in the Indo-Gangetic plain. The overall change in stream power per unit area is ~425 Wm^{-2}.

It is interesting that on the Ganges, stream power per unit area increases so drastically through the Mohand Anticline, correlating with an increase in channel slope and decrease in width of channel belt. This is a highly important area for further discussion in the next chapter. Another very interesting point to be taken from unit stream power is the relationship observed on the Yamuna in the Mohand Anticline. Unlike the Ganges, there is a minimal change in stream power and unit stream power. This is unexpected and needs to be explained. The major changes in stream power per unit area on the Ganges definitely correlate with large changes in

the channel slope. This seems true for the Yamuna too; however, it is not as stronger correlation on the Yamuna, possibly due to the much lower discharge.

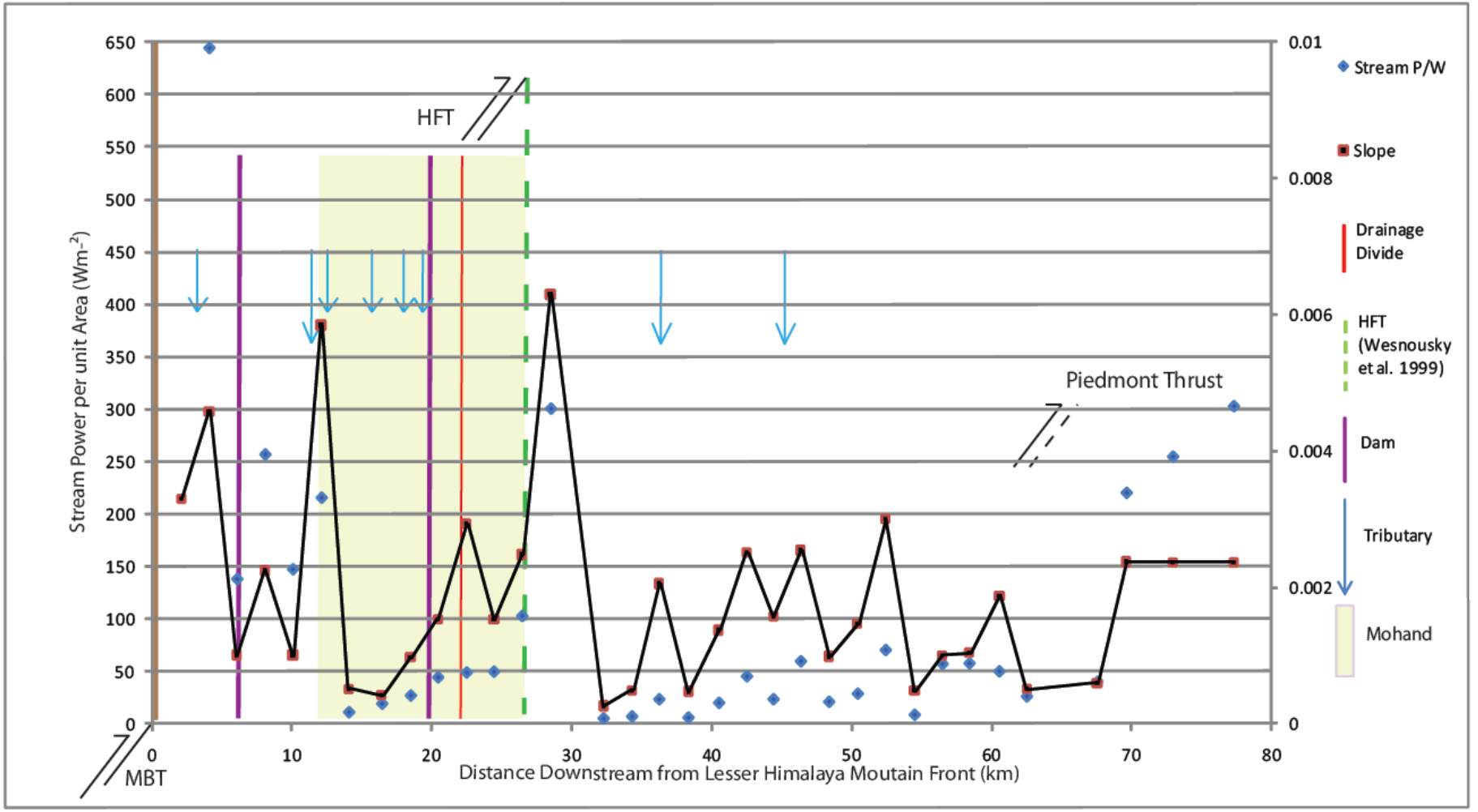

Fig 4.9 Stream power per unit area variations for the Ganges River as a function of distance downstream from the MBT. The orange box indicates the Mohand Anticline region, the red solid line indicates the drainage divide, and the dashed green line indicates the location of the HFT (from Wesnousky *et al.* 1999). Additional tributary locations have been indicated by blue arrows and dams by purple lines. The MBT has been identified by a brown line along with the possible Piedmont Thrust location.

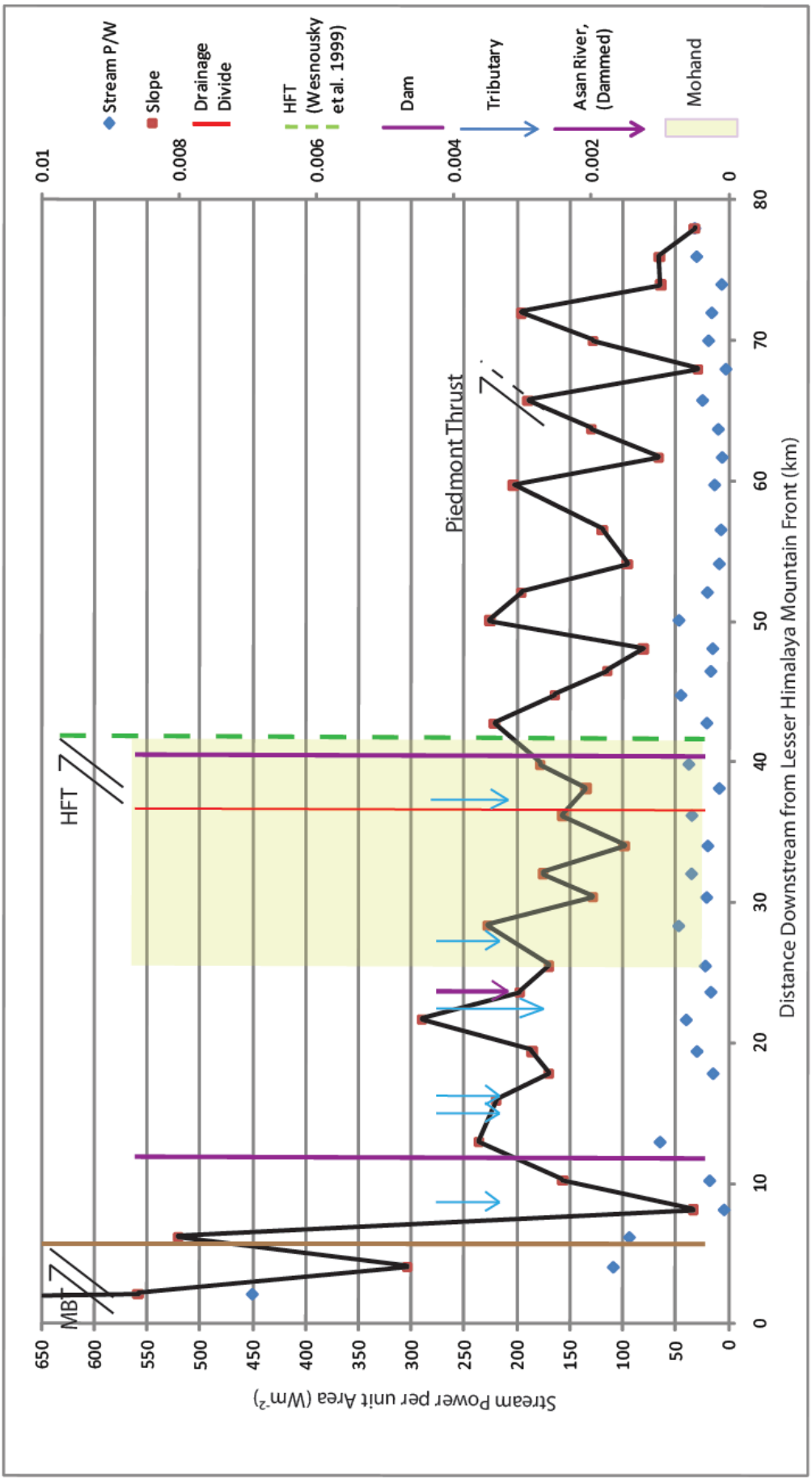

Fig 4.10. Stream power per unit area variations for the Yamuna River as a function of distance downstream from the MBT. The orange box indicates the Mohand Anticline region, the red solid line indicates the drainage divide, and the dashed green line indicates the location of the HFT (from Wesnousky *et al.* 1999). Additional tributary locations have been indicated by blue arrows and dams by purple lines. The MBT has been identified by a brown line along with the possible Piedmont Thrust location.

Grain Size Data:

The Ganges grain size data begin at approximately the MBT. It can be seen from Fig 4.11 that grain size distribution on the Ganges systematically decreases through the Dehra Dun basin and out into the Indo-Gangetic plain. There is no significant increase in grain size though the Mohand Anticline contrary to what was expected. There is one slight increase in all measured percentiles in transect 7 located at approximately the HFT with an increase in D16 from ~20 to 25 mm, D50 increasing from ~45 to ~60 mm, and D84 showing the largest increase from ~75 to ~125 mm.. The majority of the grain size data on the Ganges is within one standard deviation of the data set. The overall decrease in grain size observed is ~500 mm, with grains <2 mm (sand) at the downstream end of the study reach.

The Yamuna grain size data begin at approximately the MBT. It can be seen from Fig 4.11 that the Yamuna has a very different grain size distribution to the Ganges. Fig 4.12 shows an overall decrease in grain size through the study reach, however, the reach of river in the Mohand Anticline shows a very interesting distribution. Grain size is observed to decrease through the Dun basin, and then increase as the grains move into the Mohand. D16 increases by ~25 mm with the D50 and D84 percentiles increasing by ~50 mm. This increase continues to the HFT where the river then flows over the HFT fold axis and out into the Indo-Gangetic plain. As the river flows out of the Mohand we observe an immediate drop in grain size to levels seen upstream of the Anticline. This is an important observation and needs to be discussed further and compared with the other observations of geomorphology in this section of reach. The overall decrease in grain size across the study reach is ~250 mm, with grains <2 mm (sand) at the downstream end of the study reach.

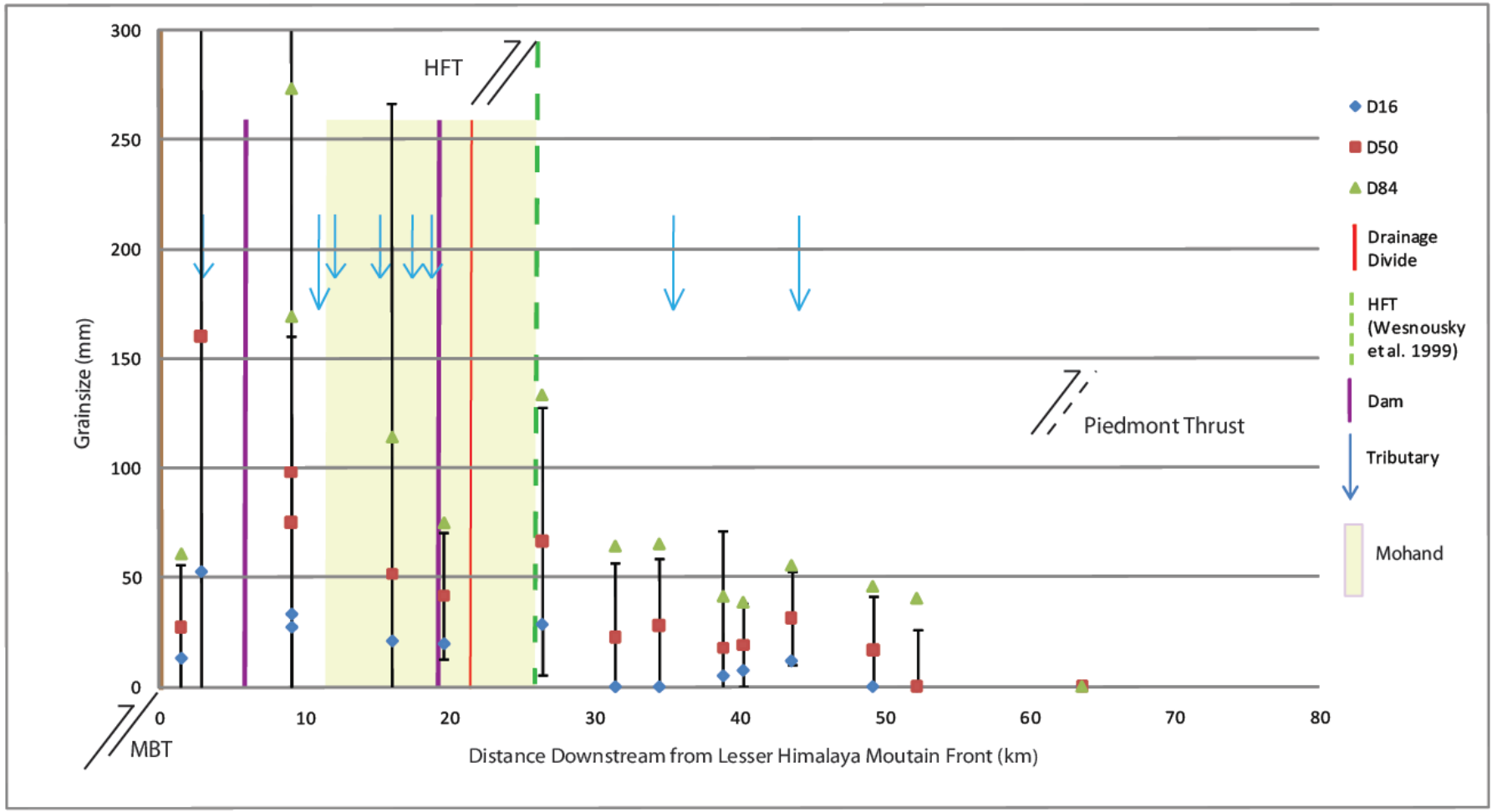

Fig 4.11. Grain size variations for the Ganges River as a function of distance downstream from the MBT. The orange box indicates the Mohand Anticline region, the red solid line indicates the drainage divide, and the dashed green line indicates the location of the HFT (from Wesnousky *et al*. 1999). Additional tributary locations have been indicated by blue arrows and dams by purple lines. The MBT has been identified by a brown line along with the possible Piedmont Thrust location. Error bars on D50 show 1. standard deviation about the mean.

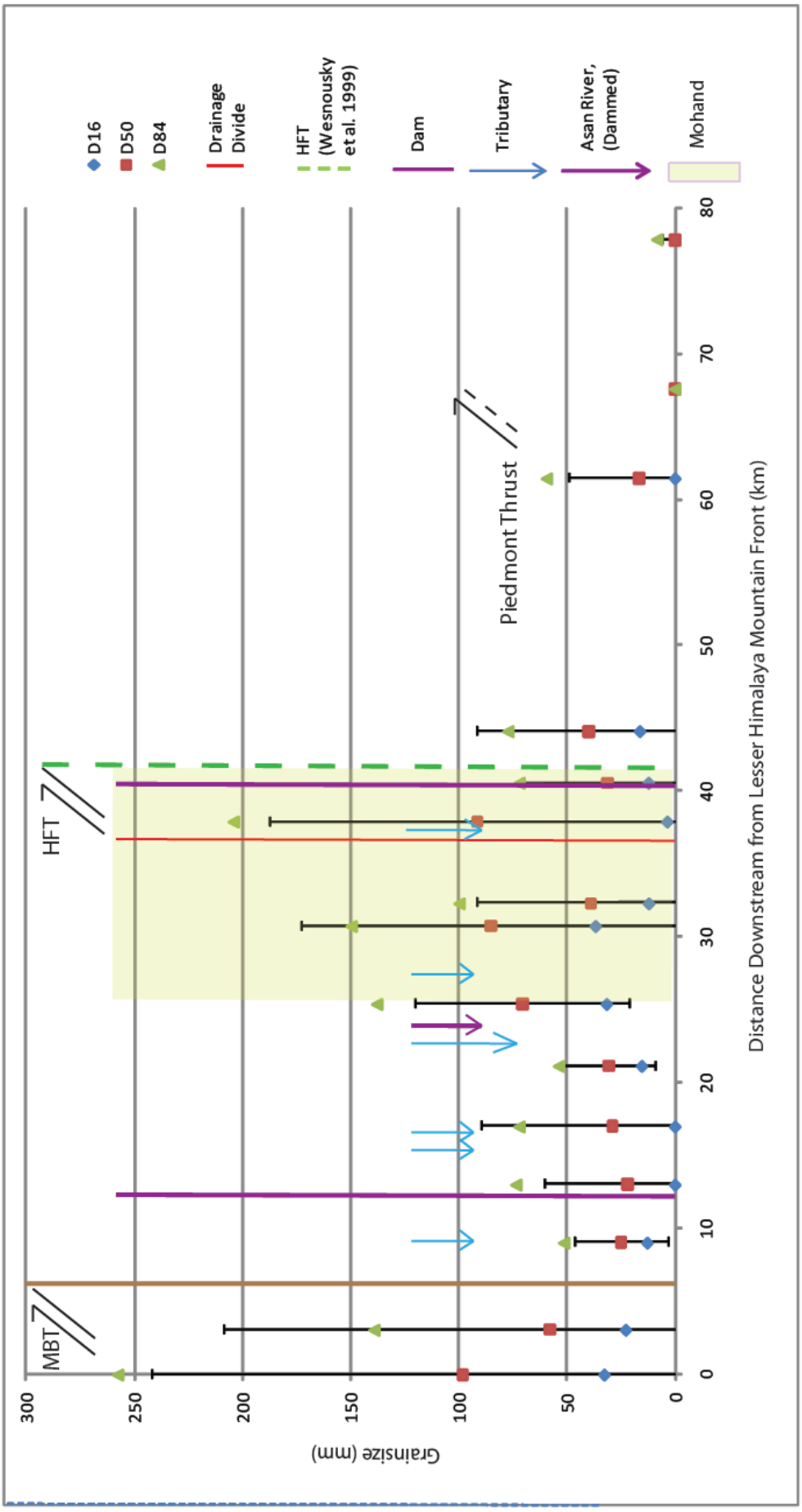

Fig 4.12. Grain size variations for the Yamuna River as a function of distance downstream from the MBT. The orange box indicates the Mohand Anticline region, the red solid line indicates the drainage divide, and the dashed green line indicates the location of the HFT (from Wesnousky *et al.* 1999). Additional tributary locations have been indicated by blue arrows and dams by purple lines. The MBT has been identified by a brown line along with the possible Piedmont Thrust location. Error bars on D50 show 1. standard deviation about the mean.

Chapter Summary

The most important things to take from the results in this section are:

1. The Ganges channel slope increases in the progression of flow towards the HFT (Fig 4.3)

2. The rivers both decrease in width as they flow through the Mohand Anticline (Figs 4.5 and 4.6).

3. The Yamuna channel slope shallows upstream proximal to the HFT (Fig 4.4).

4. The Ganges stream power per unit area increases dramatically in the Mohand (Fig 4.9).

5. The Yamuna stream power per unit area changes minimally through the Mohand (Fig 4.10).

6. The Ganges grain size distribution continues to fine through the Anticline which is not expected (Fig 4.11, Fig 1.1)

7. The Yamuna grain sizes increase in the Mohand – the more expected trend (Fig 4.12, Fig 1.1).

8. The Mohand Anticline is clearly an extremely important area of the Ganges and Yamuna reaches for determining tectonic imprint on the channel morphology of both rivers.

5. Discussion

The Ganges and Yamuna river systems in Northwest India show clear, significant fluvial geomorphological changes in the Dehra Dun valley and Mohand Anticline as they flow into the Himalayan foreland. These changes, in morphology and grain size, are consistent with the response of these rivers to tectonic activity and this study attribute them to active deformation along the HFT. In the following paragraphs I discuss and summarise the evidence for this and any divergence from the expected relationships (See river system Fig 1.1 in introduction). I also highlight the important deficiencies or gaps in the available data sets, and offer further suggestions for additional observations which would help constrain the role of tectonics in shaping these major rivers.

Patterns of Morphological Change:

To briefly recap the geomorphic changes identified in the results section: width of channel belt was observed to increase through the Dun along both rivers and decrease through the Mohand and over the HFT. Width then increased out into the foreland before decreasing once again ~15 km south of the HFT. The braiding of the rivers followed the same pattern as width. Channel slope on the Ganges decreases as the river flows out into the Dun valley across the MBT from the Lesser Himalaya. Slope on the Ganges then increases in the approach to the drainage divide in the Mohand Anticline and increases rapidly across the HFT before decreasing throughout the remainder of the study reach in the foreland. Channel slope on the Yamuna decreases through the Dun gradually then shallows in the approach to the HFT, then steepens as flow passes over the uplift axis, then shallows again gradually out into the foreland.

Slope on both rivers decreases into the Dun due to the lack of lateral confinement. When a river flows over an active fault the expected behaviour would be for the slope to shallow upstream of the fault as the hanging wall is being thrust upward relative to the hinterland (Holbrook and Schumm, 1999) (Fig 5.1). The slope would then increase as the river flows over the proximal part of the hanging wall and across the fault, reflecting the downstream drop in base level. Once downstream of the fault and on the footwall, the river would begin to shallow again as the tectonic perturbation is left upstream.

Channel slope on the Ganges actually increases as it flows into the Mohand, contrary to this expectation (Fig 4.3). The slope then increases downstream of the drainage divide across the HFT, reflecting the drop in elevation (base level) and presents excellent evidence for a response to tectonic uplift. This drop in base level appears to be sufficient enough to overcome the effects of the reclining hanging wall and maintains a high slope. It is possible that the increase in slope upstream of the Mohand drainage divide can be attributed to the anthropogenic impact of building the Dam and canal diversion at Haridwar. This dam causing deflection is controlling the localised width of the river. This would cause the channel slope to be the only variable able to change to manage discharge and therefore, the dam could be preventing the river from incising, allowing the river to maintain an artificially high slope, aiding

the river in degrading its bed and maintaining a steeper slope upstream of the HFT. The Upper Ganges Canal (UGC) system accounts for the majority of the deflection in this area of the reach. The UGC deflection of the main Ganges channel at Haridwar uses a dam to completely deflect the river to the west to flow through a man made canal network.

The Yamuna River follows the expected pattern more closely than the Ganges, with the north-tilting hanging wall causing a decrease in channel slope upstream of the HFT; this is excellent evidence for a river responding to uplift (Fig 4.4). Slope then increases slightly as the river flows downstream of the drainage divide, and across the HFT. However, slope should increase much more dramatically with a drop in base level over the HFT as illustrated in Fig 5.1, yet it does not.

The channel slope then continues to shallow, as expected, as the river flows into the foreland.

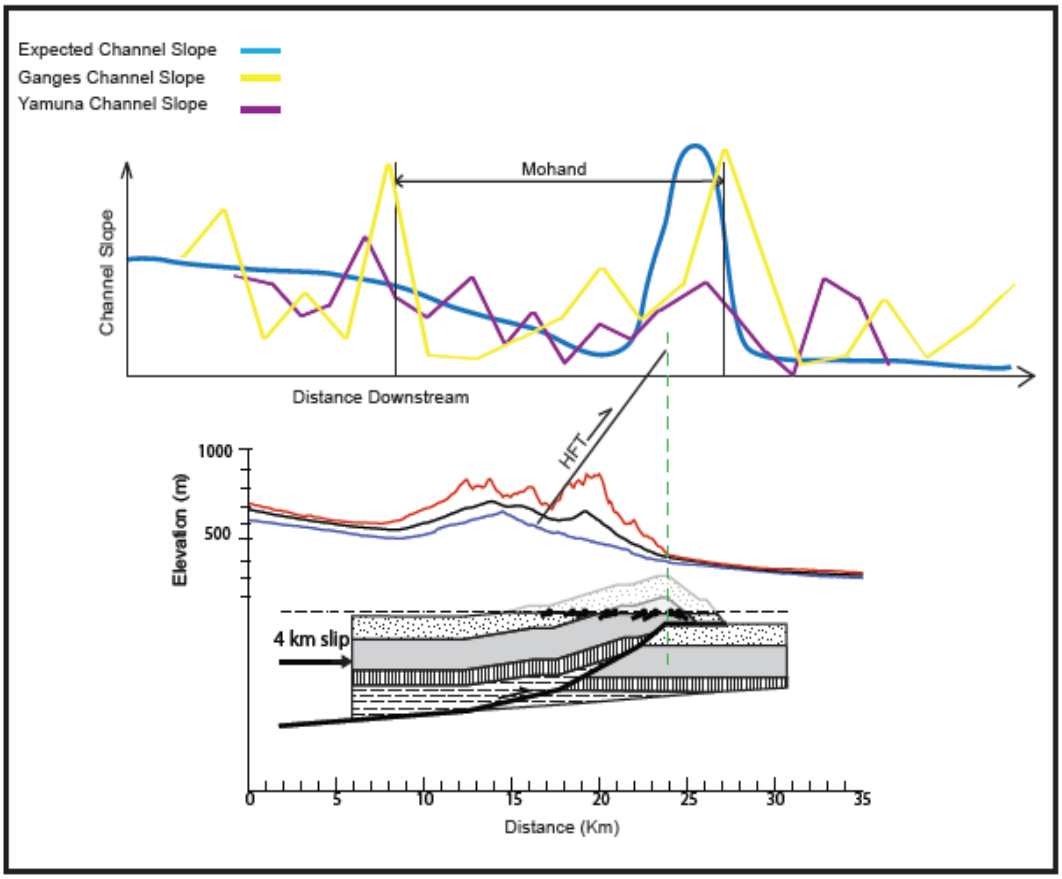

Fig 5.1. Schematic summary profile of channel slope changes associated with faulting. The blue line represents the expected channel slope of a river in this environment in cross section. The actual slopes calculated are shown in yellow (Ganges River), and purple (Yamuna River).The detailed graph shows vertically exaggerated swath-averaged minimum, mean, and maximum topographic profiles across the centre of the Mohand Anticline (Jason Barnes, pers. comm., 2009). The geologic cross-section shows the subsurface geology and HFT geometry (modified from Mishra & Mukhopadhyay 2002).The dashed green line identifies the position of the HFT.

In alluvial river systems, width of channel belt is expected to increase as the river becomes less confined by topography due to the channel banks being constituted of easily erodible material (Huggett 2003). As the Ganges and Yamuna rivers flow downstream into the Dun it is also expected that they will show a greater degree of braiding as a consequence of having a high sediment flux and a laterally relatively unrestricted channel. This pattern of braiding is observed on both the Ganges and Yamuna rivers as they flow through the Dun (Fig 4.7 & 4.8). The channels decrease in width when constricted by the Mohand Anticline, which is consistent with channel narrowing across areas of rock uplift observed by Turowski *et al*. (2006) and Holbrook and Schumm (1999). Channel narrowing along the Ganges and Yamuna rivers in uplifted areas is also consistent with Jorgenson (1990), who observed a decreasing width of channel belt immediately downstream of the axial fold on the Jefferson River in Montana, USA. Width of channel belt then increases into the unrestricted foreland when the rivers flow out of the Mohand Anticline zone, which coincides with a decreasing channel slope. Width of channel belt then builds up to a peak in the foreland for both rivers before showing a gradual narrowing for the remainder of the study reaches. The pattern of braiding highlighted by the braiding index corresponds with the changes seen in width of channel belt.

Both rivers interestingly reach a maximum in width of channel belt at similar distances downstream in the foreland. The Ganges and the Yamuna rivers both peak in width ~15 km from the HFT, which is where Yeats and Thakur (2008) placed an outboard splay of the HFT called the Piedmont Thrust (PT). Uplift would cause the width of channel belt to decrease and constrain flow in the hanging wall of the developing anticline. This mechanism could explain why width of channel belt becomes more and more constrained towards the downstream ends of the study reach. We would only be able to attribute this to uplift on the PT if the data set was extended further downstream to see if width then begins to increase again, well downstream of the PT. This decrease in width, however, could also be a signature of anthropogenic efforts to constrain the rivers as infrastructure builds up along the river banks.

Channel slope, width of channel belt, and discharge influence the variability in stream power for both rivers, however, these controls on stream power affect the two rivers in different ways. The width of channel belt decreases upstream of the HFT on the Ganges, and channel slope continues to increase, which increases the stream power per unit area because flow is forced though a narrower and steeper reach (Fig 4.9). Stream power per unit area then increases considerably as the Ganges flows over the HFT, as slope increases caused by the drop in base level induced by uplift. The controls on stream power in the Yamuna are the same yet the pattern of stream power per unit area variation is substantially different (Fig 4.10). Width of channel belt decreases as it does for the Ganges, however, due to the considerably lower discharge, and the north-tilting hanging wall causing a decrease in channel slope, stream power is much lower in the Mohand Anticline reach. Stream power per unit area only increases very slightly as the river flows over the HFT due to the increase in slope associated with the drop in base level.

Grain Size Variations:

It has long been known that grain size in a gravel bed river generally decreases downstream (Paola *et al*. 1992; Kodama, 1994; Ferguson *et al*. 1996). This downstream fining is usually ascribed to some combination of two factors: (1) abrasion, by which individual particles are diminished in size, and (2) sorting, by which finer grains are preferentially transported downstream faster and further than the coarser ones (differential transport), or in which only the fraction of the bed material smaller than a threshold size is transported by a given flow event ((selective entrainment, selective transport (Paola *et al*. 1992)).

Selective entrainment is the normal process for downstream fining, however, it has been proven by lab controlled experiments that selective entrainment can be the only process for downstream fining, with abrasion not featuring at all (Seal *et al*. 1997) or only as a minor process (Hoey & Bluck, 1999). This is a lab controlled experiment though, and may not completely reflect the actual controls within a river. This is supported by many in the field stating that abrasion is a present process (Kodama, 1994b, Werritty, 1992).)

On the Ganges, I argue that the grain size distribution in the Dun reflects downstream fining by sorting its sediment load, most likely by selective entrainment. As has already been established, channel slope decreases through the Dun which leads to decreased stream power. This causes the river to sort its sediment load according to its transport capacity, so that larger grains are deposited first and the grain sizes progressively decrease downstream as the system loses energy. Transport capacity could be tested by further research outlined in the limitations and future work section of this chapter. This relationship of stream power and slope is expected through the Dun, but not however through the Mohand Anticline. This is because channel slope and stream power are expected to decrease upstream of the HFT (Holbrook and Schumm, 1999) and the river would then be expected to deposit the larger grains (Paola *et al*. 1992), causing an increase in D50 and D84. This does not happen. The Ganges grain size distribution shows no evidence of any perturbation through the uplifting Mohand Anticline. As explained earlier, it is thought by Holbrook and Schumm (1999) that rivers with high discharge can degrade their bed over an uplift axis. This could be true for the Ganges, because the Ganges has a very large discharge it can maintain a very large stream power and continually degrade its bed as it flows through the uplift axis.

On the Yamuna, the grain size distribution in the Dun also reflects downstream fining by sorting of the sediment load. Channel slope decreases through the Dun, and decreasing stream power causes the river to deposit its sediment load, therefore relinquishing larger grains first and progressively smaller ones through the Dun. This relationship is expected to change through the Mohand Anticline, which it does. The results show that channel slope decreases in the approach to the HFT, which reduces stream power further and causes the river to deposit large grains that it would normally transport further downstream. On the upstream flank of the Mohand, D50 increases along with D84. We would expect to see D50 increase because apparently the river is still capable of transporting smaller grains through the Mohand, therefore

a larger percentage of larger grains would be seen. It is however, unexpected to see an increase in D84 distribution as it seems likely that larger grains were already deposited upstream as the sorting process dictates.

One possible explanation for this local increase in grain size, despite a decrease in slope, is that this reach acts as a trap for larger grains transported into the Mohand by seasonally controlled, large flood events. Larger grains could be moved downstream sequentially with each flood event until becoming trapped when reaching the low channel slope in the Mohand. Stream power is low because of a low slope and low discharge, perhaps due to the Asan Dam, which considerably decreases the Yamuna's normal transport capacity and inhibits boulder transport. Eventually with larger flood events the larger grains will be moved out into the foreland, but the data set is incomplete for the reach downstream of the HFT due to quarrying of large grains. The grain size data collected in the foreland reflect downstream fining, but the data are severely limited because of the extensive quarrying. Grain sizes were <2 mm (sand) at the downstream end of both Ganges and Yamuna reaches, showing the effectiveness of the sorting process over an 80 km reach.

Paola *et al*. (1992) observed a fairly abrupt transition from gravel to sand bed morphology in a flume. The gravel-sand transition has often been associated with pronounced bimodality in the bed material (Ferguson and Ashworth, 1991, Kodama, 1994). This bimodality is associated with a relative paucity of sediment in the range of 1-4 mm; samples are either composed predominantly of gravel with a median grain size in excess of 4 mm or exclusively of sand with a median grain size below 0.5 mm (Paola *et al*. 1992). This is true even through sediments with median sizes in the intervening range could be produced from the material available. The gravel-sand transition develops because of sorting processes and is not simply a reflection of the bimodality in the sediment supply (Paola *et al*. 1992). Sambrook Smith & Ferguson (1995) also found an abrupt transition between a gravel bed and sand bed, however, they attribute the transition to 3 main reasons: 1, a break in slope, 2. Lateral input (only from a large system like a bad land environment) and 3. Abrasion (only in extremely active channels) Paola *et al*. (1992) suggested there is a cut off size in the medium sand range above which grains cannot be suspended. The abrupt transition from gravel to sand was observed in the transects at the downstream end of the reach, with D16 for example decreasing from 7 mm (gravel) to 0 mm (sand) over 5 km (Fig 4.11). Another series of experiments also observed a distinct gravel front (Toro-Escobar *et al*. 2000), although their results highlighted that the gravel/sand transition was more abrupt in narrower channels than wider channels. In the Ganges, this could be true if each braid was treated as an individual channel, which for channels ~100-200 m would fit the trends seen by Toro-Escobar *et al* (2000). Another accepted explanation for rapid downstream fining is that the more concave the river profile is, the more effective downstream fining is, as shear stress is diminished with exponentially decreasing slope, less and less sediment can be transported in suspension (Ferguson et al. 1996; Hoey and Bluck, 1999; Rice, 1999).

Grain size on the Ganges locally increases in the foreland ~15 km from the HFT on the upstream flank of a proposed developing anticline related to the proposed Piedmont Thrust

(Yeats and Thakur, 2008). This is the same principle as how grain size has been interpreted in the Yamuna to show uplift and a northward tilting HFT hanging wall. The increase is, however, within one standard deviation of D50 and therefore insignificant. More work would be required to test the potential effects of the PT on the foreland river grain size distributions.

Differences between the Ganges and Yamuna Systems

The Ganges and Yamuna rivers should both have very similar regimes as they flow through the Dun and the Mohand Anticline. The main difference between the two rivers is in the stream power and discharge. The Ganges has a discharge four times that of Yamuna which could help explain the downstream fining of grain size that we see. The Ganges River has a large peak monthly discharge of 2283 $m^3 s^{-1}$ recorded at Rishikesh (Fig 2.9a). The Song and Suswa rivers flow into the Ganges downstream of Rishikesh, with some smaller channels draining the Mohand Anticline also contributing to its discharge. This large discharge helps explains why there is a minimal change in measured clast sizes in the Mohand, as the large discharge provides a very large stream power to move sediment through the system effectively. This however is not observed in the Yamuna. The Yamuna has an assumed uniform peak discharge of 777 $m^3 s^{-1}$ (Fig 2.9b), which represents June to September. This is considerably less than the peak monthly discharge of the Ganges, which may explain why larger grains are deposited and not carried through the system.

In order to gain a quantitative explanation for grain size distribution along both rivers, a Shield's approach would be needed to calculate the bed shear stress.

Shear stress acts in the direction of the flow as it slides along the channel bed and banks. Critical shear stress is the shear stress required to mobilize sediments delivered to the channel. When the shear stress equals the critical shear stress, the channel will likely be in equilibrium. Where shear stress is excessively greater than critical shear stress, channel degradation will likely result. Where the shear stress is less than critical shear stress, channel aggradation will likely result. Thus the ability to calculate or measure both shear and critical shear stress is crucial in understanding channel adjustments.

The limitation, however, is that the hydraulic radius along both river reaches are unknown and therefore shear stress cannot be calculated for this study. If hydraulic radius was known, then equations (5), (6) and (7) below would be used:

$$\tau_{ci}{}^{*} = 0.0834 \left[\frac{d_i}{d_{s50}}\right]^{-0.872} \quad (5)$$

Equation (5) (Andrews, 1984) above is used to calculate dimensionless shear stress $\tau_{ci}{}^{*}$, Where 0.0834 and -0.872 are coefficients for a gravel-cobble bed river, $d_i$is the particle size of interest, and d_{s50} is the median particle size of the sub-surface. This needs to be calculated in order to find the critical shear stress, which is the minimum amount of force the river needs to move sediment. $\tau_{ci}{}^{*}$ d50 is then inserted into equation (6), the critical shear stress equation (Knighton, 1998)

$$\tau_{cr} = \tau_{ci} x g(\rho_s - \rho_w) d_i \quad (6)$$

(6)Where: τ_{cr} is critical shear stress, τ_{ci} is dimensionless shear stress, g is acceleration due to gravity, ρ_s is the density of sediment, ρ_w is the density of water, and d_i is the particle size of interest.

As critical shear stress can now be calculated, bed shear stress can be found using the equation: (Wohl, 2000):

$$\tau = yRs \quad (7)$$

Where: τ is the fluid shear stress, y is the specific gravity of water (density x acceleration due to gravity) – (1.94 slugs x 32.2 ft/sq.sec), R is the hydraulic radius (approximately mean depth), and s is the channel slope.

This type of Shield's analysis would be very beneficial when explaining the grain size trends observed in the Ganges and Yamuna study reaches.

The Yamuna also has many tributaries, most notably the Asan and the Giri rivers within the Dun. The grain size data indicate that clast size increases considerably in the Mohand but drops off immediately as the river exits the anticline region. This is likely due to the low peak discharge, four times smaller than that of its neighbouring river, the Ganges. The lack of water therefore decreases the stream power by the same margin, thus reducing the ability of the river to move larger particles. Larger particles are left and the finer material flushed through, therefore the presence of the larger grains is most likely due to fluvial rather than tectonic influences.

An alternative explanation for the different behaviour of the Yamuna River is the damming of the Asan ~5 km upstream of Paonta Sahib (Fig 1.2). The Asan River drains the central Dun, flowing west from Dehra Dun city and parallel to the Mohand Anticline before joining the Yamuna River (Fig 1.2, 1.3b). The Asan may have had a higher percentage of larger grain sizes in its sediment load due to the smaller drainage area and limited ability to sort. Therefore larger grain sizes in the Mohand reach of the Yamuna could have been supplied by the Asan before the dam was constructed, and are now trapped within the Mohand because the Yamuna doesn't have the stream power to move them. There are also many smaller rivers draining the Donga and Dehra Dun fans which are tributaries to the Asan along with smaller streams draining the northern flank of the Mohand Anticline, contributing discharge and sediment flux. The dam therefore prevents discharge reaching a peak that the Yamuna once would have had. By altering the pattern of discharge in the Yamuna the dam reduces the potential stream power by a considerable amount. It is possible that if this dam were not in situ, then we would see a closer grain size distribution to what we see on the Ganges, although the Yamuna drainage basin is smaller than the Ganges (by a factor of ~2) so discharge would still be lower. It shouldn't be expected that the Asan dam has a direct impact on grain size, but the results might suggest that it has an indirect effect on it by directly influencing the amount of water in the system to

transport the larger grains through the Mohand. Without knowing the precise influence of the dam, however, the increased grain size in the Mohand Anticline can be attributed to tectonic uplift. Uplift induced by the HFT reduces channel slope upstream, proximal to the HFT, which causes a systematic reduction in stream power per unit area (Fig 4.10), therefore decreasing the river's transport capacity. The river therefore sorts the grains as Paola *et al*. (1992), Sambrook Smith & Ferguson, (1995), and Toro-Escobar *et al*, (2000) suggested, moving the smaller grains out into the foreland, and exposing the larger grains.

Therefore the main differences between the Ganges and the Yamuna rivers lie in the approximately four-fold difference in peak discharge. As stream power is much higher in the Ganges due to its extremely large discharge, the river has more erosive power and therefore appears capable of degrading its bed as it crosses the uplift axis (Holbrook and Schumm, 1999), maintaining a relatively steep and consistent channel slope in the uplifting face of rock. Because the Yamuna has a discharge four times smaller than the Ganges and therefore a stream power four times smaller, it is assumed that the Yamuna has not got the erosive power to overcome the effect of uplift, and the consequent reduction in slope and stream power causes the river to aggrade upstream of the HFT (Holbrook and Schumm, 1999). The relationship between stream power and uplift on the Yamuna thus represents the expected effects of uplift on an alluvial river more so than the Ganges.

Limitations and Future Work:

The major limitations of this study stem from the lack of discharge data, the unknown contributions of tributaries to the two main channels, and the accuracy of the DEM data.

Discharge is a key variable in this study for the calculation of stream power and for the interpretation of grain size variability. The Ganges discharge data were provided by taking data from four stream gauges upstream of the Dun (Fig 2.8a). However, only having four points to plot against drainage area does not allow for an accurate derivation of the power law relationship between discharge and drainage area and hence it is difficult to extrapolate to un-gauged reaches of the river. In the absence of any other data this was deemed acceptable to identify trends in the data. As for the Yamuna River, the discharge estimate was derived from one station (Fig 2.8b) at Tajewala by Jha *et al*. (1988), and this discharge value was used for the entire reach. The value was originally a value of mean annual discharge rather than peak monthly discharge, which made it difficult to compare the Ganges and Yamuna in terms of magnitudes of discharge (Fig 2.9b). Monthly discharge data is not very reliable as it does not show any particular flood events or natural variability in the discharge. Using daily discharge data would be far more accurate as it would allow the identification of higher flood events, and allow more uncertainty to be removed. If this research were to be taken further, these discharge limitations could be overcome by installing and using more gauges along the both rivers in closer proximity to each other from the MBT, through the Dun and in the Mohand in places such as Haridwar on the Ganges, and Paonta Sahib on the Yamuna (Fig 1.2).

Another main area of unreliability was the unknown characteristics of the tributary rivers for both the Ganges and the Yamuna. In particular it was not clear what grain sizes they contributed. If this study were to be investigated further, this limitation could be overcome by collecting grain size data upstream of tributary confluences. In particular, attention should be paid to streams draining the northern flank of the Mohand, streams draining the Dun, the Suswa and Song, (tributaries to the Ganges), and the Asan and Giri rivers, (tributaries to the Yamuna).

DEM resolution is another limitation for this study. Interpretation of the steps in the long river profile was complicated by the 90 m resolution of the DEM and the numerous sinks and pits. Each 90 m pixel is likely to contain a proportion of river bank and river bed. The DEM averages the elevation of each pixel and therefore the elevation in river boundary pixels is likely to carry error. In future research, transport capacity of the rivers would be needed to explain the grain size distribution in the Mohand, because if transport capacity is known, then the normal grain size distribution can be deduced easily, and the effect of uplift can truly be identified. To do this the limitation of low resolution DEMs can be overcome by using a higher resolution DEM. This would increase the amount of pixels in the channel and therefore make calculation of slope more accurate and more representative of the actual channel. Also, river depth profiles along at close intervals along both rivers would be needed to overcome the shear stress calculation limitation. By calculating shear stress, the relationship of grain size distribution to distance could be truly identified. The other limitation of data collection was the topographical maps. A lack in coverage of the region at high enough resolution prevented extraction of contour information. In future, this limitation could be overcome simply by obtaining maps of 1:50,000 m for the entire region. The 1:250,000 m maps that were available across the entire region have contours at 100 m intervals which is not good enough for this type of study because it does not indicate changes in channel morphology on a small enough scale.

The remaining limitation in the data set was with anthropogenic impacts on the channel morphology and grain size distributions. The anthropogenic influence on the Ganges River in the Mohand Anticline reach may have made the width of channel belt and slope unnatural, and therefore stream power unnatural. By controlling the hydraulic parameters of the river, its natural ability is lost, and rather forced. The Ganges and Yamuna rivers are both subjected to extensive mining operations outside of the monsoon season which was observed to be selective, removing mostly mid-size grains (~200-300 mm). This causes problems when interpreting the grain size variability and is unfortunately something that cannot be avoided. This extensive mining was at its most influential on the Yamuna. South of the Mohand Anticline quarrying was observed which caused a gap of ~15 km where no data could be collected (Fig 5.2). This limitation however cannot be overcome in this area of the study reach as the mining operations have been so disruptive and destructive.

Fig 5.2. Photograph illustrating the degree of gravel bed mining in the Yamuna downstream of the Mohand Anticline.

An issue of particular importance is the Asan Dam because it would be very useful to know the contribution of water and sediment from the channel it dams. For future studies it is recommended that both grain size data and discharge data be acquired in the immediate vicinity of the dam. The dam's properties would need to be known too, particularly its capacity, history, and frequency of releases to identify the influence of discharge that would be reaching the Yamuna if the dam were not present.

Summary:

The Ganges River is responding to active uplift on the HFT, but not in the way that might be expected (Holbrook and Schumm, 1999). Because the Ganges is such a large river with a high stream power, it degrades its bed as it flows through the Mohand which explains why the channel slope is high and the grain size distribution continues to represent downstream fining. The Ganges is interpreted to be in a state of positive feedback, whereby high stream power induces bed degradation, which induces a higher slope, which further induces higher stream power.

The Yamuna River is responding to active tectonics in a way that is more consistent with alluvial river theories, however, alike to most rivers, its morphology and grain size distribution is strongly affected by its discharge. Due to discharge being low, stream power is also low which emphasises the effect of the northward-tilting HFT hanging wall on the channel slope and grain size distribution. Because the stream power is low, the erosive ability of the river is reduced and therefore it cannot degrade its bed as the Ganges does. Due to the shallowing of the river bed, stream power decreases further and causes preferential deposition of larger grains in the

Mohand, upstream of the HFT. The major limitations faced in this study were accuracy from the 90 m resolution DEM, limited availability of discharge data, limited ability to collect a complete grain size data set, and unknown contributions of tributary rivers.

6. Conclusions

By referring back to the river system diagram (Fig 1.1) of the introduction and comparing the expected responses of the rivers to the actual responses of the rivers, it is concluded that the morphology of both rivers responded mainly as hypothesized in research question 1. The measures of width of channel belt, braiding index responded as expected, indicating active uplift on the HFT in Northern India and perturbation of both the Ganges and Yamuna rivers. Channel slope, although reflecting uplift did not respond on the Ganges as hypothesized, however, the Yamuna did. Width of channel belt increases where the river is not constrained by topography, so as both rivers flow through the Dun they widen and braid due to their low slope and high sediment load. As they flow into the Mohand Anticline, uplift by the HFT creates steeper topography and constricts the rivers. Width of channel belt decreases, forcing the rivers into a single channel as they flow over the HFT. They then flow into the Indo-Gangetic plain where they begin to braid again as the width of channel belt increases with constricting topography subsiding. This behaviour is clearly a response to active slip on the HFT.

Channel slope on the Ganges increases in the Mohand Anticline as the river flows towards the HFT. This does not necessarily mean the river is not responding to uplift as its other geomorphological variables suggest. The Ganges is a very large system with an extremely high discharge and stream power which could be allowing the river to degrade its bed as it flows through the north-tilting back limb of the Mohand and the uplift axis. Channel slope then increases dramatically as the river flows over the HFT in response to the drop in base level. Channel slope on the Yamuna is clearly controlled by/affected by slip on the HFT, as it shallows as the river progressively gets closer to the HFT and flows through the north-tilting hanging wall. Channel slope then increases as the river flows over the HFT and into the foreland reflecting the drop in base level. Both river beds shallow into the foreland with a brief steepening ~15 km downstream of the HFT.

The grain size distribution along the Ganges identifies downstream fining by selective entrainment of grains through the entire reach studied with no perturbations in the Mohand anticline. This is interpreted as a system that is in a steady state with the rate of uplift. The high discharge of the Ganges system produces a high stream power and therefore a high transport capacity. It is therefore inferred that the river transports all available sediment through the system, which explains why there is no increase in grain size in the Mohand Anticline.

The grain size distribution along the Yamuna represents a system that has a potentially low transport capacity though the Mohand Anticline, although shear stress data are needed to confirm this. The preliminary grain size distribution identified by this study does agree with the hypothesized trend, and this finding addresses research question 1. The volume of discharge is four times lower in the Yamuna and stream power approximately four times smaller, therefore removing the erosive power of the river and any ability to degrade its bed and maintain any slope that would promote removal of large grains through the Mohand. Overall we see downstream fining through the reach with boulder size grains at the MBT and sand size grains

40 km into the foreland. There are three potential reasons for the observed increase in grain size in the Mohand. The first is that because the discharge is four times lower the stream power is four times lower. So when the river flows into the Mohand the shallowing in channel slope causes the river to deposit the coarsest fraction of its load as its transport capacity suddenly decreases. The river then flushes out the smaller sediment which is why we see an increase in the distribution of mid-sized grains (D50). However, this mechanism doesn't explain why we see an increase in D84. The second reason could be that the river cannot transport larger grains in normal flow as its transport capacity is not high enough through the Dun. Seasonally-controlled large flood events are common which means larger grains could be moved downstream sequentially with each flood event until becoming trapped when reaching the low channel slope in the Mohand. Stream power is low because of a low slope and low discharge, perhaps due to the Asan Dam, which considerably decreases the Yamuna's normal transport capacity and therefore boulders cannot be moved, but smaller grains can be, emphasising the larger grain distribution in the Mohand. The third reason could be the construction of the Asan Dam. Before the Asan dam was constructed, the peak annual/monthly discharge in the Yamuna would have been much higher with water draining from the Dun and the north flank of the Mohand contributing to the main stem. The Asan River could therefore have been transporting much larger grains into the Yamuna supplied by smaller streams draining the Mohand and the Dun. Therefore the larger grains we are seeing in the Mohand could be the remnants of sediment transported in by the Asan. Once the dam was created the transport capacity of the Yamuna was completely altered as the peak annual/monthly discharge dropped significantly which is why the Yamuna can no longer transport the larger grains out of the Mohand, it can only move the smaller ones which is why we see an increase in the distribution of D50 and D84.

It is likely that the reason for an increase in grain size in the Mohand is a combination of these reasons. To determine absolute cause, more information on the Asan Dam capacity and release frequency would be needed, as well as grain size information from smaller tributaries to both the Yamuna and Asan.

To answer research question 2; this was study was found to be restricted by anthropogenic influence on two counts; the Asan Dam, and selective removal of grains from mining. The most significant gravel mining was in the foreland immediately south of the HFT. There is a major quarrying site removing large quantities of midsized grains from the river bed. This unfortunately prevents us from tracing the grain size signal through a large reach of the Yamuna. Anthropogenic influences on the Ganges exist on a large scale in the Haridwar section of the river. Extensive redirection of the main channel and levée construction could be influencing the stream power of the river and reducing the accuracy of this study in the Mohand.

A final point for further research is the effect on the rivers of the Piedmont Thrust placed approximately 15 km south of the HFT by Yeats and Thakur (2008). Width of channel belt, slope and braiding index all show the expected response of a river flowing into the north-tilting back limb of an incipient anticline. This structure may also influence the Ganges grain size distribution however the change is within one standard deviation so it may not be significant.

The Yamuna grain size across the Piedmont Thrust unfortunately cannot be assessed due to extensive quarrying. However, by looking at the grain size distribution there is an increasing trend of the data that was collected upstream of the proposed thrust, suggesting that it might be increasing due to the uplift of an anticline. Taken together, the data provide an incomplete but suggestive indication that active deformation on the Himalayan Frontal Fault system may be migrating into the foreland.

To Summarise:

Many of the conclusions remain highly speculative due to the resolution and 'type' of data used to infer the processes. Also there are considerable uncertainties in determining the sediment transport capacity of the two systems, role of tributaries and impact of dams. Unfortunately. It wasn't possible to investigate these with great rigor. It would be useful to investigate the piedmont thrust but this would require a new approach with field survey undertaken at great resolution.

References:

Adams, J. 1979. Gravel size analysis from photographs. *Journal of the hydraulics division of the American Society of Civil Engineers*, **105**, 1247-1255

Amos, C. B., and Burbank, D. W. 2007. Width of channel belt response to differential uplift. Journal *of Geophysical Research*. **112**, F0201.

An, Z. 2000. The history and variability of the East Asian palaeomonsoon climate. *Quaternary Science Reviews,* **19**, 171-187.

Andrews, E.D., Entrainment of Gravel From Naturally Sorted Riverbed Material. Geological Society of America Bulletin, v.94, p. 1225-1231, October 1983.

Avouac, J. P., J. Lave, R. Cattin, M. R. Pandey, and R.P. Tandukar. 1998. Active mountain building in the Himalaya of Nepal, Evs Trans. *American Geophysical Union, **79***, (US), Fall Meet. Suppl., F204.

Bilham, R., K. Larson, J. Freymuller, and Project Idylhim members. 1997. GPS measurements of present-day convergence across the Nepal Himalaya. *Nature*, **386**, 61-64.

Bilham, R., F. Blulme, R. Bendick, and V. K. Gaur. 1998. Geodetic constraints on the translation and deformation of India, implications for future great Himalayan earthquakes. *Current Science*, **74**, 213-229.

Bookhagen, B., and Burbank, D. W. 2006. Topography, relief, and TRMM-derived rainfall variations along the Himalaya. *Geophysical Research Letters*, **33**, L08405.

Burbank, D. W., and Pinter, N. 1999 Landscape evolution: the interactions of tectonics and surface processes. *Basin Research,* **11**, 1-6.

Burbank, D. W., McLean, J. K., Bullen, M., Abdrakhmatov, K. Y. and Miller, M. M. 1999. Partitioning of intermontane basins by thrust-related folding, Tien Shan, Kyrgyzstan. *Basin Research*, **11**, 75-92.

Burrough, P. A. 1986. 'Principals of Geographical Information Systems for Land Resources Assessment'. Clarendon, Oxford.

Buscombe, D & Masselink, G. 2009. Grain size information from the statistical properties of digital images of sediment. *Sedimentology*, **56**, 421-438

Butler, JB, Lane, SN & Chandler, JH. 2001. Automated extraction of grain size data from gravel surfaces using digital image processing. *Journal of Hydraulic Research*, **39**, 1-11

Carbonneau, P. E., and Lane, S. N. 2004. Catchment-scale mapping of surface grain size in gravel bed rivers using airborne digital imagery. *Water Resources Research*, **40**, W07202.

Chew, L. C., and Ashmore, P. E. 2001. Channel adjustment and a test of rational regime theory in a proglacial braided stream. *Geomorphology*, **37**, 43-63.

Delany, F. M., eds., '*Zagros'*, Hindu Kush, Himalaya geodynamic evolution, 3: Washington, D.C., *American Geophysical Union*, 111-121.

DeMets, C., R. Gordon, D. Argus, and S. Stein. 1994. Effect of recent revisions to the geomagnetic reversal time scale on estimates of current plate motions. *Geophysical Research Letters*, **21**, 2191-2194.

Ferguson, R., and Ashworth, P. 1991. Slope-Induced changes in channel character along a gravel-bed stream: The Allt Dubhaig, Scotland. *Earth Surface Processes and Landforms*, **16**, 65-82.

Ferguson, R., Hoey, T., Wathen, S., and Werritty, A. 1996. Field evidence for rapid downstream fining of river gravels through selective transport. *Geology*, **24,** 2, 179-182.

France-Lanord, C., Derry, L.A. 1997. Organic carbon burial forcing of the carbon cycle from Himalayan erosion. *Nature,* **390**, 65-67.

Gautam, P. and Fujiwara, Y. 1999: Magnetic polarity stratigraphy of Siwalik Group sediments from the Karnali River section in western Nepal. *In* 'Sobel, E., Appel, E., Strecher, M., Ratschbacher, L. and Blisniuk, P'., eds, '*Terra Nostir'*. Koln, Germany: Kloster Ettal, p53-54.

Gansser, A. 1981, The geodynamic history of the Himalaya, *In* Gupta, H. K., and Gansser, A. 1964. '*Geology of the Himalayas*'. Wiley Interscience, New York, 289.

Graham, D. J., Rice, S. P., and Reid, I. 2005. A transferable method for the automated grain sizing of river gravel. *Water Resources Research*, **41**, W07020.

Hodges, K. V., Hubbard, M.S., and Silverberg, D.S. 1988. Metamorphic constraints on the thermal evolution of the central Himalayan Orogen. *Royal Society of London Philosophical Transactions*, **326**, 257-280.

Hodges, K. V. 2000. Tectonics of the Himalaya and southern Tibet from two perspectives. *Geological Society of America Bulletin*, **112**, 342-350.

Hoey TB & Bluck BJ, 1999, Identifying the controls over downstream fining of river gravels, *Journal of Sedimentary Research.* **69**, 40-50.

Holbrook, J., and Schumm, S. A. 1999. Geomorphic and sedimentary response of rivers to tectonic deformation: a brief review and critique of a tool for recognizing subtle epeirogenic deformation in modern and ancient settings. *Tectonophysics*, **305**, 287-306.

Howard, A. D., Keetch, M. E., Vincent, C. L. 1970. Topological and geometrical properties of braided streams. *Water Resources Research*, **6**, 1674-1688.

Huggett, R. J. 2003. 'Fundamentals of Geomorphology'. Routledge, New York.

Jain, S. K., Agarwal, P. K., and Singh, V. P. 2007. 'Hydrology and Water Resources of India'. Springer, The Netherlands.

Jain, V., and Sinha, R. 2003. River systems in the Gangetic plains and their comparison with the Siwaliks: A review. *Current Science*, **84,** 8, 1025-1033.

Jain, V., and Sinha, R., 2005. Response of active tectonics on the alluvial Baghmati River, Himalayan foreland basin, eastern India. *Geomorphology*, **70**, 339-356.

Jain, V., Preston, N., Fryirs, K., and Brierley, G. 2006. Comparative assessment of three approaches for deriving stream power plots along long profiles in the upper Hunter River catchment, New South Wales, Australia. *Geomorphology*, **74**, 297-317.

Jarvis A., Reuter, H. I., Nelson, A., Guevara, E. 2006. Hole-filled seamless SRTM data V3, *International Centre for Tropical Agriculture (CIAT),* available from http://srtm.csi.cgiar.org.

Jha, P. K., Subramanian, V., and Sitasawad, R. 1988. Chemical and sediment mass transfer in the Yamuna river – A tributary of the Ganges system. *Journal of Hydrology*, **104**, 237-246.

Jorgensen, D. W. 1990. Adjustment of alluvial river morphology and process to localized active tectonics. *Unpublished Ph.D. Dissertation*, Colorado State University., Fort Collins, 240.

Karunakaran, C., and Rao, A. R. 1979. Status of exploration for hydrocarbons in the Himalaya region-contribution to stratigraphy and structure. Himalayan Geology Seminar 1976, *Geological Survey of India (Miscellaneous Publication)*, **415**, 1-66.

Knighton, D., Fluvial Forms and Processes A New Perspective. 1998. Oxford University Press Inc. New York.

Kodama, Y. 1994a. Downstream changes in the lithology and grain size of fluvial gravels, The Watarase River, Japan: Evidence of the role of abrasion in downstream fining. *Journal of Sedimentary Research*, **A64,** 1, 68-75.

Kodama Y, 1994b, Experimental study of abrasion and its role in producing downstream fining in gravel-bed rivers, *Journal of Sedimentary Research,* **A64**, 76-85.

Kumar, R., Ghosh, S. K., and Sangode, S. J. 2003b. Mio-Pliocene sedimentation history in the northwestern part of the Himalayan Foreland Basin, India. *Current Science*, **84,** 8, 1006-1013.

Lavé, J., and J. P. Avouac, 2000. Active folding of fluvial terraces across the Siwaliks Hills (Himalayas of central Nepal). *Journal of Geophysical Research*, **105**, 5735-5770.

Lavé, J., and J. P. Avouac, 2001. Fluvial incision and tectonic uplift across the Himalayas of central Nepal. *Journal of Geophysical Research*, **106**. 26,561-26,591.

Macfarlane, A. M. 1993. Chronology of tectonic events in the crystalline core of the Himalaya, Langtang National Park, central Nepal. *Tectonics*, **12**, 1004-1025.

Medlicott, H. B. 1864. On the geological structure and relations of the southern portion of the Himalayan ranges between the Ganges and Ravi. *Memoirs Geological Survey of India*, **3**, 1-86.

Meigs, A. J., Burbank, D. W., and Beck, R. A. 1995. Middle-late Miocene (>10Ma) formation of the Main Boundary thrust in the western Himalaya. *Geology*, **23**, 423-426.

Mishra, P., and Mukhopadhyay, D. K. 2002. Balanced structural models of Mohand and Santaurgarh ramp anticlines, Himalayan foreland fold-thrust belt, Dehra Dun re-entrant, Uttaranchal. *Journal Geological Society of India*, **60**, 649-661.

Molnar, P., and P. Tapponnier. 1977. The collision between India and Eurasia. *Scientific American*, 226, 30-41.

Mueller, E. R., and Pitlick, J. 2005. Morphologically based model of bed load transport capacity in a head water stream. *Journal of Geophysical Research*, **110**, F02016.

Ouchi, S. 1985. Response of alluvial rivers to slow active tectonic movement. *Geological Society of America Bulletin,* **96**, 504-515.

Paola, C. 1988. Subsidence and gravel transport in alluvial basins, In Kleinspehn, K. L., and Paola, C., eds., *'Frontiers in Sedimentary Geology, New Perspectives in Basin Analysis'*. New York, Springer-Verlag, 231-243.

Paola, C., Parker, G., Seal, R., Sinha, S. K., Southard, J. B., and Wilcock, P. R. 1992. Downstream fining by selective deposition in a laboratory flume. *Science*, **258**, 1757-1760.

Philip, G. and Sah, M. P. 1999. Geomorphic signatures of active tectonics in the Trans-Yamuna segment of the western Doon valley, northwest Himalaya, India. *International journal of applied earth observation and geoinformation*, **1**, 54-63.

Powers, P. M., R. J. Lillie, and R. S. Yeats. 1998. Structure and shortening of the Kangra and Derha Dun Reentrants, Sub-Himalaya, India. *Geological Society of America Bulletin*. **110**, 1010-1027.

Ranga Rao, A., Agarwal, R. P., Sharma, U. N., Bhalla, M. S., and Nanda, A. C. 1988. Magnetic polarity stratigraphy and vertebrate palaeontology of the Upper Siwalik Subgroup of Jammu Hills, India. *Journal Geological Society of India*, **31**, 361–385.

Rice, S., and Church, M. 1998. Grain size along two gravel-bed rivers: Statistical variation, spatial patterns and sedimentary link. *Earth Surface Processes and Landforms*, **23**, 345-363.

Rice S, 1999, The nature and controls on downstream fining within sedimentary links, *Journal of Sedimentary. Research,* **69**, 32-39.

Sambrook Smith GH & Ferguson RI, 1995, The gravel-sand transition along river channels, *Journal of Sedimentary Research*, **A65**, 2, 423-430.

Sangode, S. J., Kumar, R., and Ghosh, S. K. 1996. Magnetic polarity stratigraphy of Siwalik Sequence of Haripur area (H.P.), NW Himalaya**.** *Journal Geological Survey of India*, **47**, 683-704.

Schumm, S. A., Dumont, J. F., Holbrook, J.M. 2002. 'Active Tectonics and Alluvial Rivers'. Cambridge University Press.

Seal R, Paola C, Parker G, Southard JB & Wilcock PR, 1997, Experiments on downstream fining of gravel: I. Narrow-channel runs, *Journal of Hydraulic Engineering,* **123**, 10, 874-884.

Seeber, L., Armbruster, J. G., and Quittmeyer, R. C. 1981. Seismicity and continental Subduction in the Himalayan arc, *In* Gupta, H. K., and Delany, F. M., eds., 'Zagros' Hindu Kush, Himalaya geodynamic evolution, 3: Washington, D.C., *American Geophysical Union*, 215-242.

Seeber, L., Gornitz, V. 1983. River profiles along the Himalayan arc as indicators of active tectonics. *Tectonophysics*, **92**, 335-367.

Sime, LC & Ferguson, RI. 2003. Information on Grain Sizes in Gravel-Bed Rivers by Automated Image Analysis. *Journal of Sedimentary Research*. **73**, 4, 630-636

Singh, A. K., Parkash, B., Mohindra, R., Thomas, J. V. and Singhvi, A. K. 2001. Quaternary alluvial fan sedimentation in the Dehradun valley piggyback basin, NW Himalaya: tectonic and palaeoclimate implications. *Basin Research*, **13**, 449-47

Singh, A. K., Parkash, B., and Choudhury, P. R. 2007. Integrated use of SRM, Landsat ETM + data and 3D perspective views to identify the tectonic geomorphology of Dehradun valley, India. International. *Journal of Remote Sensing*, **28**, 11, 2403-2414.

Singh, C. V. 2006. Pattern characteristics of Indian monsoon rainfall using principal component analysis (PCA). *Atmospheric Research*, **79**, 317-326.

Singh, S. K., Rai, S. K., and Krishnaswami, S. 2008. Sr and Nd isotopes in river sediments from the Ganga Basin: Sediment provenance and spatial variability in physical erosion. *Journal of Geophysical Research*, **113**, F03006.

Sinha, R. 2005. Why do Gangetic Rivers aggrade or degrade? *Current Science*, **89**, 5, 836-840.

Thakur, V. C. and Pandey, A. K. 2004. Late Quaternary tectonic evolution of Dun in fault bend/propergated fold system, Garhwal Sub-Himalaya. *Current Science*, **87**, 1567-1576.

Thakur, V. C. 1992. 'Geology of Western Himalaya'. Pergamon Press, New York.

Toro-Escobar CM, Paola C, Parker G, Wilcock PR & Southard JB, 2000, Experiments on downstream fining of gravel. II: Wide and sandy runs, *Journal of Hydraulic Engineering,* **126**, 3 198-208.

Turowski, J. M., Lague, D., Crave, A., and Hovius, N. 2006. Experimental channel response to tectonic uplift. *Journal of Geophysical Research*, **111**, F03008.

Valdiya, K. S. 1992. The Main Boundary Thrust zone of the Himalaya, India. *Annals Tectonicae*, **6**, 54-84.

Valdiya, K. S. 2002. Emergence and evolution of Himalaya: reconstructing history in the light of recent studies. *Progress in Physical Geography*, **26**, 3, 360-399.

Verdú, J. M., Batalla, R. J., and Martínez-Casasnovas, J. A. 2005. High-resolution grain-size *characterisation of gravel bars using imagery analysis and geo-statistics*. Geomorphology, **72**, 73-93.

Wasson, R. J. 2003. A sediment budget for the Ganga-Brahmaputra catchment. *Current Science*, **84**, 1041-1047.

Werritty A, 1992, Downstream fining in a gravel-bed river in southern Poland: lithologic controls and the role of abrasion. In Billi P, Hey RD, Thorne CR & Tacconi P (eds) *Dynamics of Gravel-Bed Rivers*, Wiley, 333-350

Wesnousky, S. G., Kumar, S., Mohindra, R., Thakur, V. C. 1999. Uplift and convergence across Himalayan Frontal Thrust of India. *Tectonics*, **18**, 967-976.

Wohl, E. 2000. Mountain Rivers. *American Geophysical Union*. Washington, D.C. Willett, S. D., and Brandon, M. T. 2002. On steady states in mountain belts. *Geological Society of America*, **30,** 3, 175-178.

Zhao, W., Nelson, K. D., and Project INDEPTH Team. 1993. Deep seismic reflection evidence for continental underthrusting beneath southern Tibet. *Nature*, **366**, 557-559.